



Prepared in cooperation with the County of Maui Department of Water Supply

Ground-Water Availability in the Wailuku Area, Maui, Hawai'i

Scientific Investigations Report 2008–5236

U.S. Department of the Interior
U.S. Geological Survey

COVER:
Aerial view, looking west, of the Wailuku area, Maui, Hawai'i. (Photograph © by Douglas Peebles. Used with permission.)



Prepared in cooperation with the County of Maui Department of Water Supply

Ground-Water Availability in the Wailuku Area, Maui, Hawai‘i

By Stephen B. Gingerich

Scientific Investigations Report 2008–5236

U.S. Department of the Interior
U.S. Geological Survey

U.S. Department of the Interior
DIRK KEMPTHORNE, Secretary

U.S. Geological Survey
Mark D. Myers, Director

U.S. Geological Survey, Reston, Virginia: 2008

This report and any updates to it are available online at:
<http://pubs.usgs.gov/sir/2008/5236/>

For product and ordering information:
World Wide Web: <http://www.usgs.gov/pubprod>
Telephone: 1-888-ASK-USGS

For more information on the USGS—the Federal source for science about the Earth,
its natural and living resources, natural hazards, and the environment:
World Wide Web: <http://www.usgs.gov>
Telephone: 1-888-ASK-USGS

Any use of trade, product, or firm names in this publication is for descriptive purposes only and does not imply endorsement of the U.S. Government.

Although this report is in the public domain, permission must be secured from the individual copyright owners to reproduce any copyrighted materials contained within this report.

Cataloging-in-publication data are on file with the Library of Congress (<http://www.loc.gov/>).

Suggested citation:
Gingerich, S.B., 2008, Ground-water availability in the Wailuku area, Maui, Hawai'i:
U.S. Geological Survey Scientific Investigations Report 2008–5236, 95 p.

Produced in the Western Region, Menlo Park, California
Manuscript approved for publication September 9, 2008
Text edited by Peter Stauffer
Layout and design by Judy Weathers

Executive Summary

Most of the public water supply in Maui, Hawai‘i is from a freshwater lens in the Wailuku area of the island. Because of population increase, ground-water withdrawals from wells in this area increased from less than 10 Mgal/d during 1970 to about 23 Mgal/d during 2006. In response to increased withdrawals from the freshwater-lens system, water levels declined, the transition zone between freshwater and saltwater became shallower, and the chloride concentrations of water pumped from wells increased. To aid in management of ground-water resources and to plan for sustainable growth on the island, the Maui County Department of Water Supply (DWS) entered into a cooperative agreement in 2003 with the U.S Geological Survey (USGS) to study the ground-water availability in central and west Maui. The objectives of this 4.5-year study were to (1) obtain a better understanding of the ground-water flow system in the study area, (2) estimate ground-water recharge in the study area, and (3) simulate ground-water flow and transport using a numerical model to estimate the effects of selected withdrawal and recharge scenarios on water levels and the transition zone between freshwater and saltwater in the Wailuku Aquifer Sector. For management purposes, the State of Hawai‘i Commission on Water Resource Management (CWRM) divided central and west Maui into three aquifer-management sectors: Central, Wailuku, and Lahaina Sectors. Although the main area of interest for this study is the Wailuku Aquifer Sector, which includes the ‘Īao and Waihe‘e Aquifer Systems, the study area includes all of west Maui, the central isthmus, and about a third of east Maui in order to provide an understanding of the regional flow system. The most developed ground-water system in these areas comprises a lens-shaped freshwater body, an intermediate brackish water transition zone, and underlying saltwater.

Recharge and Discharge

Recharge was estimated for six periods on the basis of land use and precipitation: 1926–79, 1980–84, 1985–89, 1990–94, 1995–99, and 2000–04. Estimated recharge to central and west Maui declined 44 percent from 1979 to 2000. The period 1926–79 had the highest estimated recharge; recharge from irrigation during this period was at least 50 percent higher than in any other period considered. The period 2000–04 had the lowest estimated recharge. Recharge from irrigation during this period was 46 percent of the recharge from irrigation during 1926–79, and rainfall was the lowest of any period considered in this study.

Discharge from the aquifer in the study area is in the form of ground-water withdrawals from pumped wells, discharge to streams as base flow, and diffuse seepage to the ocean. Average withdrawals in 2000–06 were 21.4 Mgal/d in the Wailuku Aquifer Sector, about 4 Mgal/d in the Lahaina Aquifer Sector, and about 68 Mgal/d in the Central Aquifer Sector. Base flow represents ground-water discharge to streams. Most streams on West Maui Volcano receive ground-water discharge from dike-impounded ground water. Total average base flow at gaging stations operated on the 14 largest gaged streams in west Maui is about 101 Mgal/d.

Numerical Ground-Water Model

A three-dimensional numerical ground-water model capable of simulating density-dependent solute transport was developed as part of this study. Simulated water levels and salinity profiles generally were in agreement with measured water levels and salinity profiles from representative wells in the modeled area during the period 1926–2006. Within the Wailuku Aquifer Sector, simulated water levels relative to measured water levels are 1–3 ft lower north of Waihe‘e River, 1–2 ft higher between the Waihe‘e River and ‘Īao Stream, and are reasonably similar south of ‘Īao Stream. Measured salinity profiles in the Waiehu deep monitor well indicate a shallowing of the brackish-water transition zone over time, and the simulated salinity profiles are consistent with this trend. The simulated trend of the depth where ground-water salinity is 50-percent that of seawater fits the measured values best for the more recent data (1995–2006).

Future Recharge and Withdrawal Scenarios

The numerical ground-water model was used to simulate changes in ground-water level and salinity with ground-water withdrawal under various possible future withdrawal and recharge scenarios. Simulated salinities at selected DWS well fields after 30 years (a reasonable planning horizon) and 150 years (representing long-term sustainability) of withdrawal are classified as acceptable in this study if they are below 1-percent seawater salinity, cautionary if they are between 1- and 2.5-percent seawater salinity, and threatened if they are over 2.5-percent seawater salinity. This classification was developed cooperatively with the DWS to provide a basis for comparing the various scenarios investigated in this study. Scenarios included ground-water withdrawal at 2006 (most recent) and 1996 (least widespread) rates and locations assuming average recharge, and withdrawal at redistributed rates and locations assuming several different recharge scenarios.

Simulation results from the 2006 and 1996 withdrawal distributions indicate the following for the Wailuku Aquifer Sector: (1) average recharge rates and the 2006 withdrawal distribution (21.4 Mgal/d from 6 well fields) cause average water levels in wells to decrease 2–3 ft and the transition zone to become more than 200 ft shallower after 150 years, and (2) average recharge rates and the 1996 withdrawal distribution (20.1 Mgal/d from 4 well fields) cause average water levels in wells to decrease by more than 3 ft and the transition zone to become more than 300 ft shallower after 150 years. With the 2006 distribution, two of the six well fields have simulated salinity values that increase into the cautionary or threatened range after long-term withdrawal, but these two well fields are already known to be vulnerable so their degradation was deemed less critical. With the 1996 distribution, three of the four well fields have simulated salinity values that increase into the threatened range after long-term withdrawal, indicating that the 1996 withdrawal distribution was not desirable. This pair of simulations demonstrates that the amount of water that can be pumped from an aquifer system depends on the distribution of wells and pumping rates. Namely, a pumping distribution that is more spread out can provide more water with less undesirable consequences than a distribution of fewer, higher rate wells.

An idealized scenario in which ground-water withdrawal was redistributed to maximize withdrawal and minimize salinities in the withdrawn water was determined using the numerical model. The redistributed withdrawal scenario was obtained by reducing rates at existing wells and adding withdrawal from potential new well sites that, in consultation with the DWS, were determined reasonable locations for future water-system expansion. The redistribution simulates 27.1 Mgal/d of withdrawal from 14 wells or well fields in the Wailuku Aquifer Sector, with 3.5 Mgal/d from the Waihe‘e Aquifer System, 19.14 Mgal/d from the ‘Āo Aquifer System, and 4.5 Mgal/d from the Waikapū Aquifer System. The proposed rate of 4.5 Mgal/d from the Waikapū Aquifer System is higher than the current State of Hawai‘i sustainable yield estimate of 2 Mgal/d. Simulation results from the five scenarios that include the redistributed withdrawal conditions indicate the following for the Wailuku Aquifer Sector: (1) withdrawal during times of average recharge rates causes average water levels to decrease 2–3 ft and the transition zone to become more than 200 ft shallower after 150 years; (2) a 5-yr drought condition similar to the 1998–2002 drought results in additional salinity increases after 30 years (12.5 years of normal recharge after drought conditions) but only one well has salinity increases of concern; (3) additional recharge from restored streamflow significantly increases water levels, thickens the freshwater body, and decreases salinity at withdrawal sites in the Waihe‘e and ‘Āo Aquifer Systems; and (4) a complete removal of irrigation recharge decreases water levels and increases salinity in the central isthmus where irrigation is reduced, but recharge through restored streams still significantly increases water levels, thickens the freshwater body, and decreases salinity at withdrawal sites in the Waihe‘e and ‘Āo Aquifer Systems.

Contents

Executive Summary	iii
Recharge and Discharge	iii
Numerical Ground-Water Model	iii
Future Recharge and Withdrawal Scenarios	iv
Abstract	1
Introduction	1
Acknowledgements	3
Setting	3
Land Use	4
Climate	4
Geology	4
Hydraulic Properties of the Rocks	10
Hydraulic Conductivity	10
Dike-Free Volcanic Rocks	10
Dikes	14
Weathering	14
Sedimentary Rocks	14
Specific Storage and Effective Porosity	14
Dispersion Characteristics	15
Ground-Water Flow System	15
Freshwater Lens	15
Dike-Impounded System	17
Recharge	17
Recharge from Streams	18
Discharge	18
Withdrawals from Wells	18
Base Flow to Streams	23
Water Levels	27
Salinity	33
Simulation of Ground-Water Flow	33
Model Construction	35
Model Mesh	35
Boundary Conditions	35
Specified Pressures and No-Flow Boundaries	35
Recharge	35
Withdrawal	39
Initial Conditions	40
Representation of Hydrologic Features	40
Water Properties	40
Aquifer Properties	40
Simulated Historical Conditions 1926–2006	41
Water Levels	41

Salinity Profiles.....	44
Simulated Future Scenarios.....	48
Scenario 1—2006 Withdrawal Rates and Locations with 2000–04 Land Use and 1926–2006 Rainfall	51
Scenario 2—1996 Withdrawal Rates and Locations with 2000–04 Land Use and 1926–2006 Rainfall	53
Scenario 3—Redistributed Withdrawals with 2000–04 Land Use and 1926–2006 Rainfall.....	59
Scenario 4—Effects of Drought on Redistributed Withdrawals.....	61
Scenarios 5 and 6—Effects of Restoring Streamflow on Redistributed Withdrawals	63
Scenario 7—Effects of No Agricultural Irrigation or Stream Diversions.....	66
Additional withdrawal locations	68
Model Limitations.....	72
Summary.....	75
References Cited.....	76
Appendix A. Wells in the central Maui study area with stratigraphic information, Hawai'i.....	80
Appendix B. Monthly ground-water withdrawals during 1900–2006 from wells in central and west Maui, Hawai'i.....	83
Appendix C. Properties of pumped wells in the central and west Maui study area, Hawai'i.....	93

Figures

1. Location of study area and State of Hawai'i Commission on Water Resource Management aquifer-management sectors and systems, Maui, Hawai'i.....	2
2. Land use during 1926–2004 in central and west Maui, Hawai'i (modified from Engott and Vana, 2007).....	5
3. Mean annual rainfall and fog zone in central and west Maui, Hawai'i.	6
4. Generalized surficial geology in central and west Maui, Hawai'i	8
5. Geologic cross sections of the 'Īao aquifer area, Maui, Hawai'i.....	9
6. Structural contours on the top of the Wailuku Basalt and locations of wells with strati- graphic information on that unit in central and west Maui, Hawai'i.	11
7. Structural contours on the top of the Kula Volcanics/ Honomanū Basalt and wells with stratigraphic information on those units in central and west Maui, Hawai'i.....	12
8. Distribution of aquifer hydraulic conductivity in central and west Maui, Hawai'i.....	13
9. Geologic cross section of the 'Īao aquifer area, showing ground-water occurrence and movement, Maui, Hawai'i	16
10. Estimated ground-water recharge for various periods during 1926–2004, central and west Maui, Hawai'i.	19
11. Streamflow loss in Wailuku area streams, Maui, Hawai'i.....	21
12. Ground-water withdrawals from the Central Aquifer Sector, 1900–2006, Maui, Hawai'i.....	22
13. Ground-water withdrawals from the Wailuku Aquifer Sector, 1900–2006, Maui, Hawai'i.	23

14. Ground-water withdrawals from the Lahaina Aquifer Sector, 1900–2006, Maui, Hawai‘i.	24
15. Average monthly ground-water withdrawal for public supply and sugarcane production in the Wailuku and Central Aquifer Sectors, 1995–2006, Maui, Hawai‘i.	25
16. Water-level surveys of (A) December 5, 1970 and February 1979, and (B) May 17, 2005, Maui, Hawai‘i.	28
17. Measured water levels in selected wells in the Central Aquifer Sector, Maui, Hawai‘i.	30
18. Measured water levels in selected wells in the Wailuku Aquifer Sector, Maui, Hawai‘i.	31
19. Measured water levels in selected wells in the Lahaina Aquifer Sector, Maui, Hawai‘i.	32
20. Measured salinity profiles in selected wells in the study area, Maui, Hawai‘i.	34
21. Model discretization and features for the numerical model mesh of central and west Maui, Hawai‘i.	36
22. Vertical cross section of model mesh of central and west Maui, Hawai‘i.	37
23. Monthly ocean level during 1970–2006 at Kahului Harbor, Maui, Hawai‘i.	37
24. Selected withdrawal wells used in construction of the numerical model of central and west Maui, Hawai‘i.	39
25. Measured (black and green lines) and simulated (red lines) water levels in selected wells in central and west Maui, Hawai‘i. Well number shown in parentheses after well name.	42
26. Measured water levels on (A) December 5, 1970, and (B) May 17, 2005, compared with simulated water levels in central and west Maui, Hawai‘i.	45
27. Simulated water-level changes between 1926 and 2006 in central and west Maui, Hawai‘i.	47
28. Measured and simulated altitude of the top (2-percent seawater) and middle (50-percent seawater) of the transition zone in the Waiehu Deep Monitor well (5430-05), Maui, Hawai‘i.	48
29. Measured and simulated salinity profiles in selected wells in central and west Maui, Hawai‘i.	49
30. Simulated depth of 50-percent seawater salinity at end of historical simulation (2006) and locations of wells penetrating deeper than ¼ of the simulated depth to 50-percent seawater salinity in central and west Maui, Hawai‘i.	50
31. Measured (black and green lines) and simulated water-level (red lines) and simulated salinity data (blue lines) for Scenario 1 using monthly and yearly pumping rates at selected wells in the Wailuku Aquifer Sector, 2000–2157, Maui, Hawai‘i.	52
32. Measured and simulated positions of the bottom of freshwater (2-percent seawater salinity) and middle of the transition zone (50-percent seawater salinity) for Scenario 1 at the Waiehu Deep Monitor well (5430-05), 2000–2157, Maui, Hawai‘i.	53
33. Simulated change (relative to end of historical simulation) in water level, 50-percent seawater salinity depth, and 2-percent seawater salinity depth after 150 years of withdrawal at 2006 rates with long-term average recharge (1926–2006) [scenario 1], central Maui, Hawai‘i.	54

34. Predicted salinities in wells included in scenarios 1–7, central Maui, Hawai‘i.	55
35. Simulated water-level (red lines) and salinity (blue lines) data for Scenario 2 (dark lines) compared with Scenario 1 (light lines) at selected wells in the Wailuku Aquifer Sector, 2000–2157, Maui, Hawai‘i.	58
36. Simulated positions of the bottom of freshwater (2-percent seawater salinity) and middle of the transition zone (50-percent seawater salinity) for Scenario 2 at the Waiehu Deep Monitor well (5430-05), 2000–2157, Maui, Hawai‘i.....	59
37. Simulated change (relative to end of historical simulation) in water level, 50-percent sea water salinity depth, and 2-percent seawater salinity depth after 150 years of withdrawal at 1996 rates with long-term average recharge (1926–2006) [scenario 2], central Maui, Hawai‘i.....	60
38. Simulated water-level (red lines) and salinity (blue lines) data for Scenario 3 (dark lines) compared with Scenario 1 (light lines) at selected wells in the Wailuku Aquifer Sector, 2000–2157, Maui, Hawai‘i.....	62
39. Simulated positions of the bottom of freshwater (2-percent seawater salinity) and middle of the transition zone (50-percent seawater salinity) for Scenario 3 compared with Scenario 1 at the Waiehu Deep Monitor well (5430-05), 2000–2157, Maui, Hawai‘i.	63
40. Simulated change (relative to scenario 1) in water level, 50-percent seawater salinity depth, and 2-percent seawater salinity depth after 150 years of withdrawal at redistributed rates with long-term average recharge (1926–2006) [scenario 3], Maui, Hawai‘i.	64
41. Simulated water-level (red lines) and salinity (blue lines) data for Scenario 4 (dark lines) compared with Scenario 3 (light lines) at selected wells in the Wailuku Aquifer Sector, 2000–35, Maui, Hawai‘i.	65
42. Simulated positions of the bottom of freshwater (2-percent seawater salinity) and middle of the transition zone (50-percent seawater salinity) for Scenario 4 compared with Scenario 3 at the Waiehu Deep Monitor well (5430-05), 2000–35, Maui, Hawai‘i.	66
43. Simulated water-level (red lines) and salinity (blue lines) data for Scenarios 5 and 6 compared with Scenario 3 at selected wells in the Wailuku Aquifer Sector, 2000–2157, Maui, Hawai‘i.....	67
44. Simulated positions of the bottom of freshwater (2-percent seawater salinity) and middle of the transition zone (50-percent seawater salinity) for Scenarios 5 and 6 compared with Scenario 3 at the Waiehu Deep Monitor well (5430-05), 2000–2157, Maui, Hawai‘i.....	68
45. Simulated change (relative to scenario 3) in water level, 50-percent seawater salinity depth, and 2-percent seawater salinity depth after 150 years of withdrawal at redistributed rates with 12.3 Mgal/d of additional stream recharge [scenario 5], Maui, Hawai‘i.	69
46. Simulated change (relative to scenario 3) in water level, 50-percent seawater salinity depth, and 2-percent seawater salinity depth after 150 years of withdrawal at redistributed rates with 4.1 Mgal/d of additional stream recharge [scenario 6], Maui, Hawai‘i.....	70
47. Simulated water-level (red lines) and salinity (blue lines) data for Scenario 7 compared with Scenario 3 at selected wells in the Wailuku Aquifer Sector, 2000–2157, Maui, Hawai‘i.	71
48. Simulated positions of the bottom of freshwater (2-percent seawater salinity) and middle of the transition zone (50-percent seawater salinity) for Scenario 7 compared with Scenario 3 at the Waiehu Deep Monitor well (5430-05), 2000–2157, Maui, Hawai‘i.	72
49. Simulated change (relative to scenario 3) in water level, 50-percent seawater salinity depth, and 2-percent seawater salinity depth after 150 years of withdrawal at redistributed rates with no recharge from agriculture irrigation [scenario 7], Maui, Hawai‘i.	73

50. Simulated water-level (red lines) and salinity (blue lines) data for potential additional withdrawal sites in the Wailuku Aquifer Sector, 2000–2035, Maui, Hawai‘i.....	74
B1. Monthly ground-water withdrawals during 1900–2006 from wells in central and west Maui, Hawai‘i.....	83

Tables

1. Streamflow loss measurements and estimates in Waikapū, ‘Īao, and Waiehu Streams and Waihe‘e River, Maui, Hawai‘i.....	20
2. Base flow in selected study area streams, Maui, Hawai‘i.....	26
3. Estimated base flow and base flow simulated with MODFLOW-2000 model for selected study area streams, Maui, Hawai‘i.....	38
4. Recharge for historical simulation, 1926–2006, central and west Maui, Hawai‘i.....	38
5. Aquifer-property values used in the construction of the numerical ground-water model of central and west Maui, Hawai‘i.....	41
6. Withdrawal and recharge used in various simulation scenarios, central and west Maui, Hawai‘i.....	51
7. Classification of withdrawal for simulated scenarios, Wailuku Aquifer Sector, Maui, Hawai‘i.....	57
8. Selected wells and rates used in redistributed withdrawal scenarios, central and west Maui, Hawai‘i.....	61
A1. Information for wells with stratigraphic information in the central Maui study area, Hawai‘i.....	80
C1. Properties of pumped wells in the central and west Maui study area, Hawai‘i.....	93

Conversion Factors

Multiply	By	To obtain
Length		
inch (in.)	25.4	millimeter (mm)
foot (ft)	0.3048	meter (m)
mile (mi)	1.609	kilometer (km)
Area		
acre	4,047	square meter (m ²)
square foot (ft ²)	0.09290	square meter (m ²)
square mile (mi ²)	2.590	square kilometer (km ²)
Volume		
million gallons (Mgal)	3,785	cubic meter (m ³)
cubic foot (ft ³)	0.02832	cubic meter (m ³)
Flow rate		
foot per day (ft/d)	0.3048	meter per day (m/d)
foot per year (ft/yr)	0.3048	meter per year (m/yr)
cubic foot per second (ft ³ /s)	0.02832	cubic meter per second (m ³ /s)
million gallons per day (Mgal/d)	0.04381	cubic meter per second (m ³ /s)
inch per hour (in./h)	0.0254	meter per hour (m/h)
inch per year (in./yr)	25.4	millimeter per year (mm/yr)
Mass		
pound, avoirdupois (lb)	0.4536	kilogram (kg)
Pressure		
atmosphere, standard (atm)	101.3	kilopascal (kPa)
bar	100	kilopascal (kPa)
pound per square foot (lb/ft ²)	0.04788	kilopascal (kPa)
pound per square inch (lb/in. ²)	6.895	kilopascal (kPa)
Density		
pound per cubic foot (lb/ft ³)	16.02	kilogram per cubic meter (kg/m ³)
Hydraulic conductivity		
foot per day (ft/d)	0.3048	meter per day (m/d)
Hydraulic gradient		
foot per mile (ft/mi)	0.1894	meter per kilometer (m/km)
Dynamic viscosity		
Slug per foot per second (slug/ft/s)	47.88	Pascal-sec (Pa-s)

Temperature in degrees Celsius (°C) may be converted to degrees Fahrenheit (°F) as follows:

$$^{\circ}\text{F}=(1.8\times^{\circ}\text{C})+32$$

Temperature in degrees Fahrenheit (°F) may be converted to degrees Celsius (°C) as follows:

$$^{\circ}\text{C}=(^{\circ}\text{F}-32)/1.8$$

Vertical coordinate information is referenced to local mean sea level

Horizontal coordinate information is referenced to the North American Datum of 1983 (NAD 83).

Altitude, as used in this report, refers to distance above the vertical datum.

Specific conductance is given in microsiemens per centimeter at 25 degrees Celsius (µS/cm at 25 °C).

Ground-Water Availability in the Wailuku Area, Maui, Hawai‘i

By Stephen B. Gingerich

Abstract

Most of the public water supply in Maui, Hawai‘i, is from a freshwater lens in the Wailuku area of the island. Because of population growth, ground-water withdrawals from wells in this area increased from less than 10 Mgal/d during 1970 to about 23 Mgal/d during 2006. In response to increased withdrawals from the freshwater lens in the Wailuku area, water levels declined, the transition zone between freshwater and saltwater became shallower, and the chloride concentrations of water pumped from wells increased. These responses led to concern over the long-term sustainability of withdrawals from existing and proposed wells.

A three-dimensional numerical ground-water flow and transport model was developed to simulate the effects of selected withdrawal and recharge scenarios on water levels, on the transition zone between freshwater and saltwater, and on surface-water/ground-water interactions. The model was constructed using time-varying recharge, withdrawals, and ocean levels. Hydraulic characteristics used to construct the model were initially based on published estimates but ultimately were varied to obtain better agreement between simulated and measured water levels and salinity profiles in the modeled area during the period 1926–2006. Scenarios included ground-water withdrawal at 2006 and 1996 rates and locations with average recharge (based on 2000–04 land use and 1926–2004 rainfall) and withdrawal at redistributed rates and locations with several different recharge scenarios. Simulation results indicate that continuing 1996 and 2006 withdrawal distributions into the future results in decreased water levels, a thinner freshwater lens, increased salinity from pumped wells, and higher salinity at several current withdrawal sites.

A redistributed withdrawal condition in which ground-water withdrawal was redistributed to maximize withdrawal and minimize salinities in the withdrawn water was determined. The redistributed withdrawal simulates 27.1 Mgal/d of withdrawal from 14 wells or well fields in the Wailuku area. Simulation results from the five scenarios that include redistributed withdrawal conditions indicate the following for the Wailuku Aquifer Sector: (1) withdrawal during times of average recharge rates cause average water levels to decrease

2–3 ft and the transition zone to become more than 200 ft shallower after 150 years; (2) a 5-yr drought condition similar to the 1998–2002 drought results in additional salinity increases after 30 years (12.5 years of normal recharge after drought conditions) but only one well has salinity increases of concern; (3) additional recharge from restored streamflow significantly increases water levels, thickens the freshwater body, and decreases salinity at withdrawal sites in the Waihe‘e and ‘Īao Aquifer Systems; and (4) a complete removal of irrigation recharge decreases water levels and increases salinity in the central isthmus where irrigation is reduced, but recharge through restored streams still significantly increases water levels, thickens the freshwater body, and decreases salinity at withdrawal sites in the Waihe‘e and ‘Īao Aquifer Systems.

Introduction

The resident population on the island of Maui, Hawai‘i, increased from 38,691 in 1970 to 117,644 in 2000, which represents an increase of more than 200 percent (State of Hawai‘i, 2000). The total population (including visitors) on Maui in 2000 was 156,170 (State of Hawai‘i, 2000). Because of the increase in population, the demand for ground water also increased. For example, ground-water withdrawals from wells in the Wailuku area increased from less than 10 million gallons per day (Mgal/d) during 1970 to about 23 Mgal/d during 2006. Ground-water withdrawals in nearby areas also have increased, and likely will continue increasing to meet future water demands. However, the amount of ground water that is available to meet future water demands is uncertain.

For management purposes, the State of Hawai‘i Commission on Water Resource Management (CWRM) divided central and west Maui into three aquifer-management sectors: Central, Wailuku, and Lahaina Sectors. Further subdivisions of the sectors are hydrologically connected systems; Kama‘ole, Makawao, Pā‘ia, and Kahului Aquifer Systems in the Central sector; Kahakuloa, Waihe‘e, ‘Īao, and Waikapū Aquifer Systems in the Wailuku sector; and Honokōhau, Honolua, Honokōwai, Launiupoko, Olowalu, and Ukumehame Aquifer Systems in the Lahaina sector (fig. 1).

2 Ground-Water Availability in the Wailuku Area, Maui, Hawai'i

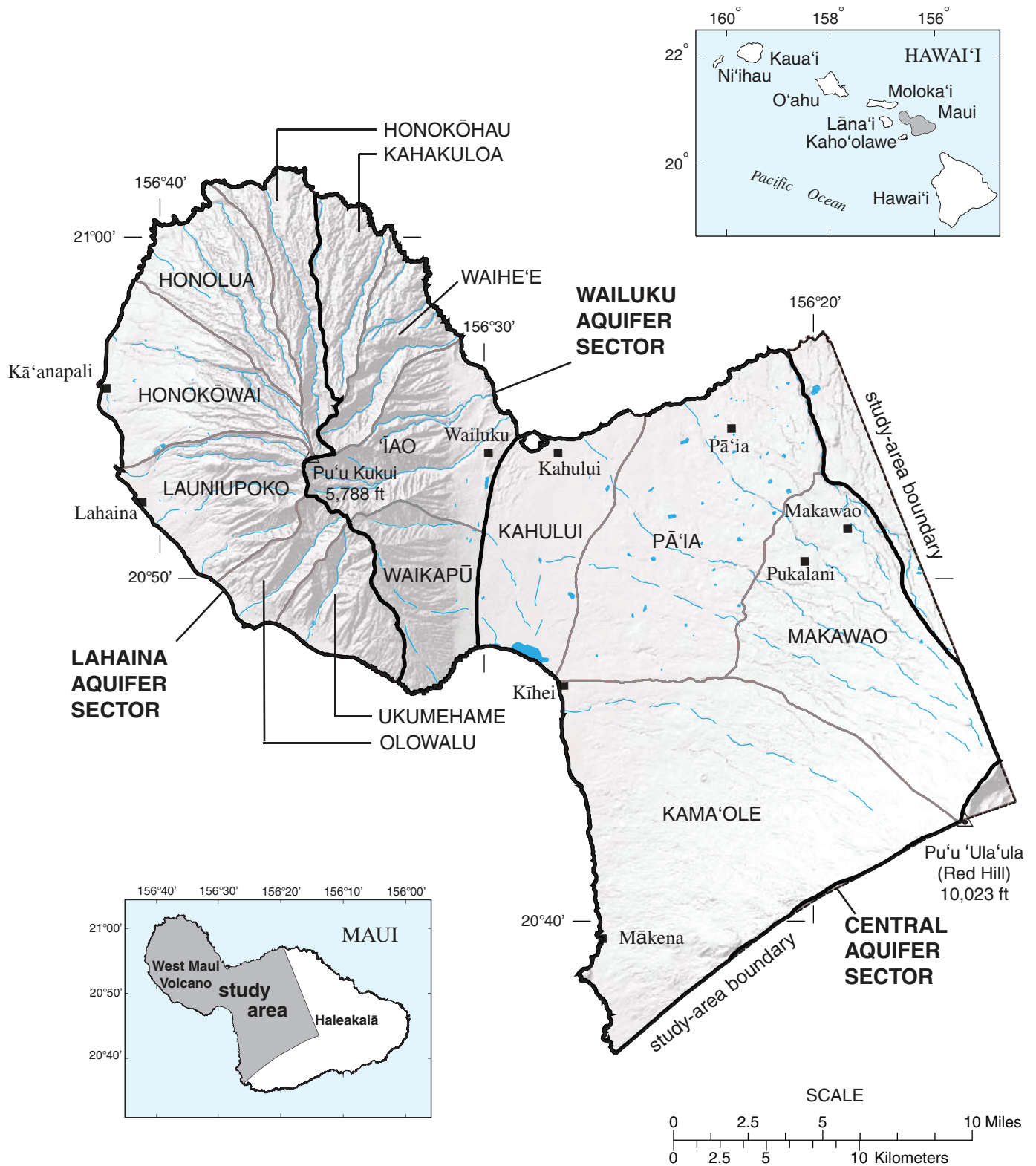


Figure 1. Location of study area and State of Hawai'i Commission on Water Resource Management aquifer-management sectors and systems, Maui, Hawai'i.

In a freshwater-lens system, increased withdrawals will, in the long term, result in a decline in water levels, a shallowing of the transition zone between freshwater and saltwater, and a reduction of natural ground-water discharge to streams or the ocean. The extent to which water levels decline and the transition zone rises is dependent on factors including the distribution and rates of withdrawals and the hydraulic characteristics of the aquifer system. In some cases, pumping from a well also may induce brackish water to enter the well if the withdrawal rate is too high or the well is too deep.

In response to increased withdrawals from the freshwater-lens system of the 'Āao aquifer, water levels declined, the transition zone between freshwater and saltwater became shallower, and the chloride concentrations of water pumped from wells increased (Meyer and Presley, 2001). Chloride concentrations in water pumped from Waiehu Heights pump 1 (State well number 5430-01) and Mokuhaul pump 2 (5330-09) have exceeded 250 mg/L, which represents the U.S. Environmental Protection Agency's recommended secondary standard for drinking water. Chloride concentrations of water pumped from other wells in the 'Āao and Waihe'e aquifers increased over time, although concentrations generally remained below 200 mg/L. The decline in water levels, shallowing of the transition zone between freshwater and saltwater, and increase in chloride concentrations in pumped water have led to concern over the long-term sustainability of withdrawals from existing wells in the 'Āao aquifer. In 2003, CWRM designated the 'Āao Aquifer System as a Ground-Water Management Area, triggered by ground-water withdrawals averaging more than 18 Mgal/d (State of Hawaii, 2003). To manage the ground-water resources and to plan for sustainable growth on the island, an improved understanding of the ground-water flow system in central and west Maui was needed.

The Maui County Department of Water Supply (DWS) entered into a cooperative agreement in 2003 with the U.S. Geological Survey (USGS) to conduct a study of the ground-water availability in central and west Maui. The objectives of this 4.5-year study are to (1) obtain a better understanding of the regional ground-water flow system in the study area, (2) estimate ground-water recharge in the study area, and (3) to simulate the effects of selected withdrawal and recharge scenarios on water levels and the transition zone between freshwater and saltwater in the Wailuku Aquifer Sector. Although the main area of interest for this study is the Wailuku area of Maui, which includes the 'Āao and Waihe'e Aquifer Systems, the study area includes all of west Maui, the central isthmus, and about a third of east Maui in order to provide an understanding of the regional flow system (fig. 1). This report describes (1) information related to the regional hydrologic system of central and west Maui, (2) development of a numerical ground-water flow and transport model, and (3) results of model simulations assessing the hydrologic effects of various recharge and withdrawal conditions on the hydrologic system.

Acknowledgements

This study was funded through a cooperative agreement between the Maui DWS and the USGS. The author is grateful to Maui DWS Director Jeffrey Eng (and former Director George Tengan) and the staff of the Maui DWS for their cooperation and assistance, especially in discussing potential withdrawal and recharge scenarios. Carl Freedman of Haiku Design and Analysis also provided valuable assistance in developing the withdrawal scenarios. Randall Moore and the staff at Hawaiian Commercial and Sugar, Inc. (HC&S) provided pumping data and arranged access and cooperation for collecting water-level data in their wells. Other well owners who kindly provided access to their wells include the County of Maui Department of Public Works and Environmental Management; the County of Maui Department of Parks and Recreation; Maui Pineapple Company, Ltd.; The Dunes at Maui Lani Golf Course; Consolidated Baseyards, LLC; and Maui Electric Company, Ltd. Glenn Bauer, Kevin Gooding, and Mitch Ohye of the CWRM assisted with water-level data collection during the synoptic water-level survey. Toby Vana, Todd Presley, and Greg Berman of the USGS provided support in resurveying measuring points, and collecting valuable water-level data during the study. Ed Carlson of the National Geodetic Survey led the effort to resurvey benchmarks and measuring points for wells throughout central Maui.

For the recharge part of the study, the author thanks the Maui Land and Pineapple Co. (ML&P) for permitting us to install climate stations on their property and Nobriga's Ranch, Inc. for providing access to a climate-station site. Randy Bartlett, ML&P Watershed Manager, and his staff, Greg Hansen and Hank Oppenheimer, provided crucial assistance in accessing, constructing, and maintaining these sites. Matt Wong and Phil Teeters of the USGS also provided support in maintaining the climate network. Special-use permits for climate stations were granted through the Hawai'i Department of Land and Natural Resources' Office of Conservation and Coastal Lands and the Natural Area Reserve System Commission. Wes Nohara (ML&P), Randall Moore and Lee Ingamells (HC&S), and Clayton Suzuki (Wailuku Water Co., Inc.) provided important agricultural data and assistance. Kevin Kodama of the National Weather Service provided rainfall data.

Finally, the author thanks the concerned citizens of Maui who continued to ask questions and provide feedback and encouragement at our presentations throughout the study. Especially notable participants include John Duey, Lucienne deNaie, David Snow, and the late Glenn Shepherd.

Setting

Maui is the second largest of the Hawaiian Islands and is located between longitudes 155°57'W and 156°47'W and

4 Ground-Water Availability in the Wailuku Area, Maui, Hawai'i

between latitudes 20°32'N and 21°03'N (fig. 1). The island comprises two shield volcanoes, the older West Maui Volcano that reaches an altitude of 5,788 ft and the younger Haleakalā Volcano that reaches an altitude of 10,025 ft. The two volcanoes are separated by an isthmus, generally at altitudes less than 300 ft, which is covered with terrestrial and marine sedimentary deposits that are as much as 5 miles wide (Stearns and Macdonald, 1942). Although the main area of interest for this study is the Wailuku Aquifer Sector, the regional study area (fig. 1) includes all of west Maui, the central isthmus, and about a third of east Maui in order to provide an understanding of the regional flow system. West Maui Volcano is deeply dissected by numerous streams, which originate from near the summit of West Maui Volcano. No perennial streams are on the part of Haleakalā that is in the study area. Topography within the study area ranges from a broad flat plain to steep interior mountains.

Land Use

Gently sloping areas around west Maui and on the isthmus between west and east Maui have been used for agriculture for over a century. The urban areas spread over the northern part of the isthmus at Wailuku and Kahului and in resort areas along the coasts. The interior of west Maui is mostly forested conservation land. The principal agricultural crops (fig. 2) have been sugarcane, pineapple, macadamia nuts, and diversified agriculture. The historical changes in agricultural land use within the study area were estimated by Engott and Vana (2007) in order to estimate the historical application of irrigation water, and the following sections on land use are summarized from their work. During the early 1900s until about 1979, land use was mostly unchanged except for some minor urbanization along the coasts. However, as large-scale plantation agriculture declined after 1979, land-use changes were more significant. During the period 1979–2004, agricultural land use declined about 21 percent, mainly from decreases in sugarcane acreage.

On the west side of West Maui Mountain, the Pioneer Mill Co. was a major sugarcane cultivator during the late 1800s until 1999, when it ceased sugarcane production and the land was subsequently bought by ML&P and other private investors. ML&P currently grows pineapple on the northwest slope of West Maui Mountain, where pineapple has a long history of cultivation, and in a small area of former Pioneer Mill Co. sugarcane lands. However, the extent of pineapple cultivation in west Maui has decreased considerably since the late 1990s.

On the east slope of West Maui Mountain, the Wailuku Sugar Co. (currently the Wailuku Water Co.) first began growing sugarcane in 1856. By the mid-1980s, sugarcane was replaced by macadamia trees on the northern extent of the plantation. Additional sugarcane lands were replaced by pineapple by the end of the 1980s. In the 1990s, Wailuku Agribusiness, as the company was then named, continued diversifying away from sugarcane and agriculture altogether. By 2005, the company had leased the southern extent of the plantation to

HC&S, halted macadamia operations, and sold much of its land for residential development.

On the central Maui isthmus, sugarcane has been grown continuously from the late 1800s until the present by HC&S and predecessor plantations. ML&P and several smaller companies currently cultivate pineapple on the lower northwest slope of Haleakalā. Pineapple has been grown in this area for more than a century.

Climate

The topography of Maui and the location of the north Pacific anticyclone relative to the island affect its climate, which is characterized by mild and uniform temperatures, seasonal variation in rainfall, and great geographic variation in rainfall (Blumenstock and Price, 1967). Average temperature in Wailuku, near the coast, is 75° F, whereas the average at Haleakalā summit is 47° F (Western Region Climate Center, 2007). During the warmer dry season (May–September), the stability of the north Pacific anticyclone produces persistent northeasterly winds, known locally as trade winds, which blow 80–95 percent of the time. During the cooler rainy season (October–April), migratory weather systems often travel past the Hawaiian Islands, resulting in less persistent trade winds that blow 50–80 percent of the time. Low-pressure systems and associated southerly winds can bring heavy rains to the island, and the dry coastal areas can receive most of their rainfall from these systems.

The variation in mean annual rainfall with altitude is extreme on Maui, with differences of more than 130 in. within one mile of Pu'u Kukui (fig. 3) where average annual rainfall exceeds 355 inches per year (Giambelluca and others, 1986). Mean annual rainfall at the coast in the dry leeward areas is less than 15 in. At higher altitudes, precipitation is a combination of rainfall and fog drip where the montane forest canopy intercepts cloud water. Giambelluca and Nullet (1991) defined the fog zone on the leeward slopes of Haleakalā as extending from altitudes of about 3,900 to 5,900 ft and estimated a thicker fog zone, at altitudes of 2,000 to 6,560 ft, along windward slopes. Precipitation is supplemented by an unknown amount of fog drip, which is fog and precipitation (not measured by rain gages) that is intercepted by vegetation and that subsequently drips to the ground surface.

Geology

The geology of Maui was described in detail by Stearns and Macdonald (1942), and some of the geologic units were subsequently reclassified by Langenheim and Clague (1987). Cox (1951), Yamanaga and Huxel (1970), and Meyer and Presley (2001) presented stratigraphic information for the basalts and overlying sediments in the Wailuku area based on drilling information.

West Maui Volcano has a central caldera and two main rift zones that trend in northwesterly and southeasterly directions

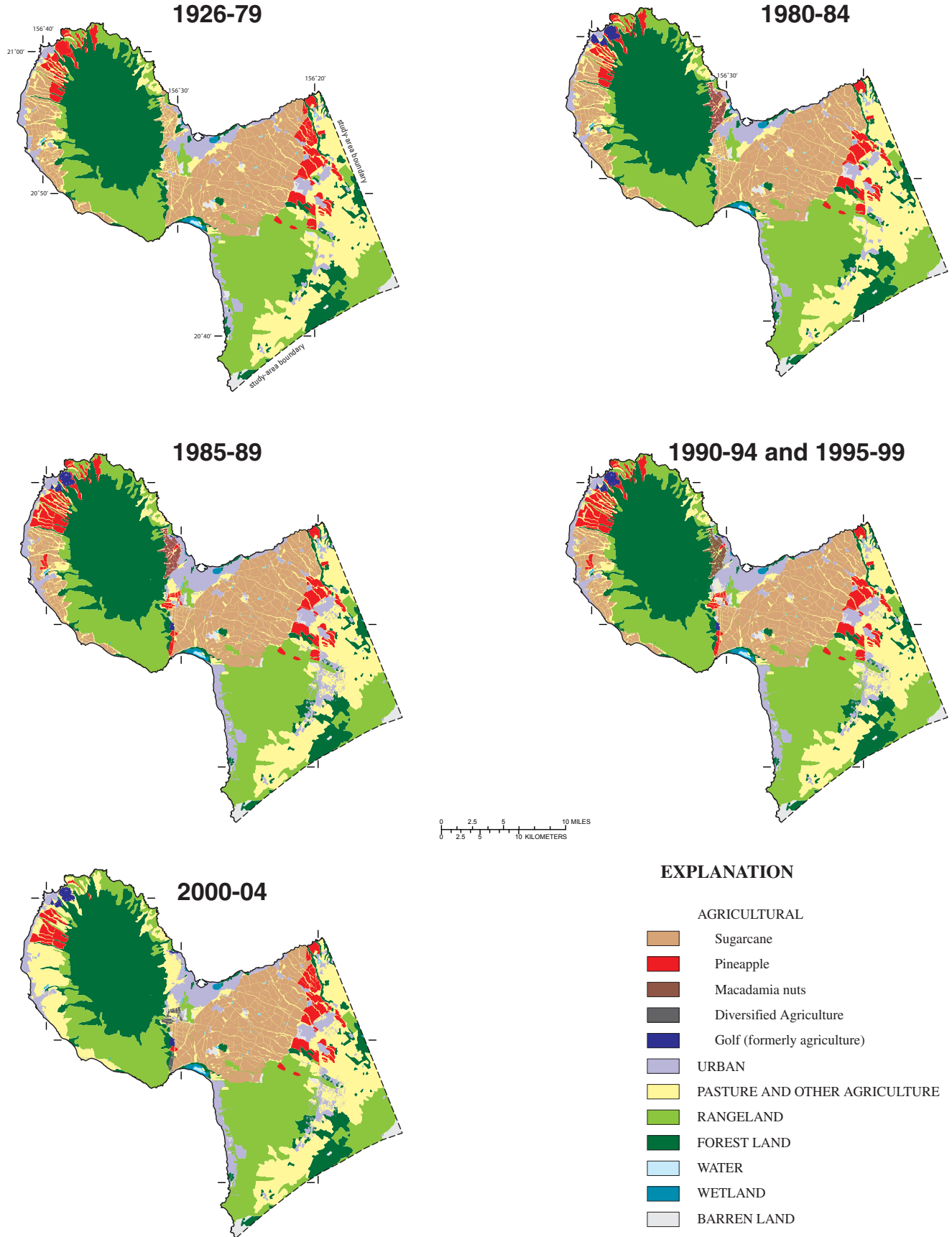


Figure 2. Land use during 1926–2004 in central and west Maui, Hawai'i (modified from Engott and Vana, 2007).

6 Ground-Water Availability in the Wailuku Area, Maui, Hawai'i

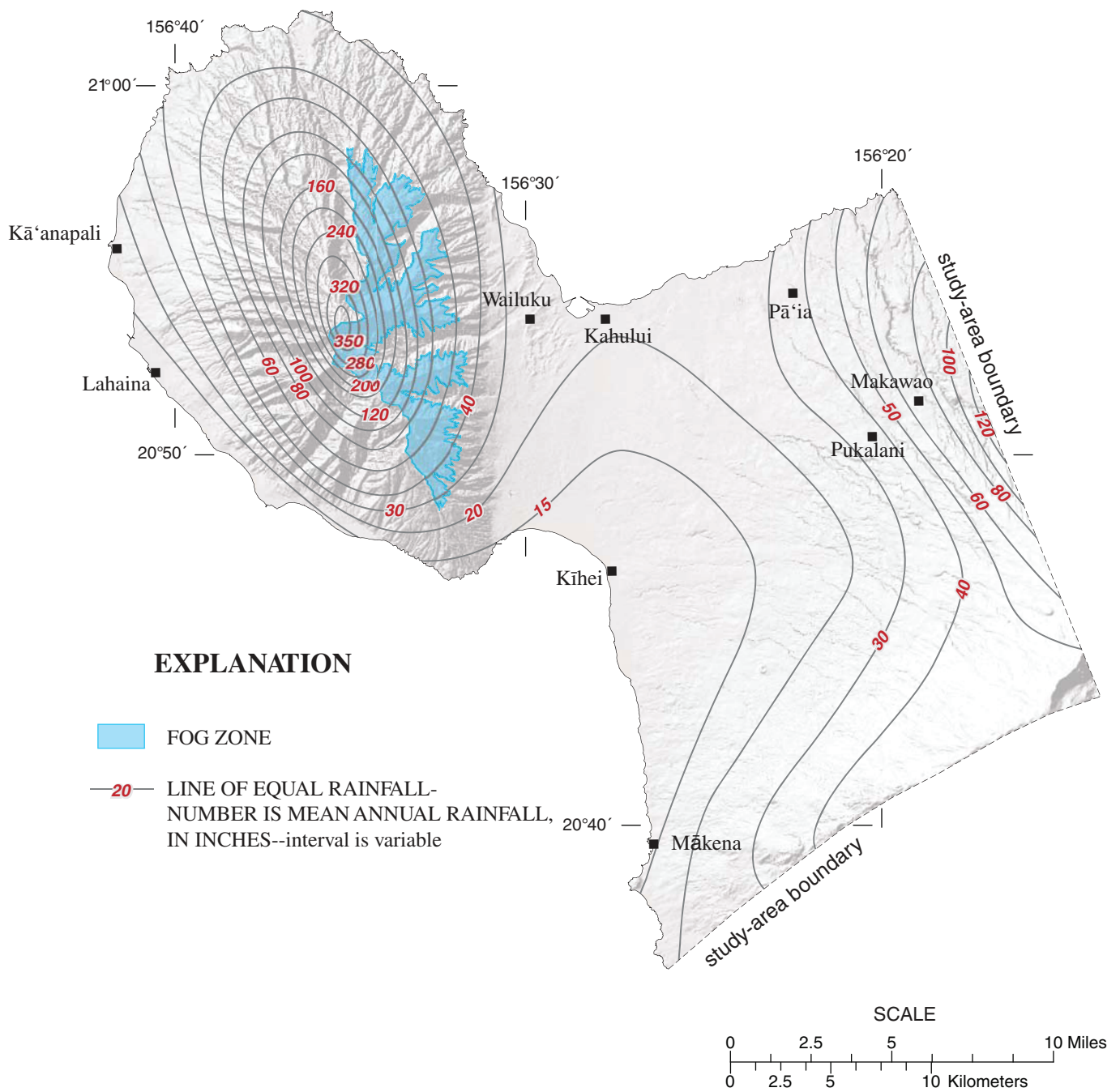


Figure 3. Mean annual rainfall and fog zone in central and west Maui, Hawai'i (modified from Giambelluca and others, 1986; Giambelluca and Nullet, 1991).

from the caldera (fig. 4). Thousands of dikes exist within the rift zones, with the number of dikes increasing toward the caldera and with depth. Additional dikes exist outside the trends of the rift zones, creating a radial pattern of dikes emanating from the caldera (Macdonald and others, 1983). Thousands of lava flows emanated from vents in and near the caldera and rift zones.

The rocks of West Maui Volcano consist of the mostly shield-stage Wailuku Basalt, which is overlain by the postshield-stage Honolua Volcanics and rejuvenated-stage Lahaina Volcanics. The Wailuku Basalt consists of tholeiitic, olivine-tholeiitic, and picritic tholeiitic basalt and postshield-stage caldera-filling lava of alkalic basalt, and it includes lava flows with associated intrusive rocks and pyroclastic and sedimentary deposits (Langenheim and Clague, 1987, p. 79). Individual lava flows range between 1 and 100 ft in thickness and dip between 5 and 20-degrees away from their sources (Stearns and Macdonald, 1942, p. 161). The Honolua Volcanics comprises mugearite, trachyte, and hawaiite, and it includes lava flows and associated domes, dikes, and pyroclastic deposits (Langenheim and Clague, 1987, p. 79). Individual flows range between 25 and 300 ft in thickness and may reach 500 ft thick near vents (Stearns and Macdonald, 1942, p. 173). These flows average about 75 ft thick and generally form a veneer on the older Wailuku Basalt. Isotopic age determinations indicate a Pleistocene age for the Wailuku Basalt and Honolua Volcanics (McDougal, 1964; Naughton and others, 1980). The Lahaina Volcanics comprises Pleistocene-age basanite and picritic basanite, and it includes lava flows and associated pyroclastic deposits (Langenheim and Clague, 1987, p. 79). These rock types are not very widespread and all lie on the west side of West Maui Volcano (Stearns and Macdonald, 1942, p. 180).

Haleakalā has three rift zones that trend in northerly, southwesterly, and easterly directions. Two of these rift zones form the eastern boundary of the study area. The rocks of Haleakalā Volcano consist of the shield-stage Honomanū Basalt, which is overlain by the postshield-stage Kula Volcanics and younger Hāna Volcanics. The Honomanū Basalt comprises tholeiitic, olivine tholeiitic, and picritic tholeiitic basalt, and it includes lava flows and associated intrusive rocks and rare pyroclastic deposits (Langenheim and Clague, 1987, p. 78). The end of the shield-building stage of the volcano is estimated to be between 0.97 and 0.93 million years ago on the basis of potassium-argon dating (Chen and others, 1991). The lavas of the Honomanū Basalt have typical dips of 2–22 degrees, with the flatter dips near the isthmus where lava flows approached the West Maui Volcano. The basalts were laid down as vesicular pāhoehoe and ‘a‘ā flows averaging about 15 ft thick (Stearns and Macdonald, 1942, p. 70).

The Kula Volcanics, which overlies the Honomanū Basalt, comprises post-shield-stage lava flows of hawaiite with some ankaramite and alkalic basalt and associated intrusive rocks and pyroclastic and sedimentary deposits (Langenheim and Clague, 1987, p. 78). The Kula Volcanics is estimated to be 0.93–0.36 million years old, with many of the

oldest rocks having chemical compositions transitional from the shield- to post-shield-stage lava (Chen and others, 1991). Exposures of this transitional phase are 50–100 ft thick and are commonly difficult to characterize as belonging to either the Honomanū Basalt or the Kula Volcanics. In some places, the two units are separated by a thin red soil layer that was altered by the weight and heat of the overlying flows. The Kula Volcanics almost completely covers the underlying Honomanū Basalt and exposures range between 2,500 ft in thickness near the summit and 50–200 ft in thickness near the coast. The thickness of individual lava flows averages about 20 ft near the summit and 50 ft near the periphery, but flows as much as 200 ft thick are not rare (Stearns and Macdonald, 1942, p. 75). The usual dip of the flows is about 10 degrees.

The Hāna Volcanics comprises alkalic basalt and basanite, and it includes lava flows and associated intrusive rocks and pyroclastic and sedimentary deposits (Langenheim and Clague, 1987, p. 78). The Hāna Volcanics is mostly ‘a‘ā and ranges between a few feet and several hundred feet in thickness where it was confined by valley walls during emplacement (Stearns and Macdonald, 1942, p. 96). The Kula Volcanics and the Hāna Volcanics are the most widespread geologic units exposed at the land surface on Maui. Sherrod and others (2003) presented age-dating, geochemical, and geological evidence for Haleakalā lavas showing that the volcano has not yet begun a classically defined rejuvenated stage of growth, and therefore the Kula (Pleistocene) and Hāna Volcanics (Pleistocene and Holocene) are products of the same stage of island formation.

The central isthmus is formed by nearly flat-lying lava flows of the Honomanū Basalt, which are interbedded with consolidated and unconsolidated sedimentary deposits (fig. 5). Beneath the isthmus, Honomanū Basalt of Haleakalā overlies older Wailuku Basalt of West Maui Volcano with a wedge of sedimentary deposits between the two units. Sedimentary deposits throughout Maui have been divided into consolidated earthy deposits, calcareous sand dunes, and unconsolidated deposits (Stearns and Macdonald, 1942). The consolidated earthy deposits are primarily older alluvium, which forms the bulk of the alluvial plains stretching from the mountains of West Maui Volcano to the coast. The older alluvium primarily consists of poorly sorted conglomerates. Within these deposits, a thin layer of Lahaina Volcanics was found while drilling Test Hole E (5430-03); this lava flow is not exposed on the surface (fig. 4). The older alluvium has been partly eroded by Waikapū and ‘Īao Streams and Waihe‘e River. Calcareous sand dunes are found seaward of the exposed older alluvium. Unconsolidated deposits are found in streambeds and in the coastal areas, and primarily consist of younger, poorly sorted alluvium.

Burnham and others (1977, p. 6) describe four principal units of the sedimentary wedge beneath the Kahului area. The base of the sediments contains a westward-thickening wedge of alluvial clay, sand, and gravel that may reach 30–50 ft in thickness within the area. Overlying the alluvium and extending

8 Ground-Water Availability in the Wailuku Area, Maui, Hawai'i

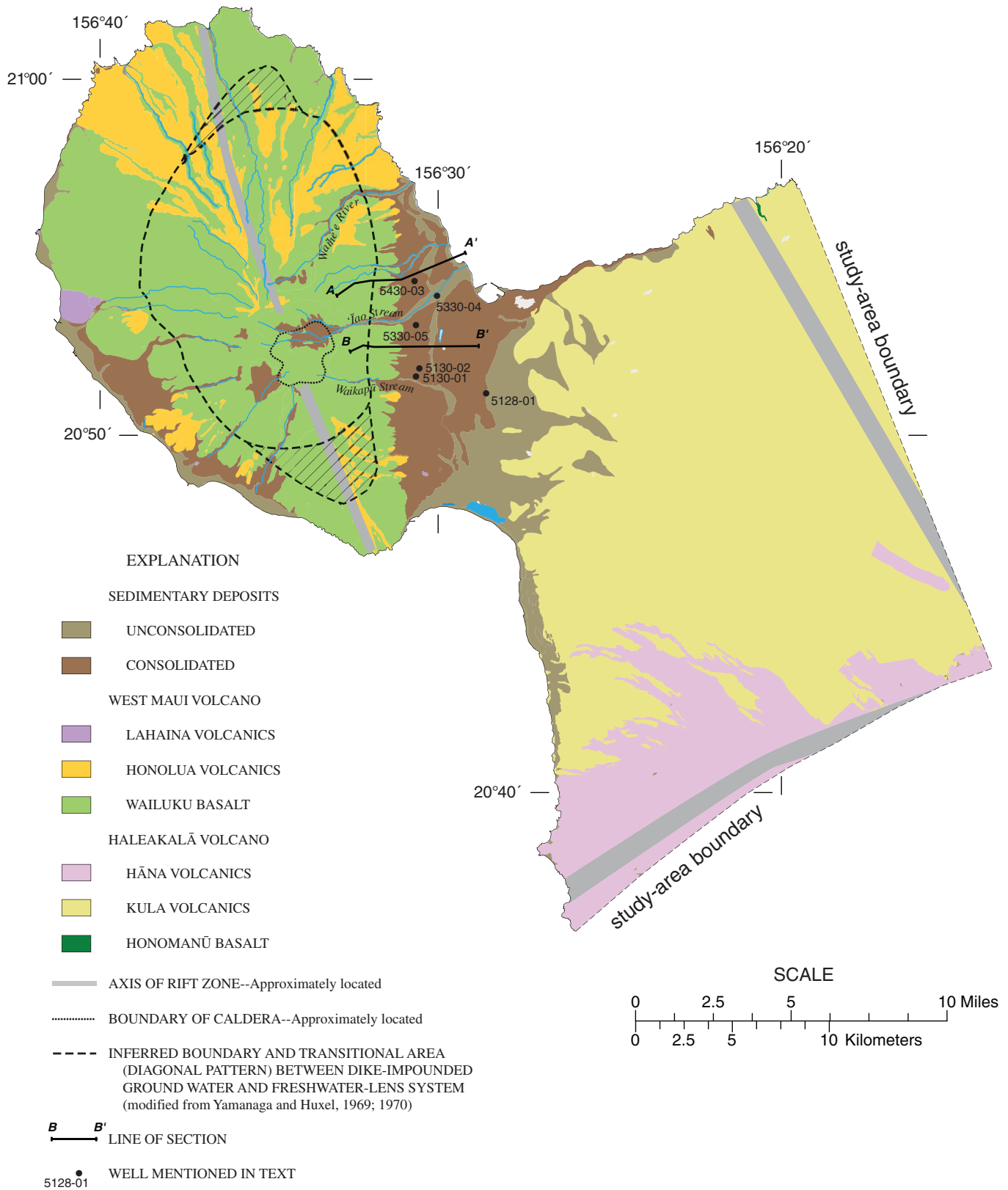
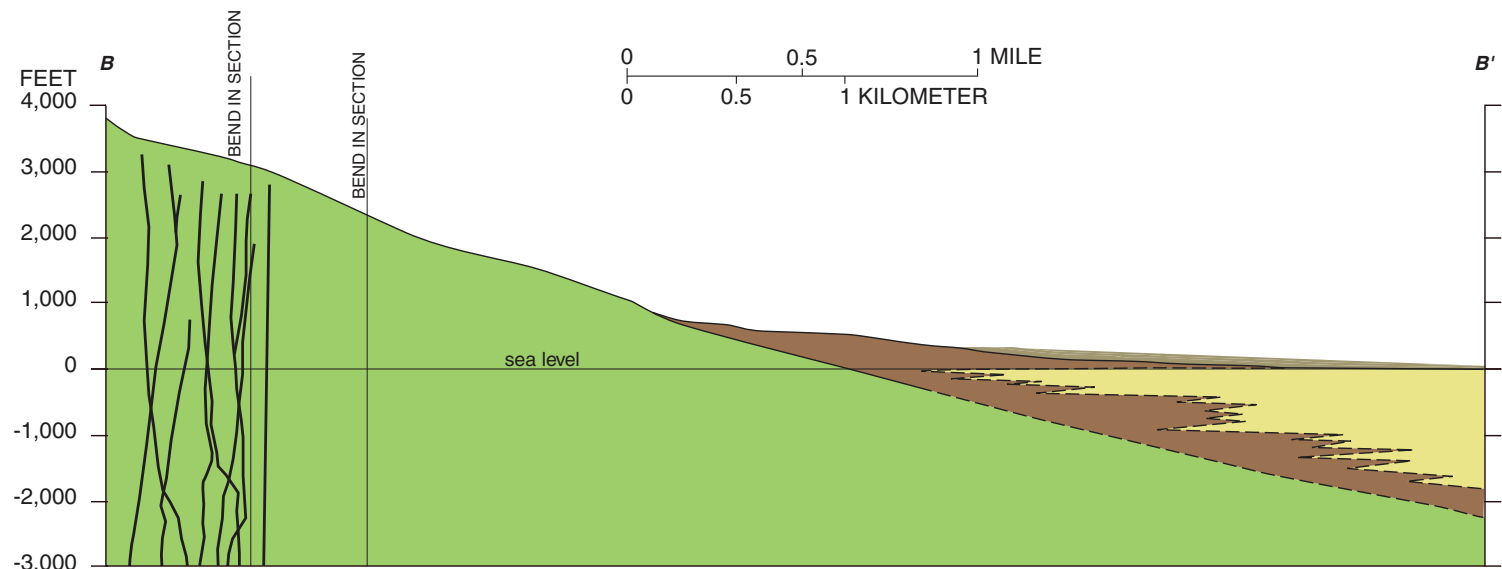
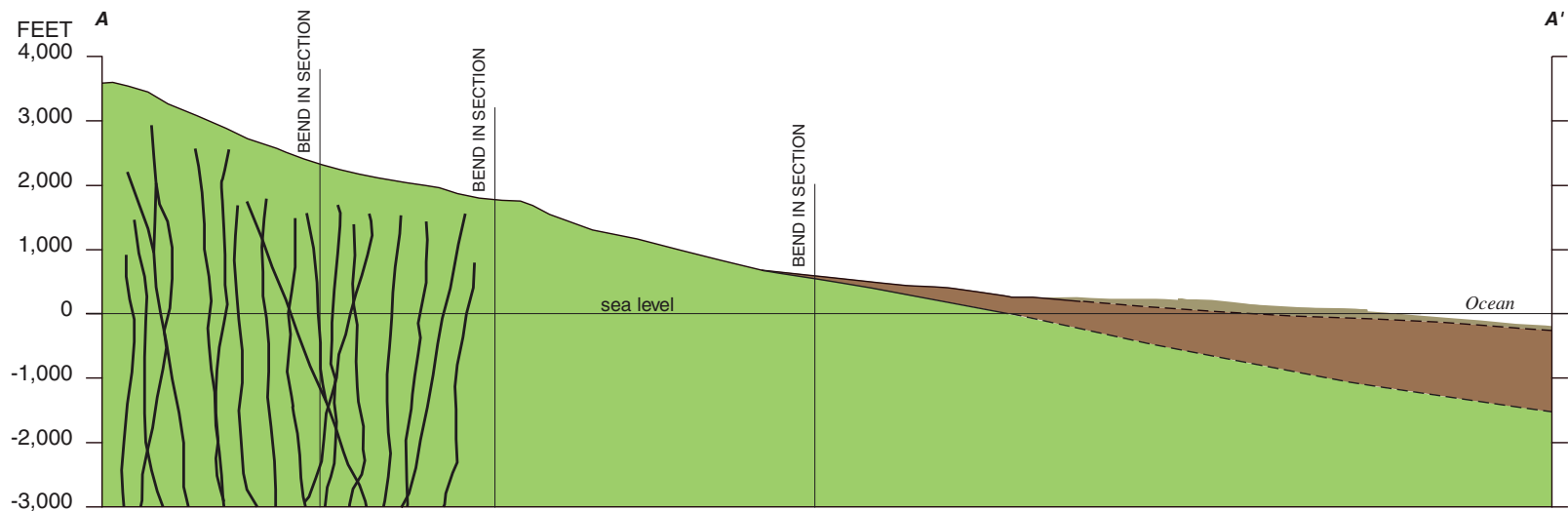


Figure 4. Generalized surficial geology in central and west Maui, Hawai'i (modified from Stearns and Macdonald, 1942; Sherrod and others, 2003).



NO VERTICAL EXAGGERATION

SEDIMENTARY DEPOSITS		EXPLANATION	
	UNCONSOLIDATED		WEST MAUI VOLCANO
	CONSOLIDATED		HALEAKALĀ VOLCANO
			KULA VOLCANICS / HONOMANŪ BASALT
			DIKES

Figure 5. Geologic cross sections of the 'Īao aquifer area, Maui, Hawai'i (modified from Meyer and Presley, 2001).

farther southeastward over residual clay on the lava is a buried coral reef complex, which appears to be the landward continuation of the present offshore reef. This reef material is dominantly coral mixed with coral debris and medium to fine sand. The reef complex is overlain by sand, which grades landward from coarse to fine and reaches thicknesses of 20–30 ft. The sedimentary materials are capped beneath the land areas by the windblown sand and soils of the present land surface (Burnham and others, 1977, p. 6). A similar sedimentary sequence would be expected across the isthmus; Stearns and Macdonald (1942, p. 109) report marine sediments 40 ft above sea level near the center of the isthmus in the Waikapū Shaft Test Hole (5128-01) (fig. 4).

Following a period of extensive erosion, during which stream valleys were deeply incised, some of the valleys were filled in by alluvial deposits during a period when sea level was higher than it is today. The deposits formed alluvial fans that extended up the stream valleys and were influenced by the growth of the Haleakalā slope to the east (Cox, 1951, p. 4). These valley-fill deposits extend below sea level, but a series of test holes drilled in the 1940's did not provide evidence of how deeply these deposits extend. Estimates of similar valley-fills in O'ahu suggest that these sediments may extend as much as 200 ft below sea level (Oki, 2005b, p. 17).

Because the sedimentary deposits are hydrologically significant owing to their relatively lower permeability compared to the volcanic rocks, the subsurface extent of these deposits was mapped using lithologic information from wells. Cox (1951, plate 2) presented an initial map of the pre-Honolua surface (top of the Wailuku Basalt) based on data from six wells in the 'Īao area, and Burnham and others (1977, fig. 2) presented a map for the Kahului area showing the depth of the top of the lava rock aquifer (Kula Volcanics or Honomanū Basalt) using data from 28 wells. Lithologic information from an additional 60 wells (appendix A) was combined with these existing maps to construct maps of the top of the Wailuku Basalt and the top of the Kula Volcanics/ Honomanū Basalt for the entire study area and extending offshore (figs. 6 and 7). Where no lithologic information was available, the approximate position of the buried surface beneath Haleakalā and offshore was determined by extrapolating the broad topographic slope of the West Maui Volcano. The subsurface extent of valley-filling deposits was estimated from borehole data and from extrapolation below sea level of the slope of the stream valley walls.

Hydraulic Properties of the Rocks

The hydraulic properties of the various rock types control the occurrence and movement of ground water in the study area. Ground-water withdrawals are primarily from a fresh-water lens system that occurs in the dike-free volcanic rocks outside of the dike-intruded rift zones. Some rocks effectively impede ground-water flow, creating barriers to flow and areas of steep hydraulic gradient.

Hydraulic Conductivity

Hydraulic conductivity is a quantitative measure of the capacity of a rock to transmit water. Hydraulic conductivity is the constant of proportionality in Darcy's law, which relates specific discharge (discharge per unit area) to the hydraulic gradient:

$$v = -K(dh/dl), \quad (1)$$

where

$$v = \text{specific discharge [LT}^{-1}\text{]},$$

$$K = \text{hydraulic conductivity [LT}^{-1}\text{]}, \text{ and}$$

$$dh/dl = \text{hydraulic gradient [LL}^{-1}\text{]}.$$

Darcy's law generally is assumed applicable to regional ground-water flow analyses in Hawai'i (Souza and Voss, 1987; Gingerich and Voss, 2005; Oki, 2005b).

Rock hydraulic conductivity can be qualitatively described by permeability. Permeability describes the ease with which fluid can move through rock. The permeability of volcanic rocks is variable and depends on many factors, including the mode of emplacement and amount of weathering. Lava viscosity and topography also can affect permeability. Thicker flows generally are less permeable and form from highly viscous lava or on flat topography (Gingerich and Oki, 2000).

Dike-Free Volcanic Rocks

The permeability of the subaerial, shield-building, dike-free lava flows in the study area generally is high. The main elements of lava flows contributing to the permeability are (1) clinker zones associated with 'a'ā flows, (2) voids along the contacts between flows, (3) cooling joints normal to flow surfaces, and (4) lava tubes associated with pāhoehoe flows. The regional horizontal hydraulic conductivity of the dike-free volcanic rocks generally ranges between hundreds and thousands of feet per day (Burnham and others, 1977; Oki, 2005b; Rotzoll and others, 2007; Hunt, 2007) (fig. 8). Because of the high permeability of the dike-free volcanic rocks, horizontal water-table gradients in these rocks are small (about 1 ft/mi). Horizontal hydraulic conductivity in the lava flows may be anisotropic—several times greater parallel to the lava flows than perpendicular to the flows (Nichols and others, 1996, p. A14).

In general, the vertical hydraulic conductivity of the dike-free lava flows may be tens to hundreds of times less than the horizontal hydraulic conductivity. In the Kahului area, Bowles (1970) suggested that horizontal permeability might be as great as ten times vertical permeability on the basis of aquifer tests on stormwater disposal wells. Burnham and others (1977) obtained acceptable results with their numerical model using horizontal hydraulic conductivity 10–100 times the vertical hydraulic conductivity near Kahului. Hunt (2007) used a ratio of horizontal to vertical hydraulic conductivity of 200 to 1 for a numerical modeling study of the Kīhei, Maui, area. Souza and Voss (1987) also estimated the ratio of horizontal to vertical

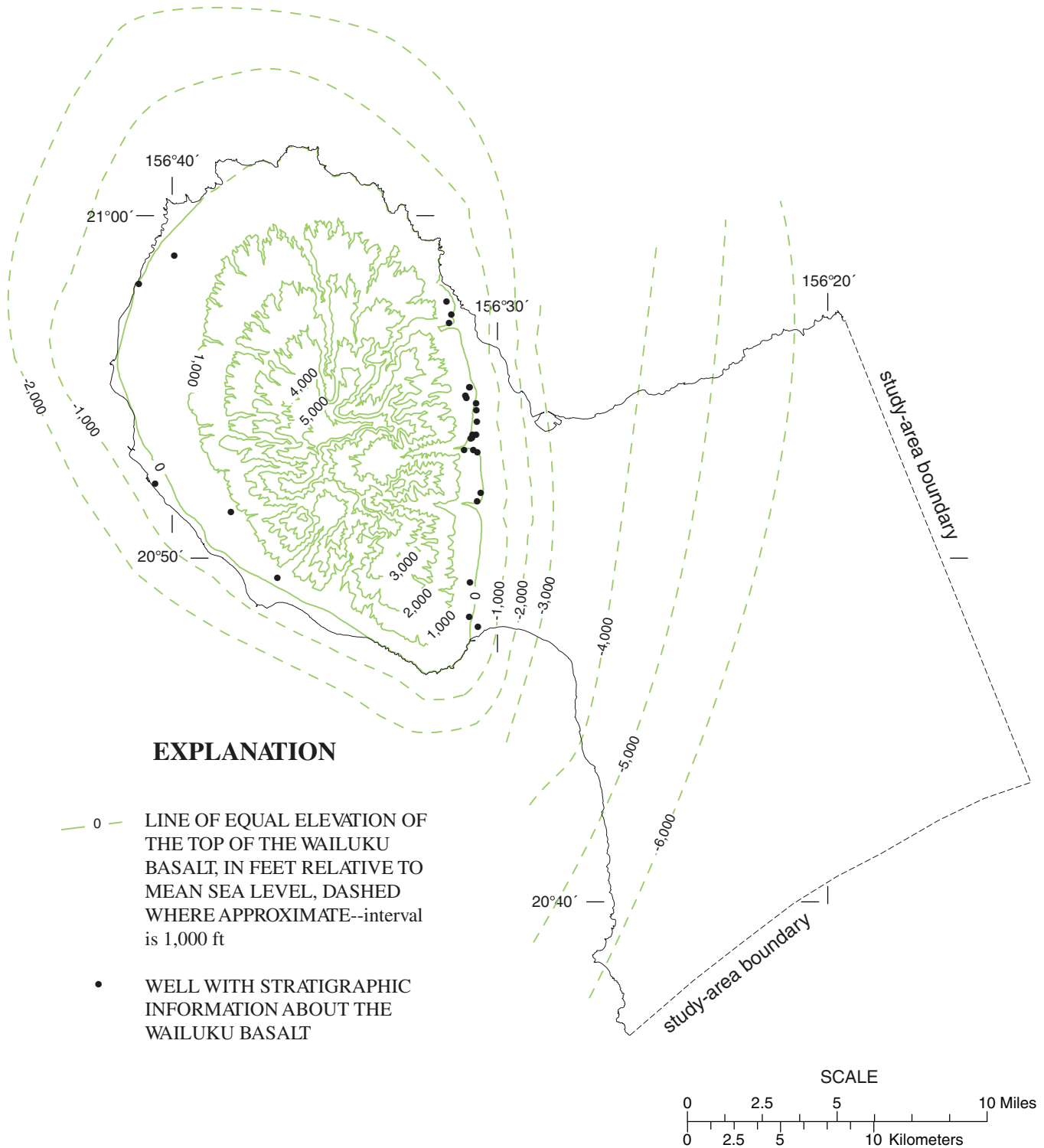


Figure 6. Structural contours on the top of the Wailuku Basalt and locations of wells with stratigraphic information on that unit in central and west Maui, Hawai'i.

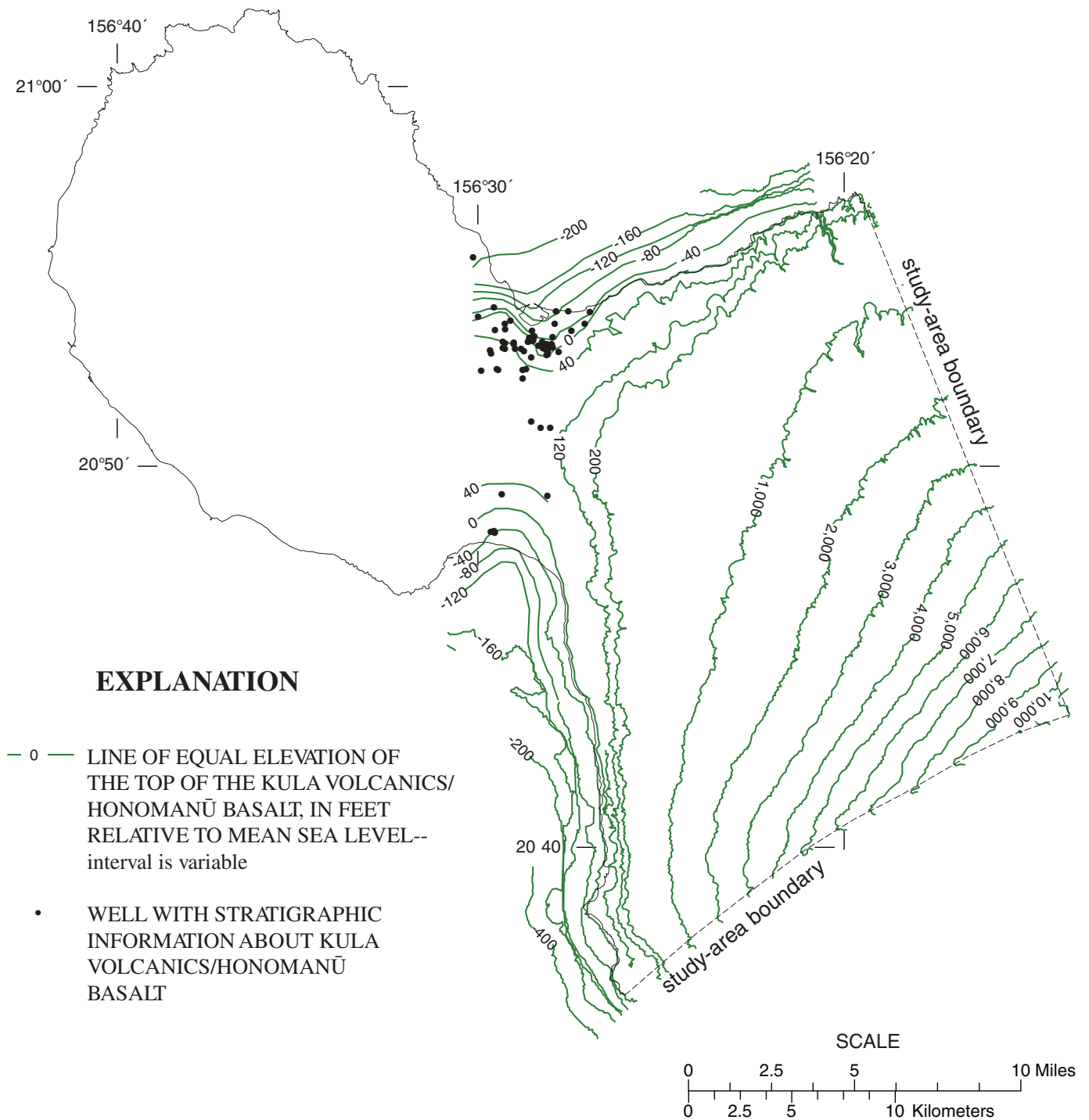


Figure 7. Structural contours on the top of the Kula Volcanics/ Honomanū Basalt and wells with stratigraphic information on those units in central and west Maui, Hawai'i.

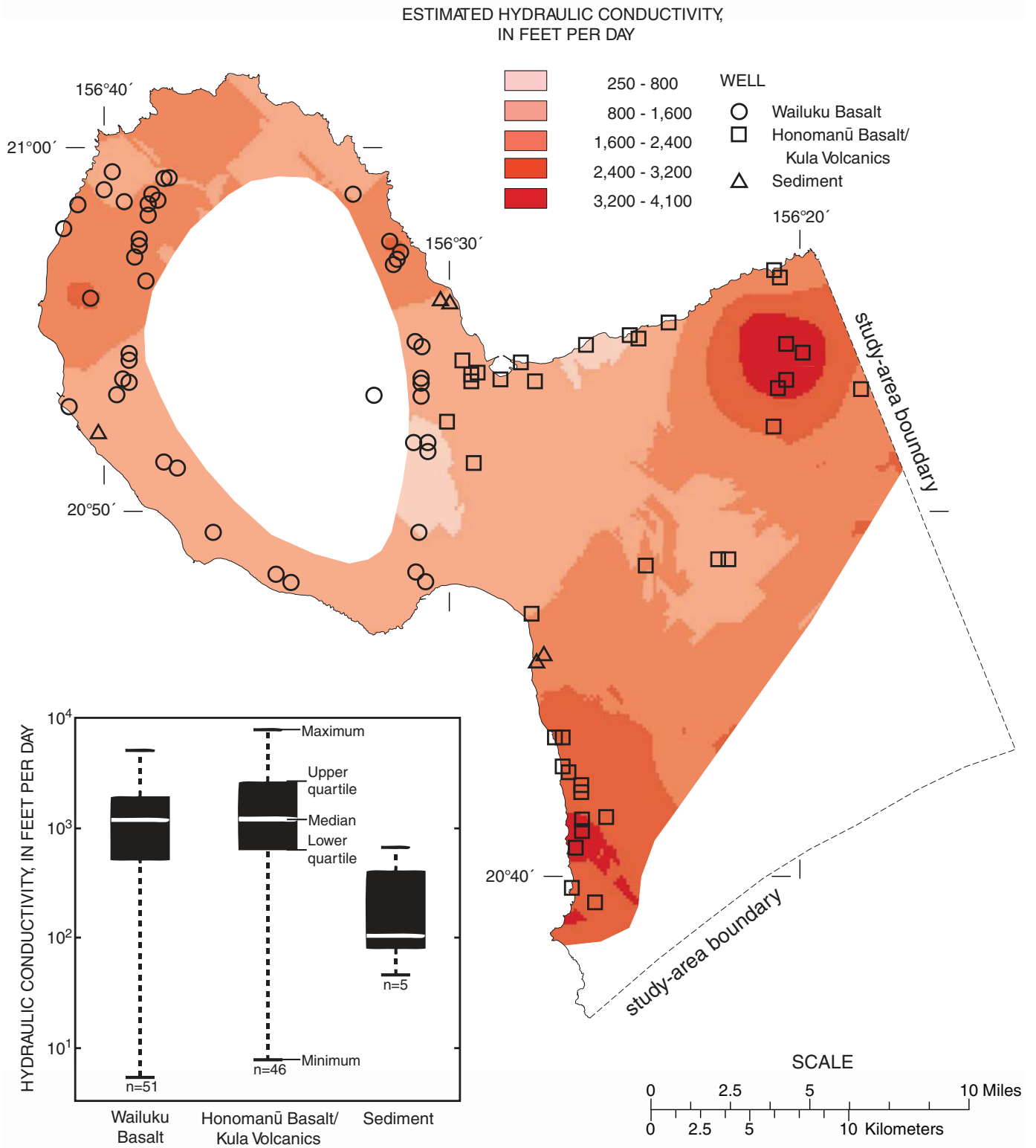


Figure 8. Distribution of aquifer hydraulic conductivity in central and west Maui, Hawai'i (modified from Rotzoll and others, 2007).

hydraulic conductivity to be 200 to 1 in their modeling study on O'ahu.

Dikes

Intrusive volcanic rocks include those rocks, such as dikes, sills, and stocks, which formed by magma that cooled below the ground surface. Dikes associated with the rift zones of the West Maui and Haleakalā Volcanoes are the dominant intrusive rocks on Maui, and they are most abundant within the central area of the rift zones and the caldera complex. Although the thickness of individual dikes generally is less than 10 ft, dikes are hydrologically significant because of their low permeability and their impounding effect on ground water. Ground-water levels in the interior of the West Maui Volcano may be as high as 3,000 ft above sea level as evidenced by tunnels tapping dike compartments (Stearns and Macdonald, 1942, p. 195).

In general, the average hydraulic conductivity of a rift zone decreases as the number of dike intrusions within the rift zone increases. In addition, hydraulic conductivity is expected to be higher in a direction along the strike of the dikes rather than perpendicular to the strike. Rotzoll and others (2007) report a hydraulic conductivity of about 20 ft/d from an analysis of an aquifer test made on a well in 'Īao Valley in the dike complex. On the basis of a numerical model analysis, Meyer and Souza (1995) suggested that the average effective hydraulic conductivity of a dike complex ranges between about 0.01 and 0.1 ft/d. These values reflect the influence of the intrusive dikes as well as the lava flows between dikes. The hydraulic conductivity of the intrusive dike material was estimated to range between 10^{-5} and 10^{-2} ft/d (Meyer and Souza, 1995).

Weathering

Weathering reduces the permeability of all types of volcanic rocks. The reduction of permeability may be attributed to secondary mineralization that clogs the primary and secondary porosity, or to clays and colloids that precipitate from percolating water (Mink and Lau, 1980). Burnham and others (1977, p. 6) report that the buried lava surface beneath the Kahului area contains a residual clay, indicating a long period of exposure, soil formation, and erosion before burial. On the basis of laboratory permeameter tests on core samples, Wentworth (1938) estimated the hydraulic conductivity of weathered basalt to be between 0.083 and 0.128 ft/d. An injection test conducted in weathered basalt beneath Waiawa Stream valley on O'ahu yielded a hydraulic conductivity of 0.058 ft/d (R.M. Towill Corporation, 1978). Miller (1987) used the water-retention characteristics of core samples collected beneath central O'ahu pineapple fields to estimate the saturated hydraulic conductivity of saprolite and found values ranging between 0.0028 and 283 ft/d. The wide range of hydraulic-conductivity values estimated by Miller was attributed to the variability in secondary porosity among samples.

Sedimentary Rocks

The sediments of greatest hydrologic significance, because of their relatively low permeability, are the older

consolidated alluvial deposits, which were created during the period of extensive erosion that carved deep valleys in the original volcanoes. These deposits are in deeply incised valleys and beneath the isthmus of Maui. The low permeability of consolidated alluvial deposits is caused by a reduction of pore space from the volume increase associated with weathering as well as from mechanical compaction (Wentworth, 1951). Wentworth (1938) estimated the hydraulic conductivity of three weathered alluvium samples from O'ahu with the use of a laboratory permeameter. Two of the samples had a hydraulic conductivity of less than 0.013 ft/d, and the third sample had a hydraulic conductivity of 1.08 ft/d. Eight samples classified as alluvium, without reference to weathering, produced a range of hydraulic conductivity between 0.019 and 0.37 ft/d (Wentworth, 1938).

The sedimentary deposits and underlying weathered volcanic rocks of the stream valleys, isthmus, and coastal plains form a low-permeability confining unit, called caprock, which overlies high-permeability volcanic rocks and impedes the seaward discharge of freshwater and the movement of water between the West Maui Volcano and Haleakalā volcanic-rock aquifers. Although the permeability of the various components of the caprock may vary widely, from low permeability in older alluvium and saprolite to high permeability in buried coral reef deposits and sand dunes, overall the caprock has lower regional permeability than the volcanic-rock aquifers. Rotzoll and others (2007) show a range of about 30–650 ft/d in hydraulic conductivity estimates from five aquifer tests in sediments of central Maui. Souza and Voss (1987) modeled a vertical cross section of the Pearl Harbor ground-water area on O'ahu and estimated a caprock hydraulic conductivity of 0.15 ft/d. In their analysis, Souza and Voss treated the caprock as a homogeneous and isotropic unit, although significant heterogeneity may exist (Oki and others, 1998). Little information about the anisotropy or vertical hydraulic conductivity of the caprock is available. Burnham and others (1977) modeled a clay layer overlying the volcanic-rock aquifer beneath Kahului using a range of vertical hydraulic conductivities between about 1 and 10 ft/d. Valley-fill deposits on O'ahu were modeled with horizontal and vertical hydraulic conductivities ranging from 0.058 to 30 ft/d (Oki, 1998; 2005b).

Specific Storage and Effective Porosity

The effective porosity and specific storage of the rocks forming an aquifer affect the timing and amount of the water-level response to natural or human-induced changes. The effective porosity represents that part of the total rock porosity that contributes to flow, and specific storage is a measure of the compressive storage of the rocks and fluid. Small values of effective porosity or specific storage result in rapid and relatively large water-level changes in response to changes in pumping or recharge, whereas large values of effective porosity or specific storage result in slower and smaller water-level changes.

Total porosity of a rock is the ratio of the volume of void spaces to the total rock volume. Pore spaces in a layered sequence of lava flows may result from (1) vesicles (small

spaces formed by the expansion of gas bubbles during the solidification of cooling lava), (2) joints and cracks, (3) separations between lava flows, (4) void spaces between fragmented rock, including 'a'a clinker, and (5) lava tubes. Total porosity of the volcanic rocks on O'ahu was measured at different spatial scales using rock samples (Wentworth, 1938; Ishizaki and others, 1967), borehole photographic logging (Peterson and Sehgal, 1974), and density logs from gravity surveys in underground tunnels (Huber and Adams, 1971). Total porosity estimates for volcanic rocks of O'ahu range from less than 0.05 to more than 0.5. Low porosity values may be associated with massive features, including dense flows, 'a'a cores, dikes, and thick lava flows, and high values may be associated with 'a'a clinker zones. Effective porosity, which includes only the hydraulically interconnected pore spaces, may be up to an order of magnitude less than total porosity. Estimates of effective porosity from modeling studies range between 0.04 and 0.10 for volcanic-rock aquifers (Gingerich and Voss, 2005; Oki, 2005b; Hunt, 2007). Rotzoll and others (2007) analyzed aquifer-test data from wells in central Maui and estimated specific storage and specific yield from one test to be 2.0×10^{-6} ft⁻¹ and 0.07, respectively.

Dispersion Characteristics

Freshwater mixing with underlying saltwater in an aquifer creates a transition zone of brackish water. The extent of mixing in an aquifer depends on several factors, including the ground-water velocity and the aquifer dispersivity. High values of dispersivity, all other factors being equal, result in greater mixing. Dispersivity values generally are larger in the (longitudinal) direction of flow relative to directions transverse to flow and may be controlled by aquifer anisotropy. Few reported dispersivity values are available for volcanic-rock aquifers. Meyer and others (1974) estimated the dispersivity to be about 200 ft for the volcanic-rock aquifer in the Honolulu, O'ahu, area, and this value likely represents a longitudinal dispersivity. Using a cross-sectional numerical model, Souza and Voss (1987) estimated the longitudinal and transverse dispersivities of the Pearl Harbor area, O'ahu, to be 250 and 0.82 ft, respectively. Liu (2005) estimated vertical dispersivity values ranging between 0.4 and 2.1 ft from salinity profiles measured in deep monitor wells throughout the Pearl Harbor area, O'ahu.

Ground-Water Flow System

Fresh ground water moves mainly from inland recharge areas to coastal discharge areas, where springs and seeps exist above and below sea level. Eastward flowing water from West Maui Volcano converges with westward flowing water from Haleakalā in the central isthmus, and the water then flows to discharge areas near the northern and southern coasts (Tenorio and others, 1970; Takasaki, 1972). Fresh ground water in the

Wailuku area is mainly in freshwater-lens systems and dike-impounded systems (Yamanaga and Huxel, 1970; Takasaki, 1972; Meyer and Presley, 2001).

Freshwater Lens

Currently, one of the most important sources of fresh ground water on Maui is from the freshwater lens in dike-free volcanic rocks in the 'Īao aquifer area (fig. 9). The main ground-water system in this area consists of a lens-shaped freshwater body, an intermediate transition zone of brackish water, and underlying saltwater. Several geologic features form boundaries of the freshwater-lens system or impede ground-water flow within the system. Features that form boundaries of the freshwater-lens system include dikes in the interior of West Maui Volcano; features that may impede flow within the system include valley-fill barriers and the coastal sedimentary caprock that thickens in a seaward direction.

The freshwater lens in the study area forms because of the density difference between freshwater and underlying saltwater. The thickness of the lens can be estimated using the Ghyben-Herzberg relation (for example, Freeze and Cherry, 1979). The relation assumes that freshwater and saltwater do not flow or mix. Although freshwater and saltwater do flow and mix in actual freshwater-lens systems, the Ghyben Herzberg relation can be used where the flow is primarily horizontal to estimate the depth at which salinity is about 50 percent that of sea water. For these conditions, the freshwater-lens thickness below sea level is directly proportional to the height of the top of the freshwater above sea level. In principle, at a place where the water table stands 1 foot above sea level, for example, 40 feet of freshwater will be below sea level, and the freshwater lens will thus be 41 feet thick. This relation exists because the ratio of the density of salt water to fresh water is 41:40. In the dike-free volcanic rocks of the Wailuku area, freshwater mixing with underlying saltwater creates a brackish-water transition zone that may be hundreds of feet thick. (For the purposes of this report, brackish water has salinity that ranges between greater than 2-percent and less than 100-percent seawater salinity.)

The water table in the dike-free volcanic rocks is less than a few tens of feet above sea level. In general, the water-table altitude in the dike-free volcanic rocks is lowest near the coast and increases landward at a rate of about 1 ft/mi, although local variations may exist near areas of converging flow caused by pumping from wells. Although freshwater flow is predominantly horizontal in the dike-free volcanic rocks, the flow may have an upward or downward component in some areas.

The lower permeability sedimentary caprock between West Maui Volcano and Haleakalā is a confining unit that impedes the flow of fresh ground water between the Wailuku area and the Haleakalā lavas in the isthmus and also ground-water discharge to the coast. The caprock extends offshore, beyond the seaward extent of the freshwater lens. The freshwater-lens system in the

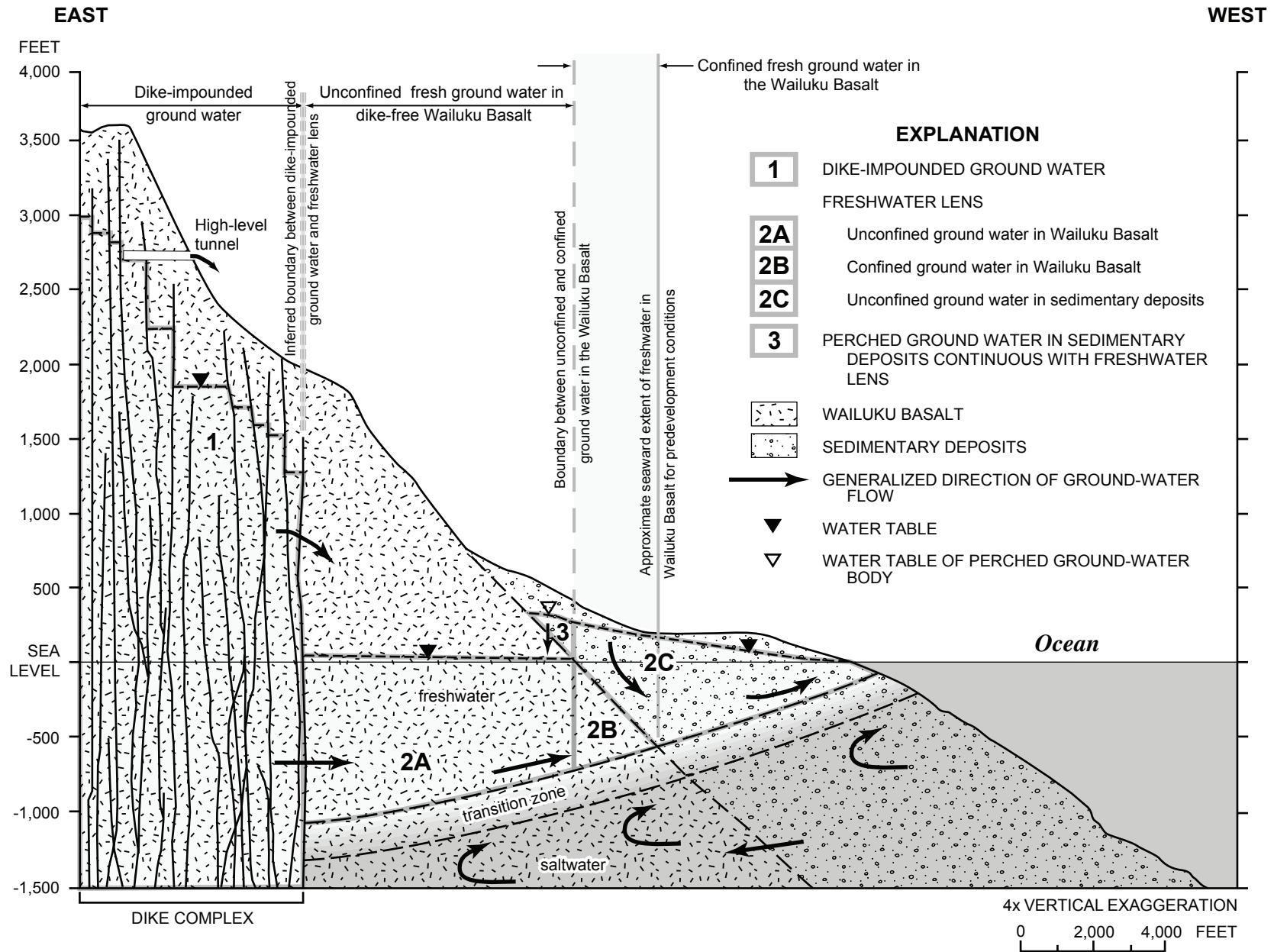


Figure 9. Geologic cross section of the 'Iao aquifer area, showing ground-water occurrence and movement, Maui, Hawai'i (from Meyer and Presley, 2001).

dike-free volcanic rocks is mainly unconfined inland from the caprock. Within the caprock, the freshwater lens is unconfined.

The lower permeability valley-filling sediments likely impede the flow of ground water to the north and south. Water levels often are an indicator of a low-permeability barrier to flow if abrupt differences in ground-water levels are found on either side of the suspected hydrologic barrier. The presence of valley-fill barriers in the ʻĪao area was first postulated by Cox (1951, p. 6), who cited a 3-ft difference between the head north and south of ʻĪao Valley and a much greater head drop (18 ft) from just south of ʻĪao Valley to south of Waikapū Valley. Later, drilling on the north side of Waikapū Stream revealed a head difference of about 4 feet between the Waikapū 1 (5130-01) and Waikapū 2 (5130-02) wells located about 1,600 ft apart but not near any known hydrologic feature. Mink and Lau (1990) subsequently located the boundary separating the ʻĪao and Waikapū Aquifer Systems between these two wells rather than along Waikapū Valley. Water-level differences between these wells and wells closer to ʻĪao Stream were 4 to 7 ft, also indicating that some type of hydrologic barrier is located in this area but not one necessarily corresponding to the surface expression of the current Waikapū Valley. Water levels drop more than 5 ft from south to north across Waiheʻe Valley, indicating that the valley-filling sediments here also are a partial barrier to flow.

A saltwater-circulation system exists beneath the freshwater lens. Saltwater flows landward in the deeper parts of the aquifer, flows upward, and then mixes with seaward-flowing fresher water (fig. 9). This mixing creates the brackish-water transition zone. When water is pumped from the freshwater lens system, water levels will decrease and the transition zone will rise until a new equilibrium is reached between the amount of recharge to the system and the amount of discharge to wells and the coast. In the ʻĪao/Waiheʻe Aquifer Systems, the coastal caprock that impedes the discharge of freshwater also impedes the flow of ocean water into the aquifer. This causes the balance between fresh and salt water to be out of equilibrium for tens of years as ocean water moves slowly into the aquifer to balance the freshwater that has been removed. Hence, the midpoint of the freshwater lens is deeper than would be expected by assuming the Ghyben-Herzberg principle. Only after a new equilibrium is reached will the depth of the midpoint of the transition zone be about 40 times the head at the water table.

Dike-Impounded System

Dike-impounded systems are found near the caldera and rift zones of the volcanoes, where low-permeability dikes have intruded other rocks. Near-vertical dikes tend to compartmentalize areas of permeable volcanic rocks. Dikes impound water to heights as much as 3,000 ft above sea level in the interior of West Maui Volcano, as evidenced by tunnels tapping dike compartments (Stearns and Macdonald, 1942, p. 195). In some stream valleys, where extensive erosion exposed dike compartments, ground water discharges directly to streams.

Nevertheless, the evidence supplied from gaining streams, ground-water tunnels, and wells indicate that ground water is impounded to high levels. The extent of the dike-impounded water body is inferred from the dikes exposed in valley walls, tunnels, and water levels in wells (Yamanaga and Huxel, 1969, fig. 6; 1970, fig. 7). No data from wells are available for determining the depth to which freshwater extends below sea level within the dike-impounded system. Where erosion or tunneling extends to below the water level in the stream valleys, ground water discharges directly to the streams as base flow. Fresh ground water that does not discharge to streams or tunnels or is not withdrawn from wells in the dike-impounded system flows to downgradient areas in the freshwater-lens system. Although preferential flow to downgradient areas in some parts of the West Maui Volcano is likely, no evidence is available indicating where these areas might be.

Recharge

Ground-water recharge generally is greatest in the inland mountainous regions, where rainfall is highest, but the plantation-scale sugarcane cultivation (and, to lesser degrees, pineapple and macadamia nuts) have profoundly affected the amount and location of recharge to the ground-water system in agricultural areas (Engott and Vana, 2007). Since the early 20th century, about 100 billion gallons of surface water has been diverted each year from island streams for crop irrigation within the study area. More than half of this diverted water, about 59 billion gallons per year, originates outside the study area, in east Maui. Under natural conditions, most stream water would flow to the ocean; instead, stream water diverted for irrigation is applied to the plant-soil system, creating an artificial increase in ground-water recharge.

Irrigation rates in the study area have been steadily decreasing since the 1970s, when large-scale sugarcane plantations began a conversion from furrow to more-efficient drip irrigation methods and began reducing the acreage dedicated to sugarcane production. However, stream diversions were not reduced during this period. During 1979–2004, agricultural land use decreased about 21 percent, mainly because of decreased sugarcane acreage. During the same period, on the leeward (west) side of West Maui Mountain, sugarcane cultivation ceased altogether. Decreasing irrigation coincided recently with periods of below-average rainfall, leading to substantially reduced recharge rates in many areas.

Engott and Vana (2007) used a daily water-budget method to estimate ground-water recharge during six periods as part of this study. Their mass-balance procedure accounted for water entering (rainfall, irrigation, and fog drip), leaving (runoff, evapotranspiration, and ground-water recharge), and being stored within the plant-soil system. Estimated recharge for central and west Maui declined 44 percent during the period 1926–2004. The period 1926–79 had the highest estimated recharge. Recharge from irrigation during this period was at least 50 percent higher than in any other period considered. The

period 2000–04 had the lowest estimated recharge. Recharge from irrigation during this period was 54 percent of recharge from irrigation during 1926–79, and rainfall was the lowest of any period.

The spatial recharge distributions over the period 1926–2004 (fig. 10) indicate several patterns: (1) changes in agricultural land use resulted in corresponding changes in recharge distribution; (2) the reduction in sugarcane irrigation rates resulted in less pronounced differences between the recharge rates of adjacent sugarcane and non-sugarcane lands; (3) in nonagricultural areas, the spatial recharge distributions varied according to the amount and spatial distribution of rainfall; and (4) in agricultural areas, the spatial recharge distribution varied with the rainfall and irrigation distribution.

Recharge from Streams

Downstream from the area of dike-impounded water, where the water table of the freshwater-lens system is below the streambed, potential exists for streamflow infiltration to recharge the freshwater-lens system. The only water flowing in these diverted streams is runoff immediately after rainfall, because at other times all low flow is captured by the diversion ditches for irrigation. The water budget estimates (Engott and Vana, 2007) calculated for this study did not account for historical recharge through streambed seepage, because streams were dry most of the time. In the future, some streams may be fully or partially restored to natural flow conditions, potentially changing future recharge. The report by Engott and Vana (2007) did include an estimate of recharge assuming no irrigation, but did not include the effects on recharge of restoring all streamflow. For this report, the effects of restored streamflow on recharge were investigated for only the Wailuku Aquifer Sector, because data were unavailable elsewhere.

Most water diverted from Waikapū, 'Īao, and Waiehu Streams and Waihe'e River is transported to the isthmus and used for irrigation outside the area contributing recharge to the Wailuku Aquifer Sector. This causes a net decrease in recharge to the Wailuku Aquifer Sector because of a lack of seepage through the streambeds of these four streams. The potential amount of water that is lost recharge from streambeds of these four streams can be estimated using gaging station and flow measurement data (table 1). Seepage-loss measurements were made in losing sections of the four streams during periods when streamflow was being returned to the stream or was overtopping the diversion. The flow measurements and the length of stream channel between measurements were used to calculate stream loss, in gallons per day per foot of stream channel (fig. 11). Estimates of loss rate for the same stream reach on different days were averaged, and these average rates were extrapolated to nearby reaches on the same stream where flow measurements were not available. The estimate of total streamflow loss at undiverted streamflow conditions, which becomes recharge to the underlying ground-water system, is about 12.3 Mgal/d (table 1). Streamflow-loss estimates for the individual streams are: Waihe'e River, 1.3 Mgal/d; Waiehu

Stream, 2.7 Mgal/d; 'Īao Stream, 5.5 Mgal/d; Waikapū Stream, 2.8 Mgal/d. Waikapū Stream has the potential to lose more than 7 Mgal/d at high flows, but the average diverted flow is only about 2.8 Mgal/d; therefore 2.8 Mgal/d is the maximum flow that could infiltrate on an average basis.

Discharge

Discharge from the study area is in the form of ground-water withdrawals from pumped wells, discharge to streams as base flow, and diffuse seepage to the ocean. Withdrawals from pumped wells and base flow in streams have been measured in most locations, although records are incomplete for some periods and locations. Diffuse seepage to the ocean has not been measured.

Withdrawals from Wells

Withdrawals from dug wells in the study area began after 1894 and increased substantially after the first Maui-type skimming shaft was constructed in 1900 (Stearns and Macdonald, 1942). Reported withdrawals were compiled from published records (Stearns and Macdonald, 1942; Yamanaga and Huxel, 1969, 1970; Takasaki, 1972; Meyer and Presley, 2001), information contained in USGS files (unpub. data, USGS Pacific Islands Water Science Center data files), and a CWRM digital database (unpub. data, 2007). Stearns and Macdonald (1942) present withdrawal records from individual wells starting in 1902. Earlier withdrawal records are not available. During the early period of ground-water development, most of the water used was for sugarcane cultivation in the central isthmus and the Lahaina area.

Ground-water withdrawals from the Central Aquifer Sector increased steadily and peaked in the 1960s and 1970s before declining in the 1980s (fig. 12). During 1902–49, withdrawals averaged about 70 Mgal/d, all from the Pā'ia and Kahului Aquifer Systems. During 1950–79, average withdrawals increased to about 168 Mgal/d. After the 1970s, average withdrawals began declining and spreading out into the Makawao and Kama'ole Aquifer Systems. During 1980–1999, average ground-water withdrawal from the Central Aquifer Sector was 107 Mgal/d. During 2000–06, average withdrawals decreased to about 68 Mgal/d. The CWRM sustainable yield estimate for the Central Aquifer Sector is 27 Mgal/d (State of Hawaii, 1990).

Ground-water withdrawals (fig. 13) from the freshwater lens in the Wailuku Aquifer Sector did not begin until 1948, when Shaft 33 (5330-05) (fig. 4.) was built above Wailuku. During 1948–69, most of the average withdrawal of 5 Mgal/d, exclusively in the 'Īao Aquifer System, was for sugarcane irrigation. Pumping increased during the 1970s through the 1990s and peaked in the 2000s with all of the water pumped after 1984 for public supply (Meyer and Presley, 2001, table 4). Average withdrawals from the 'Īao Aquifer System during these decades were as follows: 1970–79, 13.5 Mgal/d; 1980–89, 12.7 Mgal/d; 1990–99, 19.3 Mgal/d; and 2000–06, 21.4 Mgal/d. Withdrawal

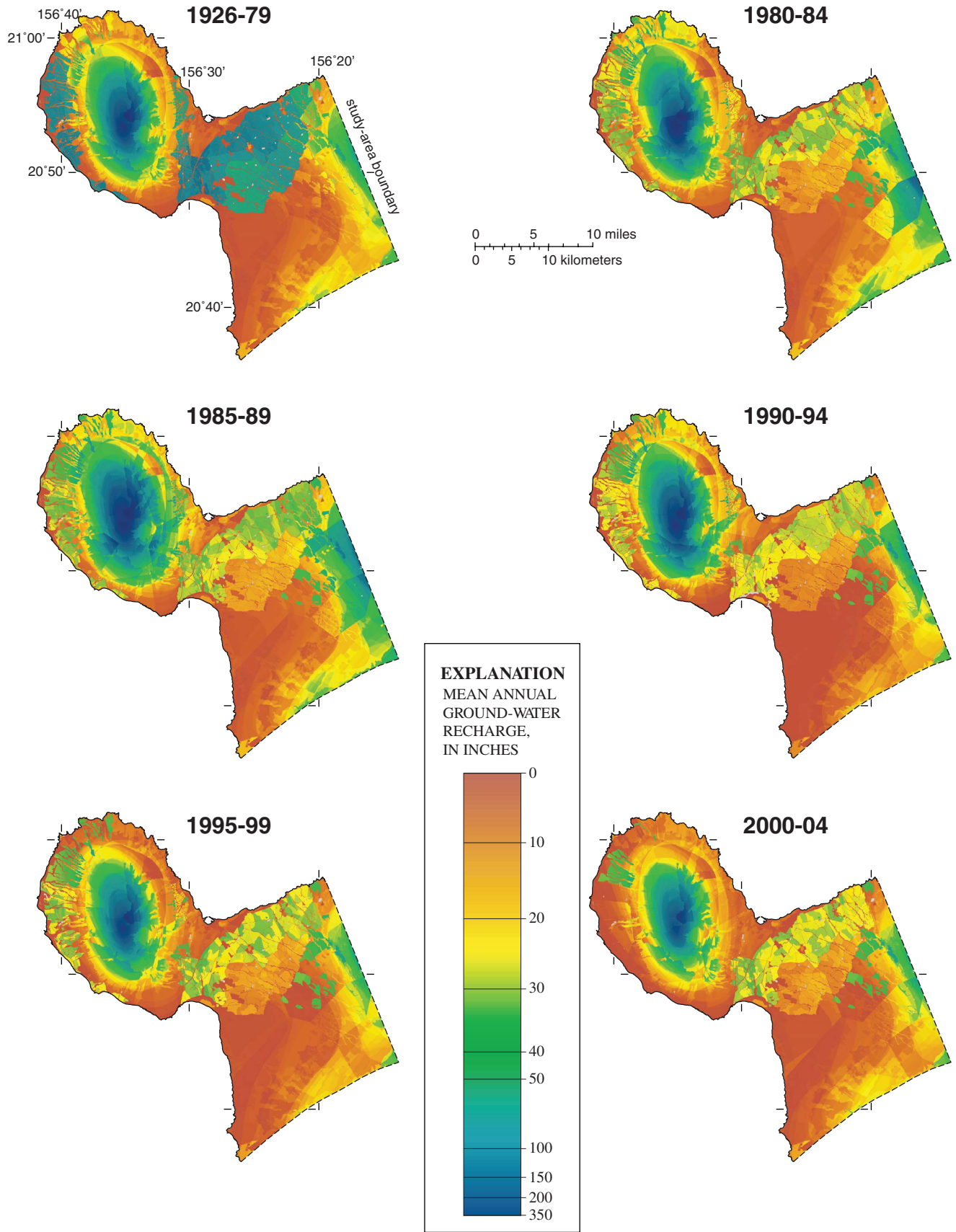


Figure 10. Estimated ground-water recharge for various periods during 1926–2004, central and west Maui, Hawai'i (modified from Engott and Vana, 2007).

Table 1. Streamflow loss measurements and estimates in Waikapū, Īao, and Waiehu Streams and Waihe'e River, Maui, Hawai'i

[Mgal/d, million gallons per day; ft, feet; gal/d, gallons per day; USGS PIWSC, U.S. Geological Survey Pacific Islands Water Science Center; Waikapū-lower total estimated loss rate is the average flow of the stream at the diversion minus the total estimated loss rate of the Waikapū-upper reach]

Stream	Date	Flow at measurement site (Mgal/d)		Streamflow loss (Mgal/d)	Distance between measurements (ft)	Loss per ft of channel length (gal/d/ft)
		Upstream	Downstream			
Waihe'e	12/12/2006	1.61	1.44	0.17	908	187
Waiehu						
North	3/7/2007	2.21	1.57	.64	3,036	211
North	3/6/2007	1.68	1.31	.37	2,376	155
North	3/7/2007	1.57	1.30	.27	2,376	114
North	3/6/2007	1.31	0.96	.36	3,415	104
North	3/7/2007	1.30	0.94	.36	3,415	104
South	7/26/2006	1.60 ^a	1.45	.16	1,060	146
South	7/27/2006	1.80	1.45	.35	2,642	132
Lower	3/6/2007	1.23	0.85	.39	5,007	78
Lower	3/7/2007	1.45	1.03	.42	5,007	84
Īao						
Upper	2/11/2008	29.08	26.82	2.26	5,015	451
Upper	2/12/2008	26.11	23.33	2.78	5,015	554
Upper	2/13/2008	23.20	21.72	1.49	5,015	296
Upper	2/14/2008	22.43	19.84	2.59	5,015	516
Upper	2/15/2008	20.71	19.52	1.20	5,015	238
Lower	2/13/2008	8.40	6.79	1.61	7,154	226
Lower	2/14/2008	6.22	4.21	2.01	7,154	281
Waikapū						
Upper	9/6/2006	1.54	1.33	0.21	4,171	50
Upper	5/3/2007	2.48	2.33	0.15	4,171	36
Lower	4/2/2007	4.78	3.64	1.14	7,665	149
Lower	3/18/2004	10.53	4.59	5.95	15,837	375
Lower	3/18/2004	4.59	3.71	0.88	3,068	286

^acombined flow from stream and diversion

Stream	Length of losing reach (ft)	Average loss per ft of channel (gal/d/ft)	Estimated loss rate (Mgal/d)
Waihe'e	7,000	187	1.31
Waiehu-north	7,070	138	0.94
Waiehu-south	7,360	139	1.02
Waiehu-lower	9,390	81	0.76
Īao-upper	8,730	411	3.59
Īao-lower	7,400	253	1.87
Waikapū-upper	10,790	43	0.46
Waikapū-lower	26,570	270	2.38
Total			12.34

began in the Waihe'e Aquifer System in 1997. Presently (2007), no significant withdrawals are reported from the Waikapū and Kahakuloa Aquifer Systems. The CWRM sustainable yield estimate for the Wailuku Aquifer Sector is 38 Mgal/d (State of Hawaii, 1990).

In the Lahaina Aquifer Sector, wells were constructed as early as 1897 but withdrawal records are only available after 1918 (Stearns and Macdonald, 1942, p. 218). Ground-water withdrawals increased steadily during the 1920s and averaged 33 Mgal/d during 1918–29 (fig. 14). During 1930–79, average withdrawals were about 44 Mgal/d, mostly from the Honokōwai and Launiupoko Aquifer Systems. After 1979,

sugarcane irrigation decreased and domestic withdrawals began increasing and spreading into the Honolua Aquifer System. Average withdrawals during 1980–2000 were about 21 Mgal/d. During 2000–06, average withdrawals decreased to about 4 Mgal/d. The CWRM sustainable yield estimate for the Lahaina Aquifer Sector is 40 Mgal/d (State of Hawaii, 1990).

Ground-water withdrawals generally follow a seasonal pattern controlled by the amount of rainfall available for irrigation. During 1995–2006, the withdrawals for domestic uses in the Wailuku Aquifer Sector were highest in July and August and the withdrawals for sugarcane irrigation in the Central Aquifer Sector were highest in September and October (fig. 15).

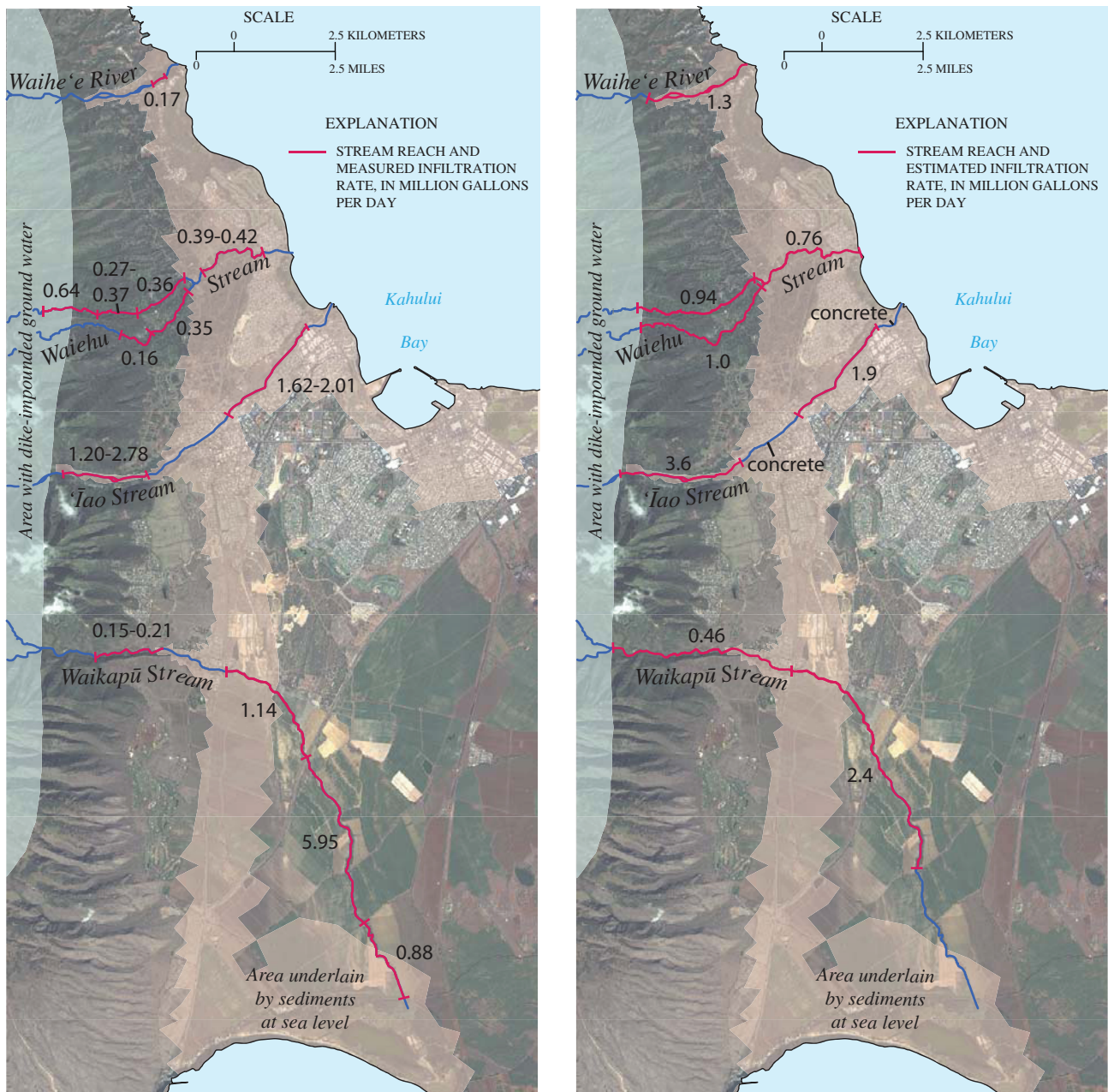


Figure 11. Streamflow loss in Wailuku area streams, Maui, Hawai'i.

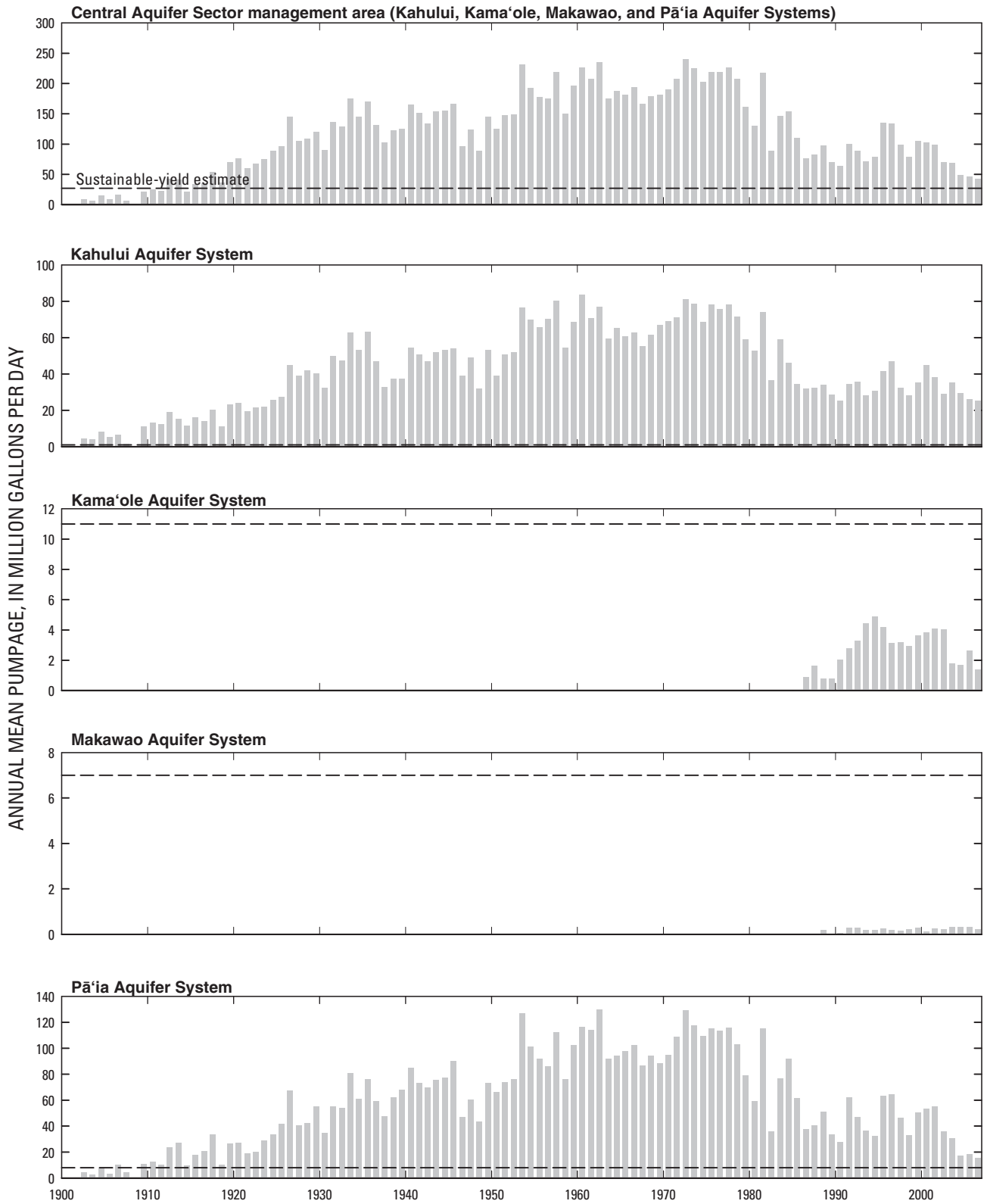


Figure 12. Ground-water withdrawals from the Central Aquifer Sector, 1900–2006, Maui, Hawai'i. Sustainable-yield values (dashed lines; of 2007) are from the State of Hawai'i Commission on Water Resource Management.

Ground-water withdrawals from the sedimentary caprock in Kahului are mainly for landscape irrigation or industry. These withdrawals may total a few Mgal/d, but records of these withdrawals are limited.

Base Flow to Streams

Base flow represents ground-water discharge to streams. Nearly all perennial streams on West Maui Volcano depend on ground-water discharge from the dike-impounded water body for their supply (Stearns and Macdonald, 1942, p. 195). No perennial streams are in the study area on Haleakalā. The base-flow component of streamflow can be estimated from daily streamflow records. Daily streamflow records are available from gaging stations operated on the 14 largest streams on West Maui Volcano by the U.S. Geological Survey (table 2). Some streamflow records are from gaging stations that measured streamflow upstream of any diversion, and others were

reconstructed from records collected on ditches and tunnels diverting the streams of interest. Streamflow from ungaged streams was considered a minor part of the total streamflow and was not included.

The base-flow component of streamflow was estimated using a computerized base-flow separation method described by Wahl and Wahl (1995). Two variables, N (number of days) and f (turning-point test factor) must be assigned values in the method. The method divides the daily streamflow record into nonoverlapping N -day periods and determines the minimum flow within each N -day window. If the minimum flow within a given N -day window is less than f times the adjacent minimums, then the central window minimum is made a turning point on the base-flow hydrograph. Wahl and Wahl (1995) recommend a value of 0.9 for the turning-point test factor for most applications. The value of N , determined independently for each stream, was 4 for all streams in this study.

Because the gaging stations were established at different dates and over varying time lengths, the streamflow records

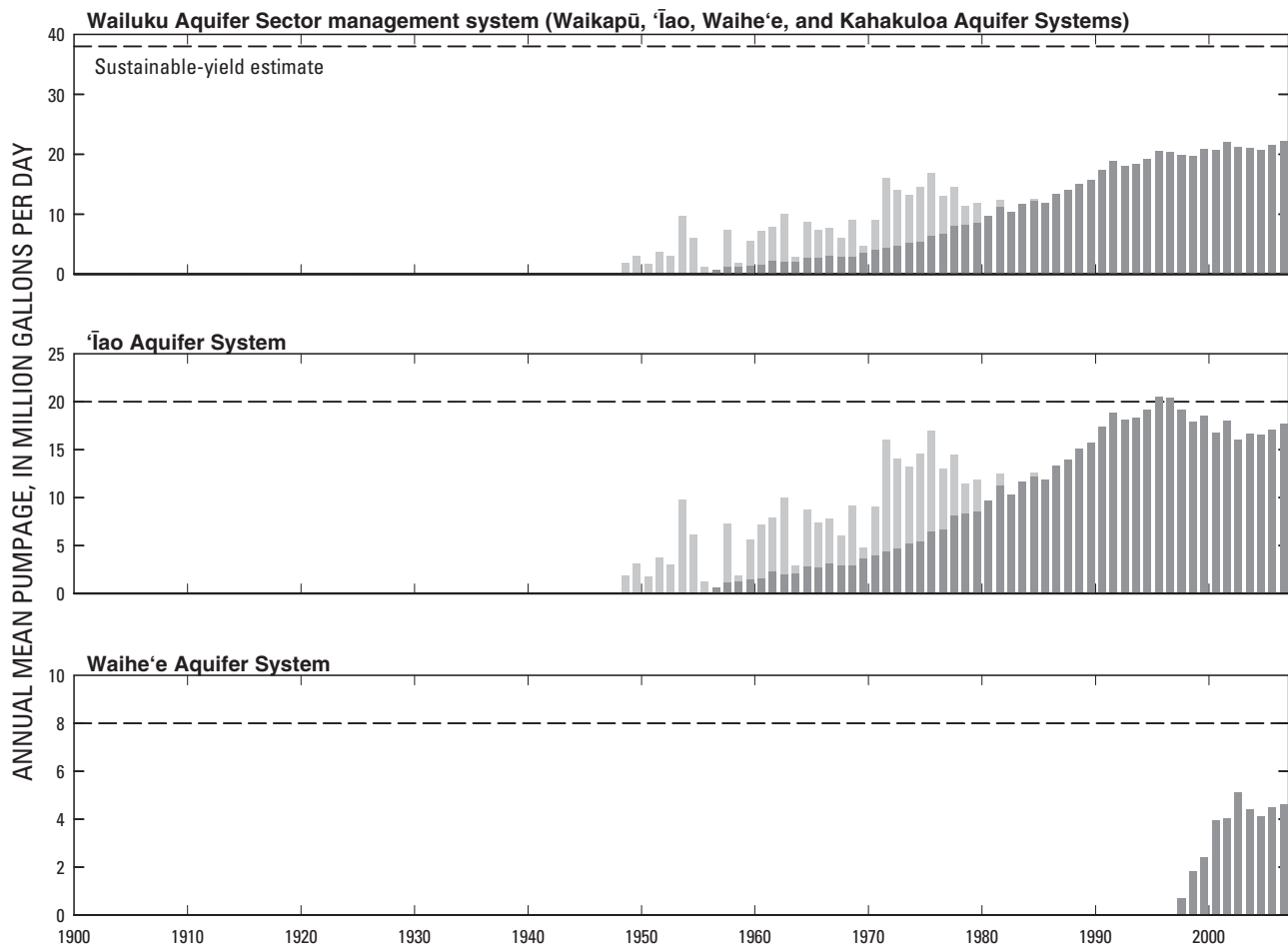


Figure 13. Ground-water withdrawals from the Wailuku Aquifer Sector, 1900–2006, Maui, Hawai'i. Sustainable-yield values (dashed lines; as of 2007) are from the State of Hawai'i Commission on Water Resource Management. No pumpage reported in Waikapū and Kahakuloa Aquifer systems. Pumpage for public supply shown in dark gray.

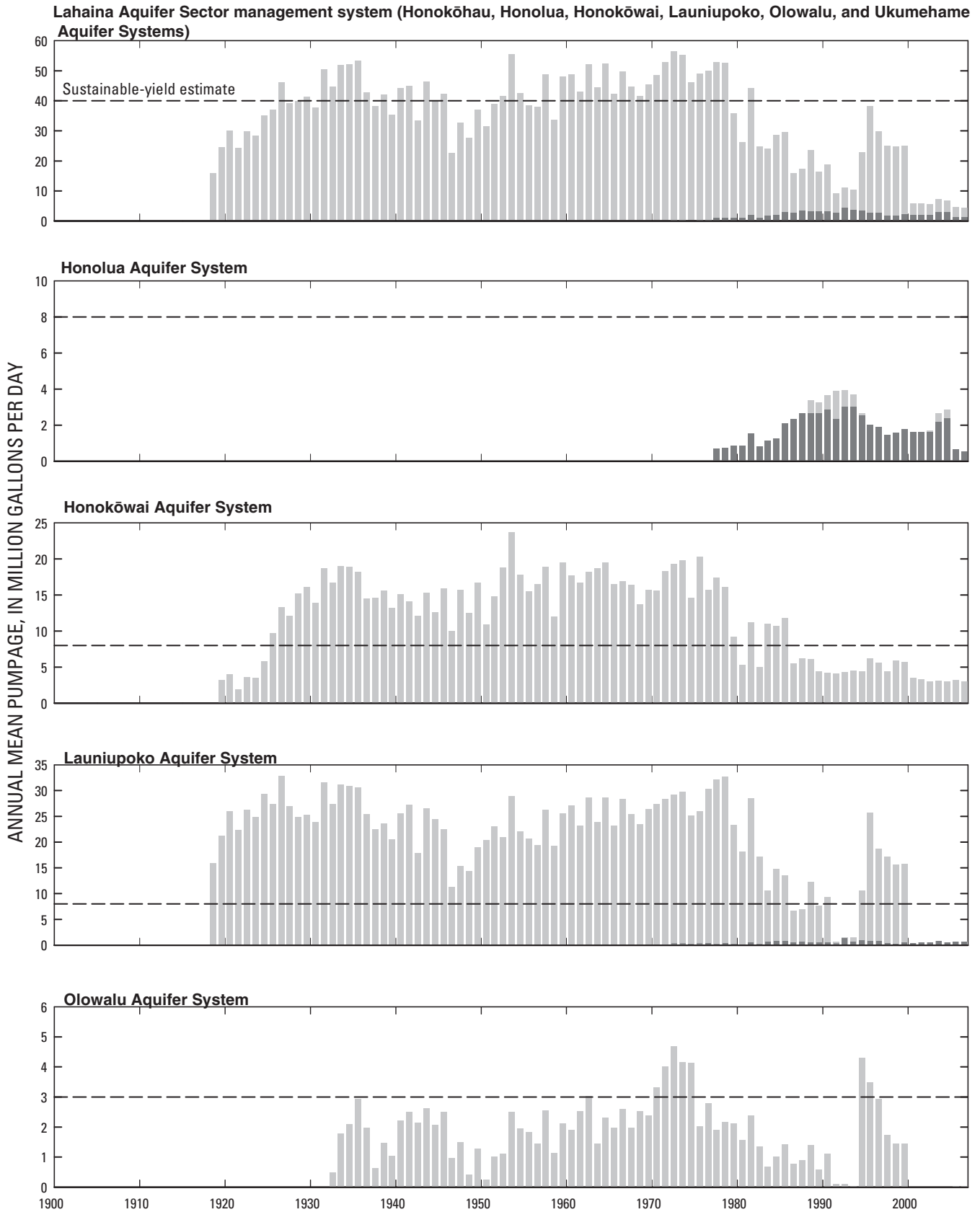


Figure 14. Ground-water withdrawals from the Lahaina Aquifer Sector, 1900–2006, Maui, Hawai'i. Sustainable-yield values (dashed lines; as of 2007) are from the State of Hawai'i Commission on Water Resource Management. No pumpage reported in Honokōhau Aquifer system. Pumpage for public supply show in dark gray.

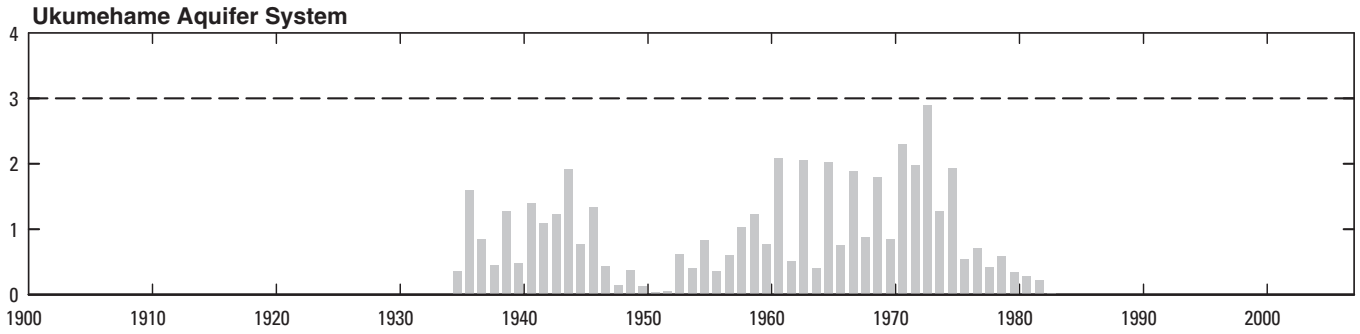


Figure 14.—Continued.

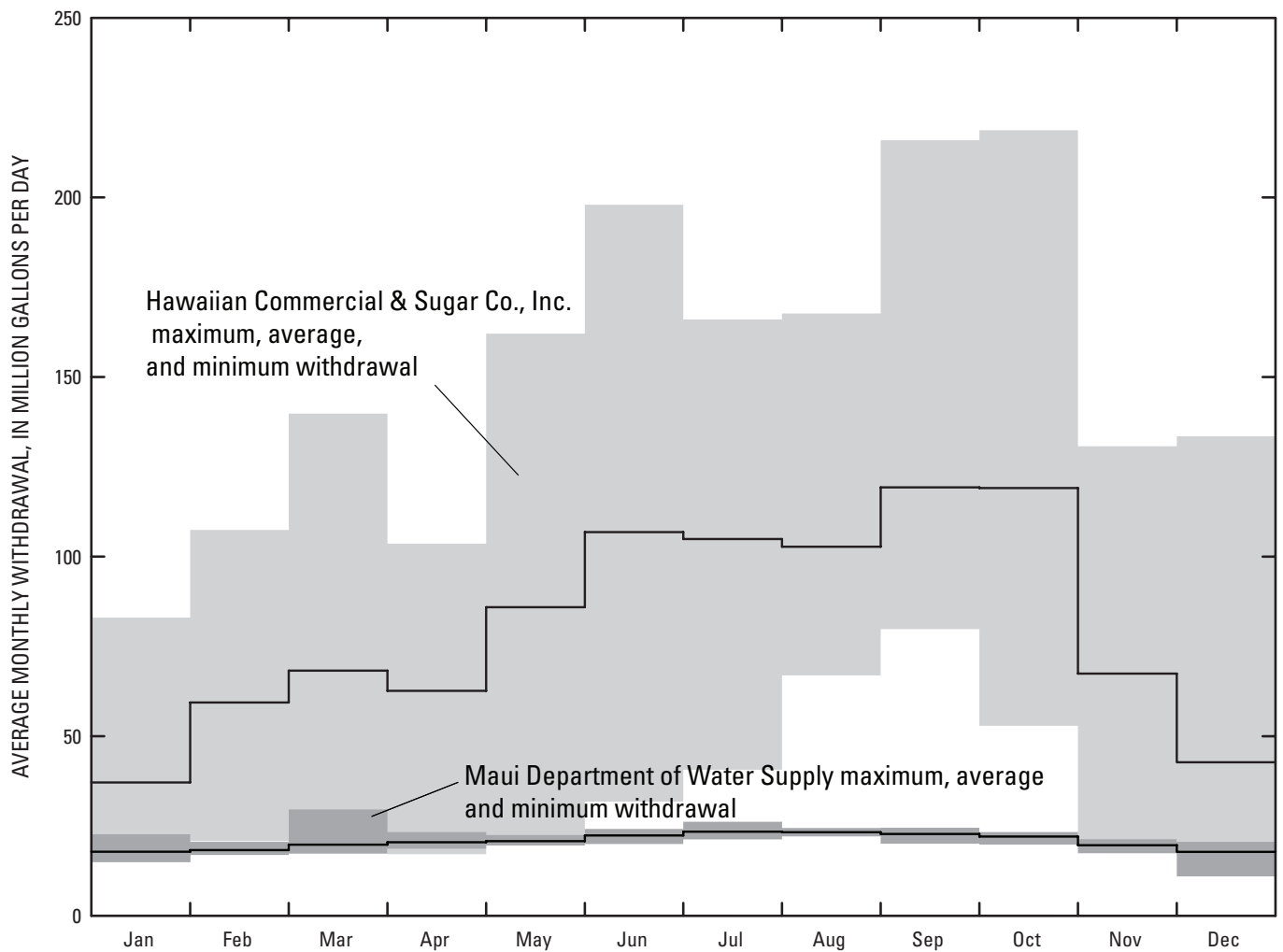


Figure 15. Average monthly ground-water withdrawal for public supply and sugarcane production in the Wailuku and Central Aquifer Sectors, 1995–2006, Maui, Hawaii.

Table 2. Base flow in selected study area streams, Maui, Hawai'i.

[Mgal/d, million gallons per day; index station shown in **bold**; number of days (*N*) in base-flow separation method window is 4 for all streams (Wahl and Wahl, 1995); adjustment factor calculated by dividing the average base flow of Honokōhau Stream during 1913–2005 by the average base flow of Honokōhau Stream during the concurrent period of record]

Stream name	USGS gaging station numbers	Concurrent period of record	Average base flow during concurrent period (Mgal/d)	Adjustment factor	Average base flow adjusted to index station (Mgal/d)	Comments
Waikapū	16648000, 16649000	1913-17	6.9	0.63	4.3	Combined flow in South side Waikapū Ditch and Pālolo Ditch
Īao	16604500	1983-2005	19.	1.05	20.	Flow upstream of Māniania Ditch intake
Waiehu	16610000	1913-17	4.8	0.63	3.1	Flow in South Waiehu Stream
Waihe'e	16614000	1983-2005	30.	1.05	32.	Flow upstream of Waihe'e Ditch intake
Kahakuloa	16618000	1939-43, 1947-70, 1974-2005	4.5	1.03	4.6	
Honokōhau	16620000	1913-2005	12.3	1.00	12.3	Flow upstream of Honokōhau Ditch
Honolua	16623000	1913-17	1.5	0.64	1.0	Flow upstream of Honolua Ditch
Honokōwai	16629000	1913-67	3.7	.96	3.6	Flow in Honokōwai Ditch
Kahoma	16633000, 16634000	1913-17	5.3	.64	3.4	Combined flow from Kahoma Stream and tunnel
Kanahā	16636000	1916-32	2.9	.92	2.7	Flow upstream of pipeline intake
Kaua'ula	16641000	1914-17	6.8	.61	4.1	Flow upstream of Kaua'ula Ditch
Launiupoko	16644000	1913-17	1.1	.63	0.7	Flow upstream of diversion intake
Olowalu	16645000	1913-67	3.7	.96	3.6	Flow in Olowalu Ditch
Ukumehame	16647000	1913-19	5.2	.74	3.9	
Total average base flow					101.	

were adjusted to a concurrent period using gaging station 16620000 (Honokōhau Stream near Honokōhau, Maui) as an index station that operated throughout the period of record (1913–2005). The average base flow from the index station streamflow record determined over the entire period that the index station was operated was divided by the average base flow from the index station streamflow record, determined for the concurrent period for the gaging station to be adjusted. This adjustment factor ranges between 0.61 and 1.05 for the selected gaging stations (table 2). The base flow from the selected gaging station was multiplied by the appropriate adjustment factor, determining the base flow adjusted to the concurrent period for the selected gaging station. Adjusted base flow values range from 0.67 Mgal/d in Launiupoko Stream to 32 Mgal/d in Waihe'e River (table 2). Total average base flow during 1913–2005 from the 14 gaged streams was about 101 Mgal/d.

Sixteen tunnels were constructed during 1900–26 to increase streamflow by developing water from the dike-impounded water body in West Maui Volcano (Stearns and Macdonald, 1942, p 195). Little evidence is available to determine whether these tunnels increased streamflow by capturing additional water not discharging to any stream or if they just redistributed streamflow by capturing water that would eventually discharge into the streambed farther downstream.

Water Levels

Ground-water flow directions commonly are inferred from ground-water levels measured in wells. Ground-water levels also are an indicator of changes in recharge or withdrawals from the ground-water system, and can be an indicator of freshwater-lens thickness. In the study area, ground-water levels vary spatially (horizontally and vertically) and temporally.

In general, measured water levels in the study area are lowest near the coast. Water levels increase inland toward the recharge areas of West Maui and Haleakalā Volcanoes (Yamanaga and Huxel, 1969, 1970; Takasaki, 1972; Souza, 1981; Meyer and Presley, 2001). On December 5, 1970, a ground-water-level survey was made in the central Maui isthmus area after wells were shut off for 10 days (Takasaki, 1972, fig. 12). Water levels measured in the 1970 survey ranged between 3.2 and 17.7 ft above mean sea level (fig. 16). An additional synoptic water-level survey was completed on May 17, 2005, on 38 wells as part of this study by the USGS with the assistance of staff from the County of Maui DWS, Hawaiian Commercial and Sugar Co., and the State of Hawai'i CWRM (U.S. Geological Survey, 2006a). Water levels measured on May 17, 2005, ranged from 0.84 feet above sea level near the coast to about 637 feet above mean sea level in the dike-impounded aquifer. Before these measurements, wells were pumping on their regular pumping schedules. In general, measured water levels in the freshwa-

ter lens were lowest in the central isthmus and were highest where sediments impede flow in the 'Āao aquifer area (fig. 16). In the Lahaina area, simultaneous water levels were reported for 10 wells during February 1979 and 1980 and ranged between 2.0 and 6.5 ft above mean sea level (Souza, 1981, sheet 1).

Water levels were not corrected for tidal fluctuations in any of the water-level surveys, nor for the effects of nearby actively pumping wells, and thus the water levels represent the configuration of the water-table surface at only a specific point in time. Nevertheless, the water-table configuration throughout the year is probably represented by the measured water levels.

Measuring points for each of the wells measured in the synoptic survey were resurveyed to tie all wells in to a common, updated sea-level datum (U.S. Geological Survey, 2006b). Existing measuring-point elevations changed as much as 1.88 ft as a result of the resurvey. Owing to the measuring-point changes, the accuracy of the historical water-level records became questionable, because the timing of the change in measuring-point elevations is unknown. The original measuring-point elevations could have been wrong initially, they could have changed over time owing to settling or land-surface change, or they could have changed abruptly due to damage, earthquake, or other causes. Because the timing of the measuring-point changes is unknown, water levels measured before October 1, 2003 (to coincide with the beginning of the USGS water year), were unadjusted and subsequent water levels were adjusted using the new measuring-point elevations.

The magnitude of the horizontal hydraulic gradient varies spatially and is about 0.00004–0.0002 ft/ft (about 0.2–1 ft/mi) in the central isthmus area and about 0.0005 ft/ft (about 2.6 ft/mi) in the Lahaina area. Burnham and others (1977, p. 28) estimated a hydraulic gradient of about 1.6 ft/mi in the volcanic rocks in the isthmus near Kahului. In the Wailuku area, where valley-filling and caprock sediments are assumed to impede flow, gradients are much higher. Water-level information is not available for determining vertical gradients, but it is likely that near inland recharge areas, heads in the aquifer may decrease with depth, whereas near coastal discharge areas heads in the aquifer may increase with depth.

The first successful well drilled on Maui was in the Lahaina area and was completed in 1883 (McCandless, 1936), and the first shaft or skimming tunnel (tunnel and sump constructed at or near sea level to collect water from the top of the freshwater lens) was constructed in 1900 in the central isthmus (Stearns and Macdonald, 1942, p. 126). However, published water levels from wells are not available earlier than 1935. Water levels in the central isthmus and Lahaina areas ranged between 2 and 7 ft above mean sea level at the time of these first recorded measurements (figs. 17–19). Water levels before development from the basaltic aquifer of the 'Āao Aquifer System were first measured in 1940 in the 'Āao Valley Test hole (5331-01) and ranged between about 31 and 37 ft above sea level during 1940–42 (fig. 18). Water levels in the Waihe'e Aquifer System were first measured in 1988 and were about 11 ft above sea level in North Waihe'e 1 (5631-02).

A

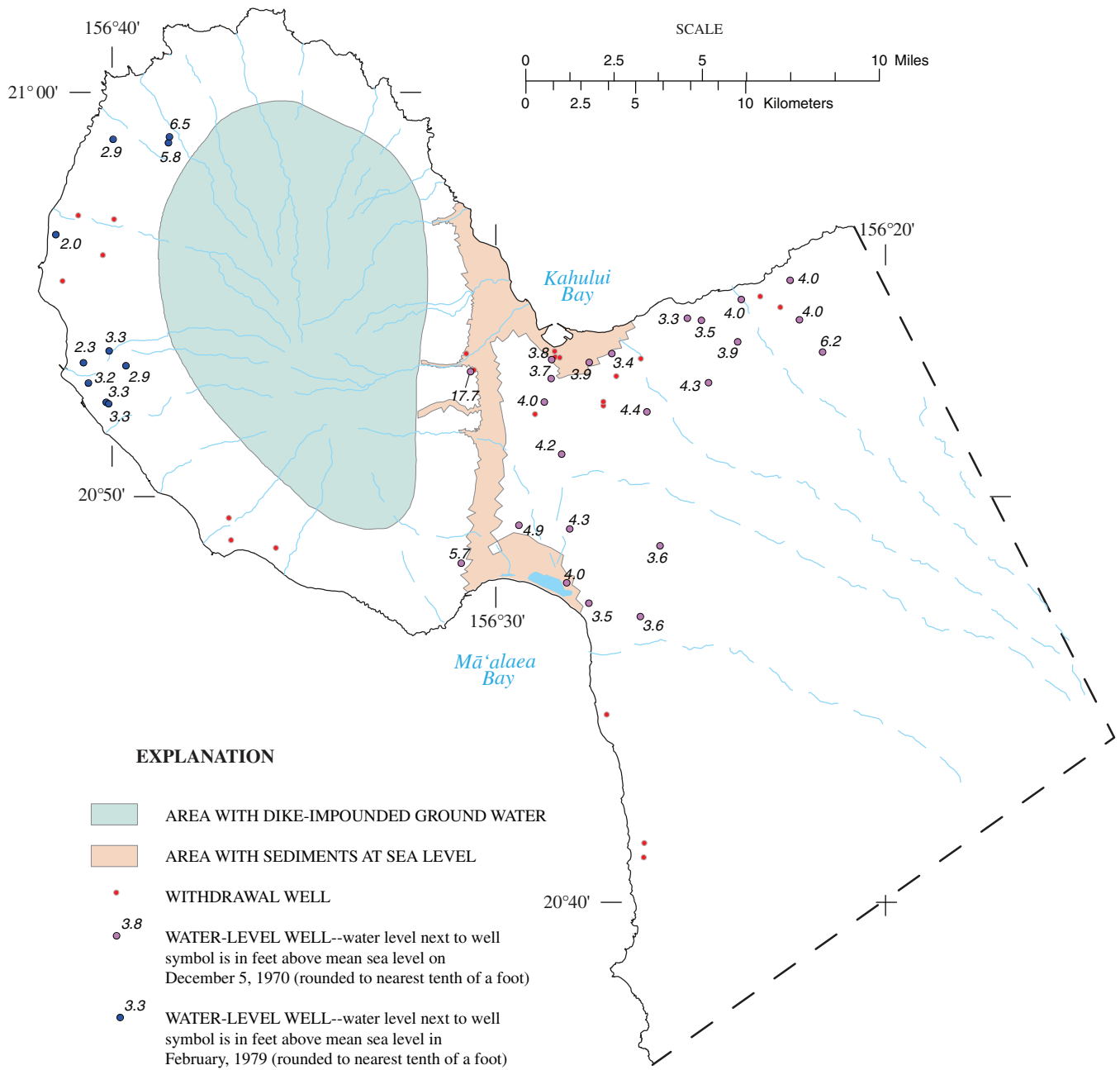
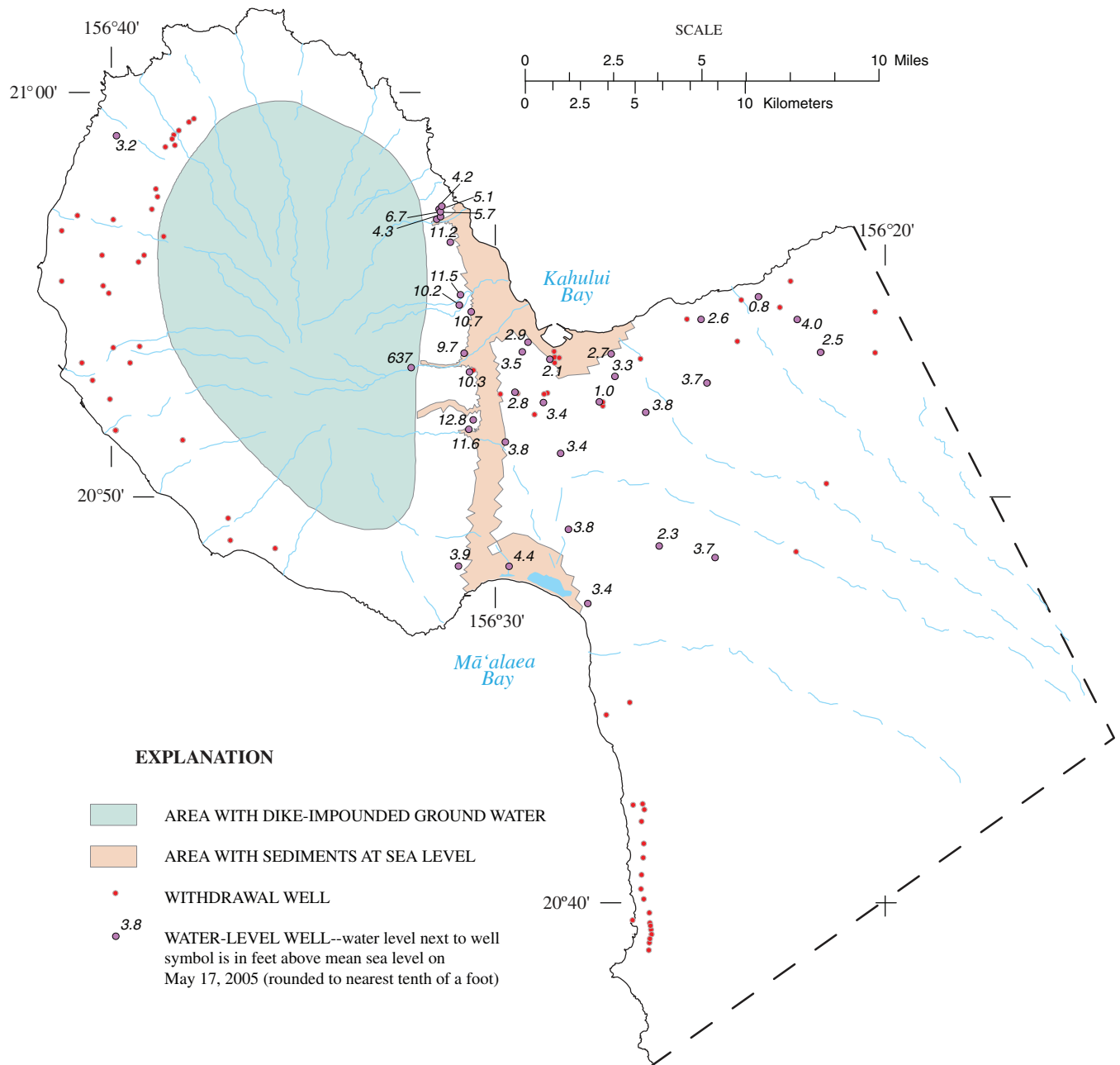


Figure 16. Water-level surveys of (A) December 5, 1970 and February 1979, and (B) May 17, 2005, Maui, Hawai'i (historical water levels from Takasaki, 1972, and Souza, 1981).

B



EXPLANATION

- AREA WITH DIKE-IMPOUNDED GROUND WATER
- AREA WITH SEDIMENTS AT SEA LEVEL
- WITHDRAWAL WELL
- 3.8 WATER-LEVEL WELL--water level next to well symbol is in feet above mean sea level on May 17, 2005 (rounded to nearest tenth of a foot)

Figure 16.—Continued.

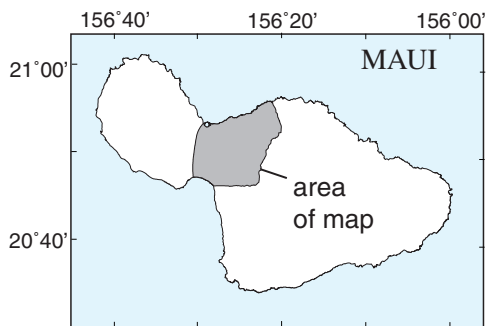
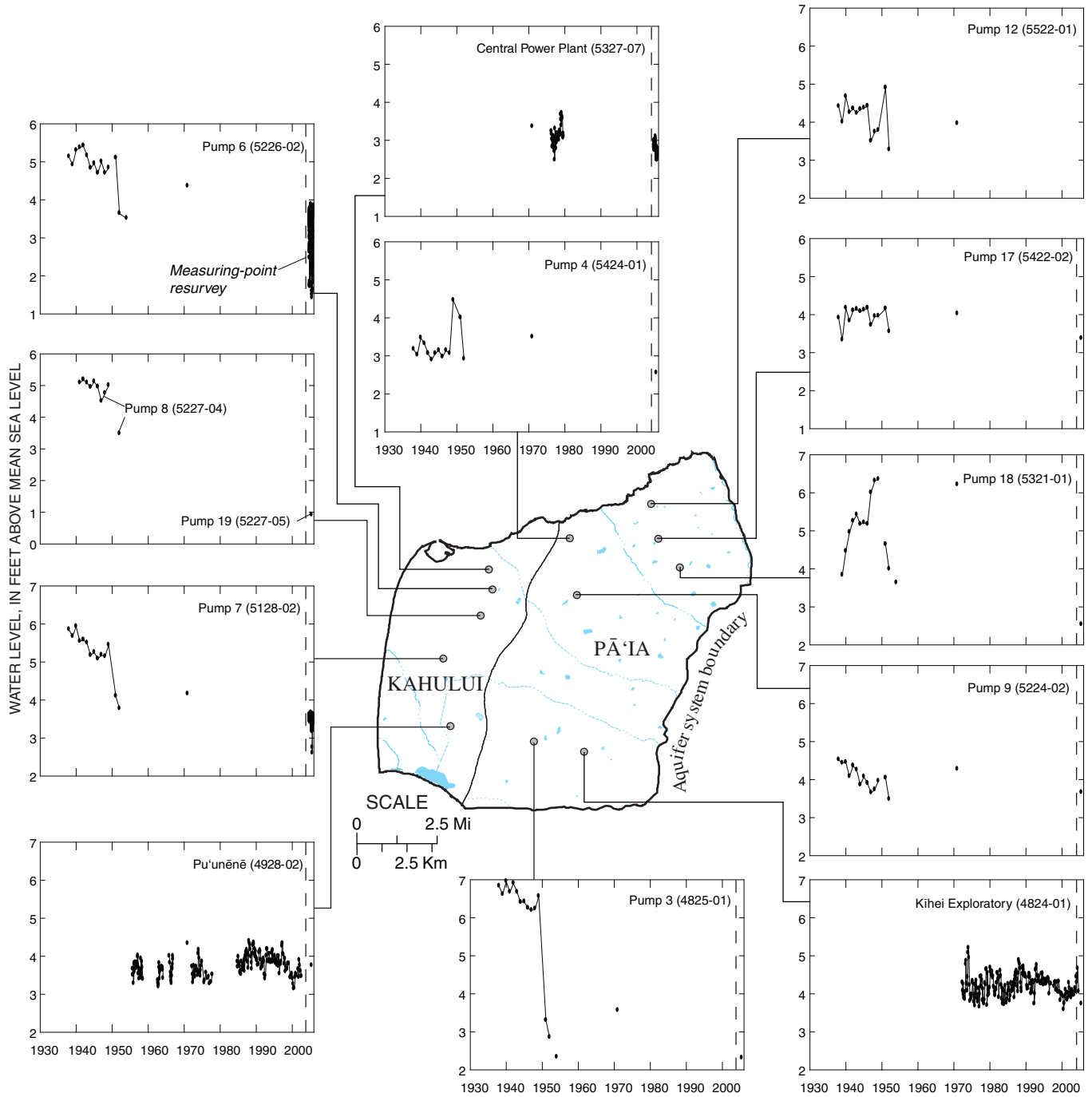


Figure 17. Measured water levels in selected wells in the Central Aquifer Sector, Maui, Hawai'i.

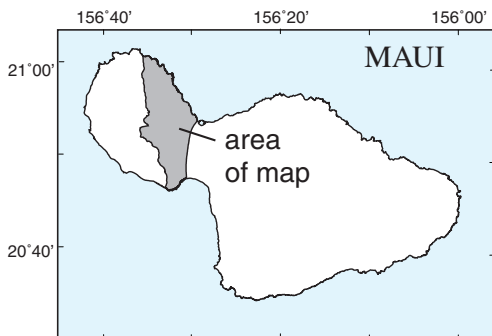
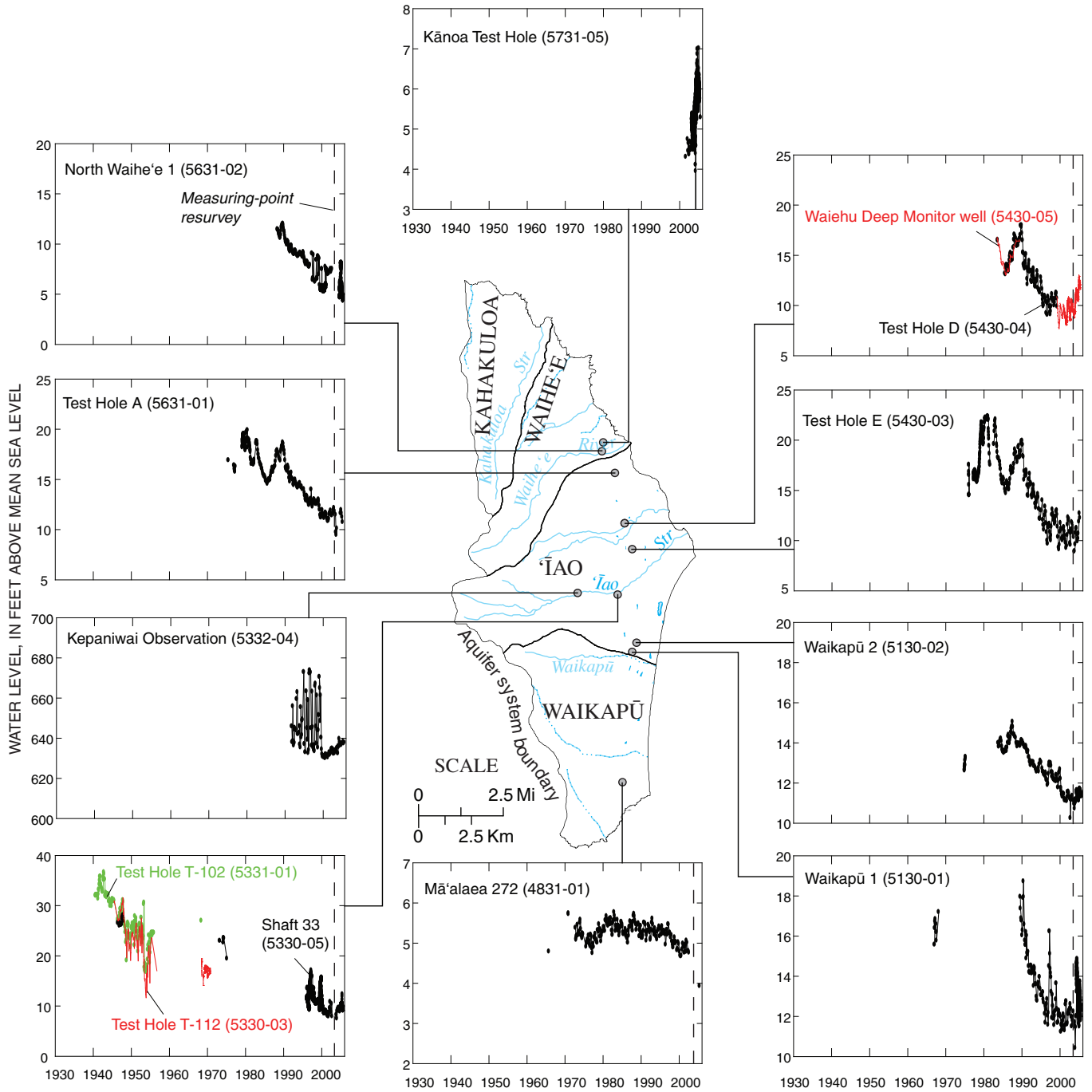


Figure 18. Measured water levels in selected wells in the Wailuku Aquifer Sector, Maui, Hawai'i.

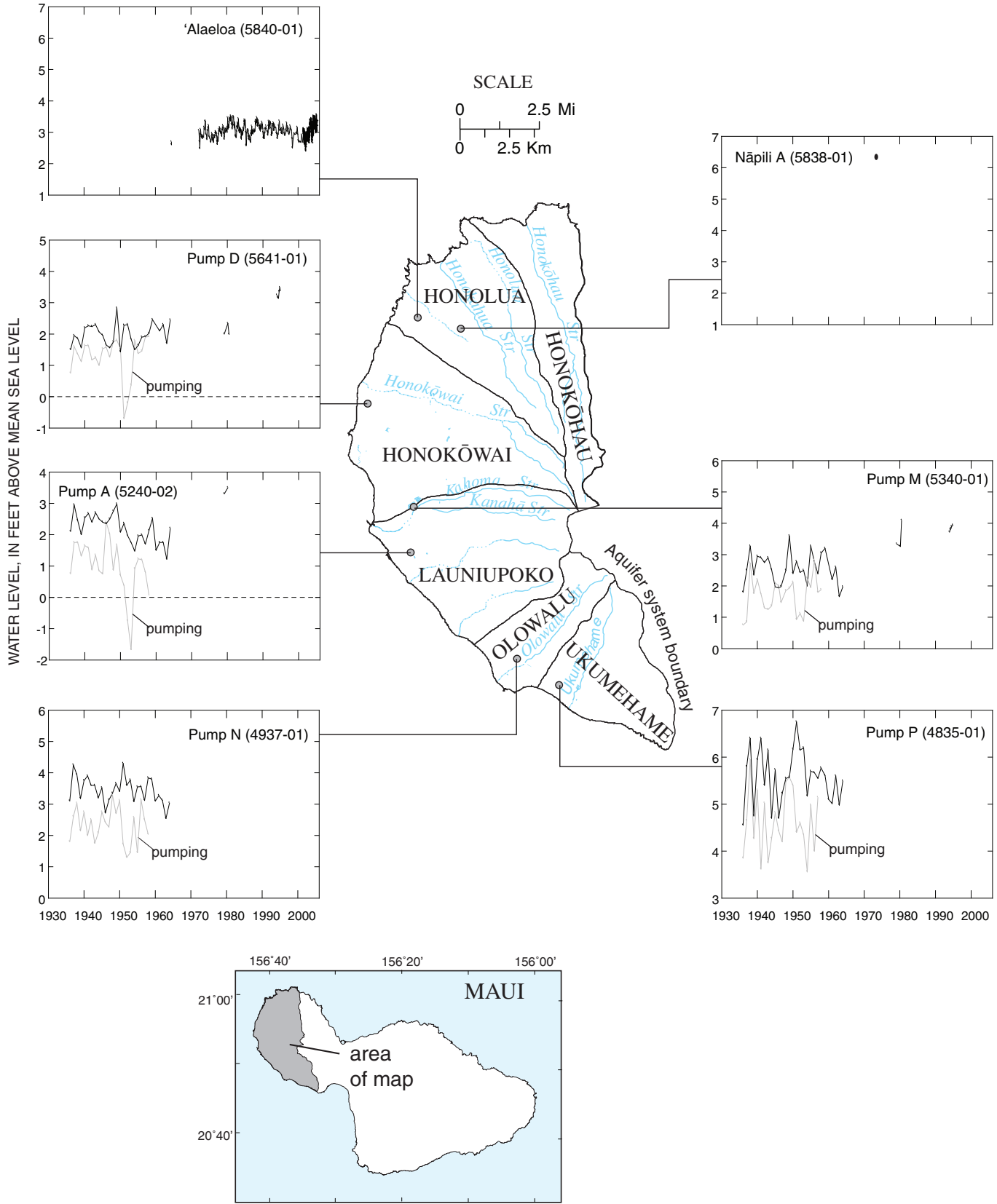


Figure 19. Measured water levels in selected wells in the Lahaina Aquifer Sector, Maui, Hawai'i.

The history of water-level decline in wells in the ʻĪao and Waiheʻe Aquifer Systems was documented by Meyer and Presley (2001). Water levels in these areas indicate seasonal variations and a long-term downward trend during the early 1980s to the early 2000s (fig. 18). Water levels in several wells declined 7–10 feet during 1980–2000. However, water-level data during 2001–present show no downward trend in water levels. The 20-yr water-level decline (1980–2000) was caused by a combination of increased ground-water withdrawals from the aquifer over time and variations in rainfall (Meyer and Presley, 2001). Oki (2005a) documented a statewide downward trend in rainfall during 1913–2001 that may have contributed to the overall water-level decline. Water levels in the ʻĪao and Waiheʻe Aquifer Systems also are strongly affected by the seasonal pattern of recharge and ground-water withdrawals for public supply. This effect is evident at Test Hole E (5430-03) where measured water levels vary by about 2–3 ft from highs in January–March, after the months when withdrawal is lowest, to lows in September–November, after the summer when withdrawal is highest (fig. 18).

Salinity

Salinity is one of the main factors controlling ground-water availability in the study area. Generally, with few exceptions, the salinity of water withdrawn from wells in the area increases with depth, proximity to the coast, and withdrawal rate. Public supply wells in the ʻĪao and Waiheʻe Aquifer Systems mostly produce water with 1 percent or less of seawater salinity (Meyer and Presley, 2001), but occasionally as high as 2.5 percent of seawater salinity (U.S. Geological Survey, 2006c). Before the addition of irrigation water from east Maui surface-water sources, ground water beneath the central isthmus was believed to be naturally brackish (Stearns and Macdonald, 1942, p. 129). Many of the older, high-capacity irrigation wells and shafts operated by sugarcane plantations in central Maui produce water exceeding 4 percent of seawater salinity; some reported values are as high as 20 percent of seawater salinity (Stearns and Macdonald, 1942, p. 220). Saltwater intrusion is a problem at these wells because of the high withdrawal rates and low water levels.

Measuring the salinity profiles in deep open boreholes that fully penetrate the freshwater lens is a common method used in Hawaiʻi to monitor the distribution of salinity with depth in freshwater-lens systems. Salinity profiles are usually measured in terms of chloride concentration or of fluid specific conductance. For this study, seawater was assumed to have a chloride concentration of 19,600 mg/L and a fluid specific conductance of 50,000 $\mu\text{S}/\text{cm}$, values that are near the maximum values measured in deep boreholes (Meyer and Presley, 2001, p. 48). Measured values of concentration or fluid specific conductance were divided by 19,600 mg/L or 50,000 $\mu\text{S}/\text{cm}$ as appropriate and multiplied by 100 to obtain salinity in terms of percent of seawater salinity.

Measured salinity profiles provide an indication of the freshwater volume in the aquifer. Collection of salinity profiles

over time provides an indication of the changes in freshwater volume. In the ʻĪao Aquifer System, two deep wells have been drilled for monitoring salinity profiles. The Waiehu Deep Monitor well (5430-05) has been sampled for chloride concentration at discrete depths by the U.S. Geological Survey since 1985 and additionally for specific electrical conductance by the CWRM since 1999. The ʻĪao Deep Monitor well (5230-02) was monitored for specific electrical conductance by the CWRM since 2006. Salinity profiles collected from the Waiehu deep monitor well indicate a shallowing of the brackish-water transition zone and a reduction of freshwater thickness over time (fig. 20). Based on measurements from the Waiehu Deep Monitor well (U.S. Geological Survey, 2006c), the middle of the transition zone (depth of 50-percent seawater salinity) rose by about 154 ft during 1985–2006. Trends are not discernible from measurements in the ʻĪao Deep Monitor well because of limited temporal data.

Transition-zone information from the Central Aquifer Sector is limited to a few measurements indicating that the freshwater lens is relatively thin in this area. Data from two wells (5328-24, -43) in Kahului collected during 1936–70 show that the middle of the transition zone was about 80–160 ft below sea level (fig. 20) (Burnham and others, 1977, fig. 7). Burnham and others (1977, p. 18) concluded that even though these data were widely spaced in time, the configuration of the transition zone in the area probably remained the same. Since 2002, fluid specific conductance measurements in the Lahaina Aquifer Sector made in the Māhinahina Deep Monitor well (well 5739-03) by the CWRM indicate that the middle of the transition zone is around 140 ft below sea level (fig. 20).

Salinity profiles from deep open boreholes may be affected by flow within the borehole (Paillet and others, 2002). Borehole flow can be caused by natural and withdrawal-induced vertical-head differences in the aquifer. Head may increase with depth in the aquifer near coastal discharge areas and near partially penetrating pumped wells, and increasing head in the aquifer with depth may lead to upward flow within an open borehole that is in hydraulic communication with zones of contrasting head in the aquifer. Upward borehole flow may cause saltwater to flow upward in the borehole, which in turn may lead to an underestimate of the freshwater-lens thickness based on the recorded salinity profile. In areas where head decreases with depth, downward borehole flow may lead to an overestimate of the freshwater-lens thickness based on the recorded salinity profile.

Simulation of Ground-Water Flow

The numerical model developed for this study is a three-dimensional model that simulates the transition from fresh water to ocean water and incorporates hydrogeologic features such as the sediments forming the less-permeable caprock, valley fill, and layer between the lavas of West Maui and Haleakalā Volcanoes. The model code used for this study was SUTRA (version

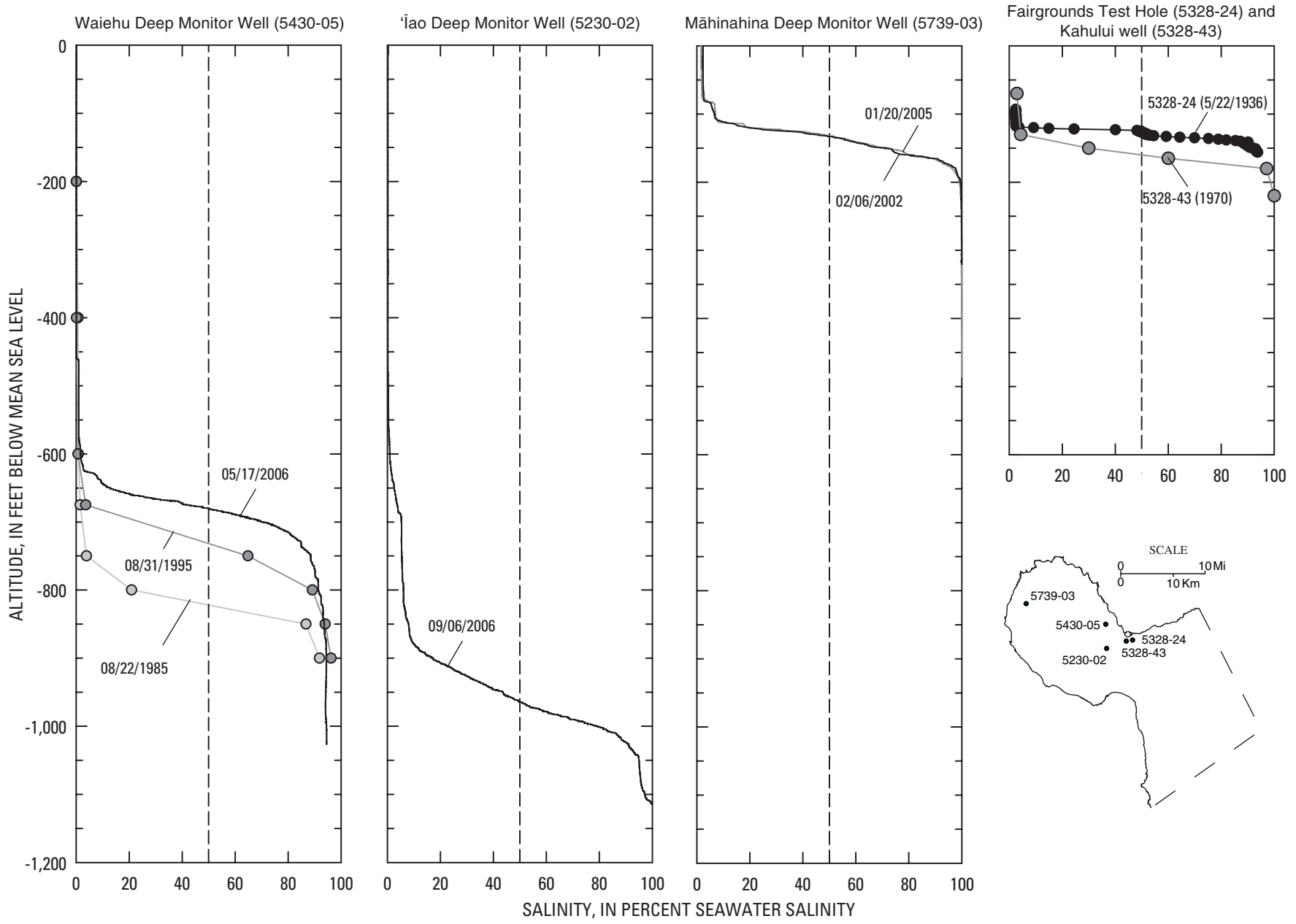


Figure 20. Measured salinity profiles in selected wells in the study area, Maui, Hawai'i. Salinity profiles from Burnham and others (1977) [5328-24, -43]; U.S. Geological Survey data [5430-05]; and the Commission on Water Resource Management [5430-05, 5230-02, and 5739-03].

2D3D.1) (Voss and Provost, 2003), modified to account for water-table storage (Gingerich and Voss, 2005) using the aquifer specific yield. SUTRA is a finite-element code that simulates fluid movement and the transport of dissolved substances in a ground-water system. SUTRA (version 2D3D.1) is capable of simulating three-dimensional, variable-density ground-water flow and solute transport in heterogeneous anisotropic aquifers. Model construction was facilitated using a graphical user interface (SutraGUI) (Winston and Voss, 2003) capable of reading geographic information system (GIS) spatial data and writing files used by SUTRA (version 2D3D.1).

Model Construction

The numerical model of ground-water flow and transport was developed to simulate ground-water levels and salinity movement within the freshwater-lens system during 1926–2006, and it incorporates time-varying recharge, withdrawals, and ocean level. Model construction includes designation of spatial and temporal discretization, assignment of boundary conditions and initial conditions, and delineation of fluid and aquifer properties.

Model Mesh

The model finite-element mesh used for this study comprises 346,256 nodes and 330,924 elements, covers the entire freshwater-lens system in central and west Maui, and extends 1–2 miles offshore to include the zone where fresh ground water discharges to the ocean (fig. 21). The model mesh excludes dike-intruded areas as described by Yamanaga and Huxel (1969, 1970) in the West Maui Volcano interior, although flow from these excluded areas to the freshwater-lens system is included in the model.

The top of the onshore model domain is assumed equal to sea level. Although the top water-table boundary in onshore areas is truncated at sea level, the aquifer transmissivity is underestimated by less than 1 percent using this assumption. The top of the offshore model domain is defined by ocean-bottom bathymetry (National Geophysical Data Center, 2004). The modeled domain extends to 5,906 ft below mean sea level, coinciding with an assumed aquifer bottom similar to that used for a Pearl Harbor model on O‘ahu (Souza and Voss, 1987; Oki, 2005b). Node spacing is variable in the vertical and horizontal directions and is finest in the upper part of the aquifer and near areas of increased ground-water withdrawal and discharge. Horizontal spacing is variable but identical at all depths in the aquifer. Onshore, the vertical spacing between nodes varies from 33 ft within the top 1,312 ft of the aquifer to 328 ft within the bottom 1,640 ft of the modeled domain; offshore, the vertical spacing between nodes is dependent on the bathymetry within the top 1,312 ft of the aquifer, but it is the same as the onshore spacing within the bottom 4,594 ft of the modeled domain (fig. 22).

Boundary Conditions

The model domain extent is defined by vertical boundaries that are either specified-pressure, no-flow, or recharge boundaries.

Specified Pressures and No-Flow Boundaries

The offshore, vertical boundaries of the model domain are a specified-pressure (hydrostatic ocean water) boundary condition. Pressure at each node along the offshore boundary is equal to the pressure of a column of ocean water extending from the node to sea level. For simulations before 1970, when ocean level data are not available, specified pressures were held constant in time. During 1970–2006, the pressures were varied to match the observed ocean levels at the Kahului Harbor (fig. 23). For simulations of future conditions, pressures also were held constant in time. Water may either enter or exit the flow system across the offshore vertical boundary of the model. Water entering along this boundary has salinity equal to that of ocean water, and water exiting along the boundary has salinity equal to that of water in the adjacent aquifer.

The top of the offshore model domain is defined by the ocean-bottom bathymetry (National Geophysical Data Center, 2004) and is a specified-pressure (hydrostatic ocean water) boundary condition. These pressures were also held constant for simulations before 1970, varied to match observed ocean levels during 1970–2006, and held constant for simulations of future conditions. Ocean water may enter the model domain at the top of the boundary in offshore areas, and water from the aquifer may exit at the top boundary in offshore areas.

The eastern boundaries are formed by the northern and southern rift zones of Haleakalā Volcano and are treated as no-flow boundaries in the model. The interior model boundary in west Maui represents the contact between the dike-intruded areas and the lavas of West Maui Volcano. Flow from the dike-intruded area recharges the model along this boundary, and the determination of the amount and distribution of inflow to the model from the dike-intruded area is described below. Below altitudes of -98 ft, this boundary is a no-flow boundary. The model bottom is assumed to be a no-flow boundary.

Recharge

Recharge was added to the model for the periods 1926–79, 1980–84, 1985–89, 1990–94, 1995–99, and 2000–04 based on the distributions (fig. 10) estimated by Engott and Vana (2007). Recharge enters the model at the top, water-table boundary in onshore areas. Because the modeled area did not include the West Maui Volcano interior, recharge around the interior model boundary was distributed with the aid of a simple ground-water flow model constructed using MODFLOW-2000 (Harbaugh and others, 2000). Recharge from the interior boundary enters the model between altitudes of -20 ft and -98 ft relative to mean sea level. This interval was chosen because it is below the top layer of nodes, avoiding assigning two sets of recharge (lateral and areal) at the same node

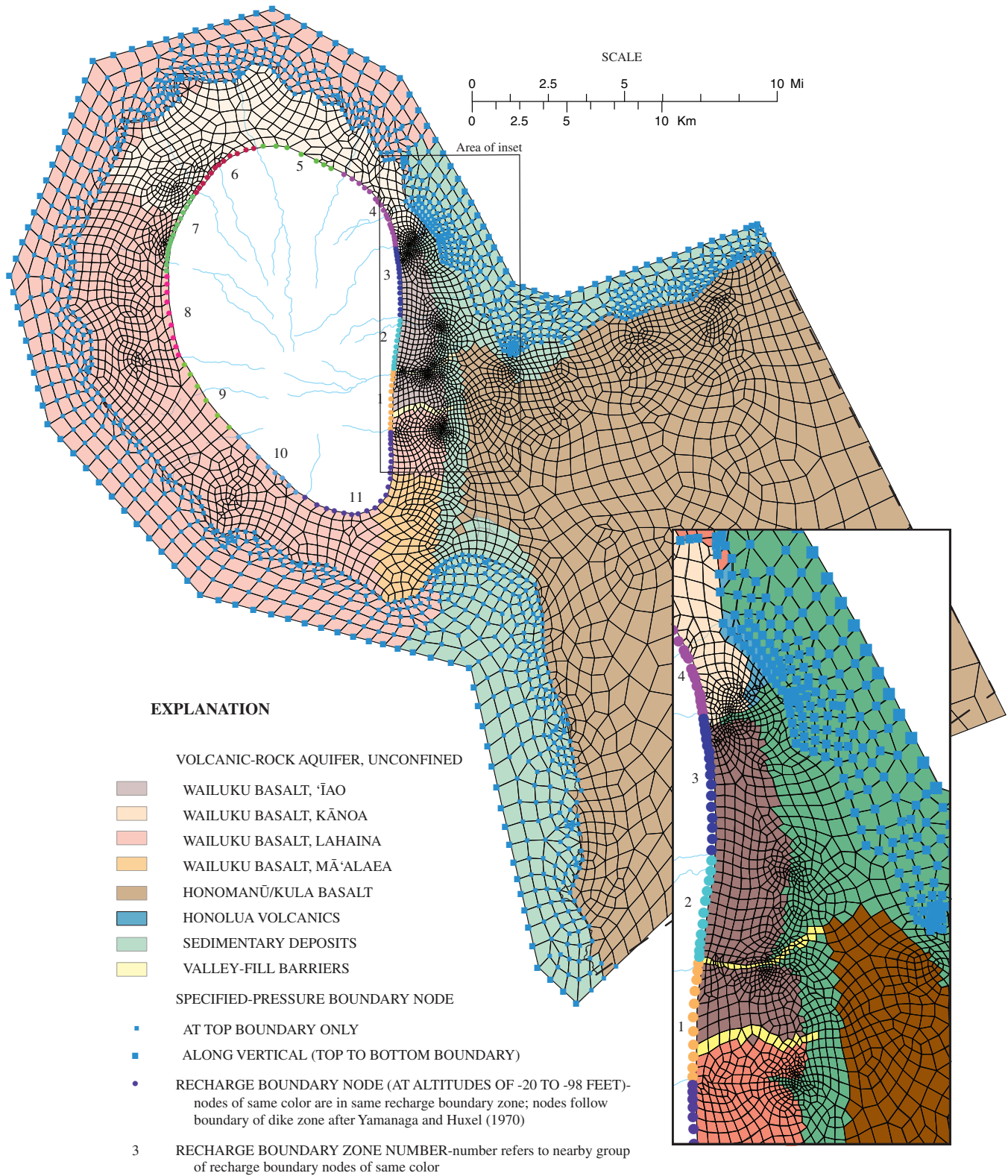


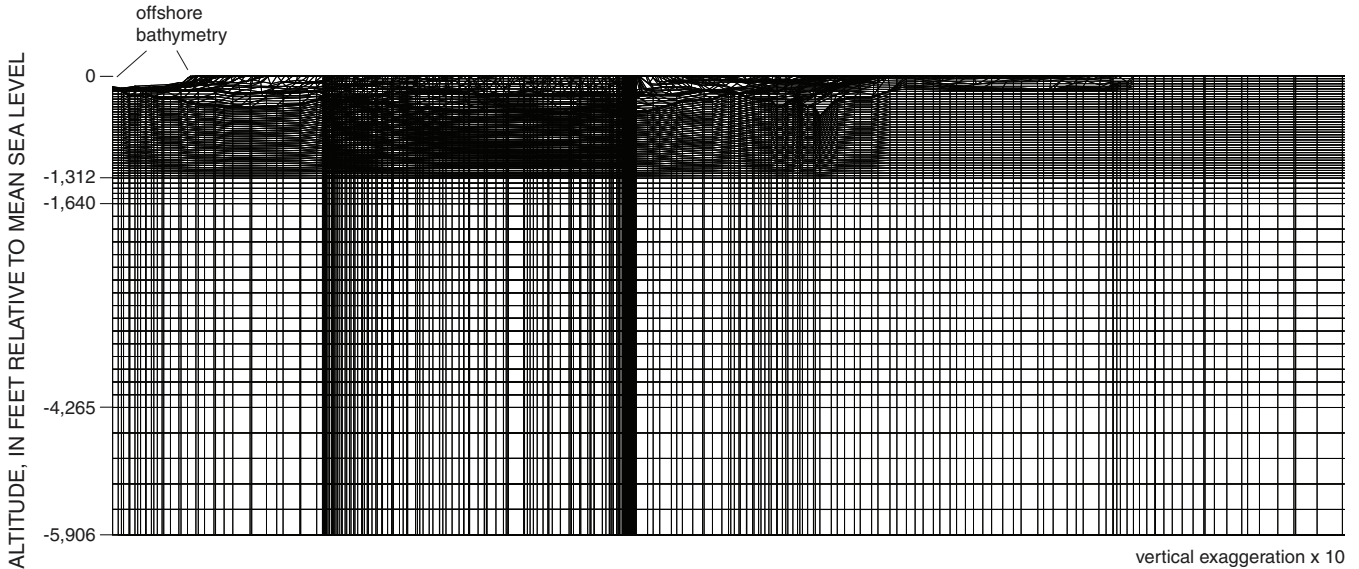
Figure 21. Model discretization and features for the numerical model mesh of central and west Maui, Hawai'i.

in SUTRA, and shallow enough to avoid adding fresh water to a node of simulated saltwater. All recharge was assigned a salinity concentration of 0.000036 kg/kg, about equal to a chloride concentration of 20 mg/L, the average concentration measured in flow from a water-supply tunnel tapping the dike-impounded water body (U.S. Geological Survey, 2006c). The water is assumed to be representative of recharge reaching the freshwater-lens system.

The MODFLOW model was constructed to represent the ground-water flow system of West Maui Volcano, including the low-permeability caldera and dike complexes of the volcano interior and the deeply incised stream valleys that drain much of the interior. This model, which simulates only freshwater flow, is applicable because the ground-water flow system in the dike complex is tens to thousands of feet above sea level and contains only freshwater. Aquifer hydraulic conductivity (assumed homogenous because of the lack of hydraulic conductivity data) and streambed leakage values

were adjusted in the model until simulated discharge from the aquifer to the stream valleys for the 1926–79 recharge period roughly matched estimated base flow flowing from the volcano’s interior during the same period as determined from the historic records of West Maui’s stream gaging stations (table 3). For subsequent recharge periods, the best-fit adjusted values of hydraulic conductivity and streambed leakage were used in the MODFLOW model to calculate base flow based on the specified recharge for the period.

The program ZONEBUDGET (Harbaugh, 1990) was used to calculate the flow amount from 11 regions (roughly the space between adjacent streams) of the dike-impounded water body (fig. 21) into adjacent parts of the freshwater-lens system. Because no data exist to determine areas of preferential flow to the adjacent freshwater-lens system, the flow was distributed uniformly on the basis of the length of the boundary of each of the 11 regions. The amount of flow through each of the 11 regions as a percentage of the total flow from the



Perspective view looking north of southern edge of numerical model mesh.

Figure 22. Vertical cross section of model mesh of central and west Maui, Hawai‘i.

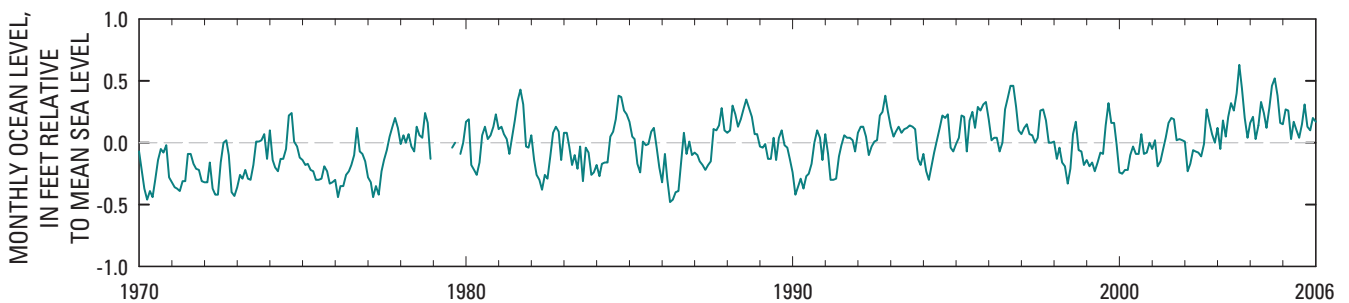


Figure 23. Monthly ocean level during 1970–2006 at Kahului Harbor, Maui, Hawai‘i (data from National Oceanic and Atmospheric Administration, 2007).

Table 3. Estimated base flow and base flow simulated with MODFLOW-2000 model for selected study area streams, Maui, Hawai'i.

[Mgal/d, million gallons per day]

Stream name	Estimated average base flow during 1926-79 ^a (Mgal/d)	Simulated base flow using 1926-79 recharge (Mgal/d)	Difference between simulated and estimated average base flow	
			Mgal/d	Percent
Waikapū	4.19	5.47	1.28	31
Īao	19.09	20.66	1.57	8
Waiehu	2.98	2.99	0.01	0
Waihe'e	30.93	33.02	2.09	7
Kahakuloa	4.45	4.62	0.17	4
Honokōhau	11.91	11.12	-0.79	-7
Honolua	0.93	0.68	-0.25	-27
Honokōwai	3.50	3.88	0.38	11
Kahoma	3.31	5.47	2.16	65
Kanahā	2.59	3.12	0.53	20
Kaua'ula	4.01	4.76	0.74	18
Launiupoko	0.65	0.00	-0.65	-100
Olowalu	3.50	3.75	0.25	7
Ukumehame	3.74	2.69	-1.05	-28
Total	95.79	102.22	6.43	7

^aEstimated from daily streamflow records**Table 4.** Recharge for historical simulation, 1926–2006, central and west Maui, Hawai'i.

[All values in million gallons per day; estimated recharge from Engott and Vana (2007); total recharge used in simulation is the sum of the estimated recharge to the modeled area and the estimated flow from the dike complex; estimated base flow to streams estimated using MODFLOW simulations; estimated flow from dike complex to surrounding aquifers divided into zones based on the following percentages: zone 1–7.1%, zone 2–5.8%, zone 3–5.8%, zone 4–5.3%, zone 5–7.0%, zone 6–5.8%, zone 7–9.3%, zone 8–12.8%, zone 9–15.1%, zone 10–13.9%, zone 11–12.1%]

Model period	Estimated recharge		Estimated base flow to streams from dike complex	Estimated flow from dike complex to surrounding aquifers	Total recharge used in SUTRA simulation
	Modeled area	Dike complex			
1926–79	481	202	96	106	587
1980–84	314	218	107	111	425
1985–89	342	276	151	125	467
1990–94	241	229	113	116	357
1995–99	229	181	86	95	324
2000–04	214	163	70	93	307
Future average conditions	244	206	98	108	352
1998–2002 drought	167	162	78	84	251

dike-impounded system to the freshwater-lens system ranges from 5.3 percent in recharge boundary zone 4 to 13.9 percent in recharge boundary zone 10 (table 4). These flow percentages were used for each recharge period to determine the amount of water added to the SUTRA model along the interior boundary for the entire modeled period. Recharge across the interior boundary ranged between a high of 125 Mgal/d during 1985–89 and a low of 93 Mgal/d during 2000–04 (table 4). Total recharge to the SUTRA model was highest during 1926–79 at 587 Mgal/d and lowest during 2000–04 at 307 Mgal/d.

Withdrawal

Reported monthly withdrawals from wells during 1926–2006 were simulated in the numerical model (appendix B). Reported withdrawals were compiled from published records (Stearns and Macdonald, 1942; Yamanaga and Huxel, 1969, 1970; Takasaki, 1972; Meyer and Presley, 2001), information contained in USGS files (unpub. data, USGS Pacific Islands Water Science Center data files), and a CWRM digital database (unpub. data, 2007).



Figure 24. Selected withdrawal wells used in construction of the numerical model of central and west Maui, Hawai'i.

Withdrawal wells (fig. 24) were represented in the model by the nearest vertical column of nodes to the withdrawal well. Within the nearest vertical column of nodes from a withdrawal well, only those nodes corresponding to the well interval open to the aquifer (appendix C) were used to simulate withdrawal. Withdrawal from the aquifer was assumed uniform within the well interval open to the aquifer. Withdrawals from shafts with large-capacity infiltration tunnels were represented in the model by several nodes along the reported orientation of the tunnels (Takasaki, 1972). In several cases where wells are closely spaced, a model node represented more than one well. In the model, withdrawals were not simulated from the top layer of nodes, thus avoiding assigning areal recharge and pumpage at the same node in the model.

Initial Conditions

Initial conditions for the historical simulation during 1926–2006 were estimated from a steady-state simulation using average (1926–79) recharge and average withdrawals for the period 1902–26. Average total recharge of 587 Mgal/d was used in the steady-state model, and simulated withdrawal, mainly from sugar irrigation wells, was about 39 Mgal/d. A two-step iterative process was used to determine model adjusted hydrologic properties and initial conditions. Firstly, selected hydrologic properties were adjusted to improve the match between simulated heads and salinities, and historically measured values during the simulation of 1926–2006 conditions; and secondly, the steady-state simulation was repeated with the adjusted properties to compute new initial conditions. The process was repeated until the change in model adjusted hydrologic properties was small.

Representation of Hydrologic Features

Several hydrogeologic features of low permeability were represented in the numerical model. Valley-fill barriers associated with Waikapū and ʻĪao Valleys were represented as partially penetrating, vertical, low-permeability zones continuing inland from the low permeability sedimentary wedge (fig. 21). The penetration depth of the valley-fill barriers is uncertain because of a paucity of available information. The final location of the valley-fill barrier representing Waikapū Valley was determined through trial and error by matching the head differences measured on either side of the presumed feature. A simulated valley-fill barrier was not required beneath Waiheʻe Valley to match the drop in head across the valley.

A uniform thickness of about 800 ft was specified for the sedimentary layer between West Maui Volcano and Haleakalā on the basis of stratigraphic information from one well and the assumed slope of the top of the Wailuku Basalt. The Wailuku Mill Test Hole (5330-04) (fig. 4) likely penetrated lavas from Haleakalā between altitudes of -16 and -191 ft and sediments below the lavas to -524 ft (Meyer and Presley, 2001, fig. 9). The slope of the top of the Wailuku Basalt beneath the location

of this test hole projects to an altitude of -1,000 ft, indicating that the total thickness of the sedimentary wedge is at least 800 ft (from about -200 to about -1,000 ft altitude).

Water Properties

Water was assigned a fluid compressibility of $2.14 \times 10^{-8} \text{ ft}^2 \text{ lb}^{-1}$ ($4.47 \times 10^{-10} \text{ Pa}^{-1}$) and a dynamic viscosity of $2.1 \times 10^{-5} \text{ slug ft}^{-1} \text{ s}^{-1}$ [$1.00 \times 10^{-3} \text{ kg m}^{-1} \text{ s}^{-1}$]. Solute concentrations in the model are expressed as a mass fraction: mass of total dissolved solids (TDS) per unit mass of fluid. Freshest water was assigned a TDS concentration of zero and 100 percent ocean water was assigned a TDS concentration of $3.57 \times 10^{-2} \text{ kg/kg}$. The density of water was assumed to increase linearly with salinity from 62.42 lb ft^{-3} ($1,000 \text{ kg m}^{-3}$) for freshwater to 63.98 lb ft^{-3} ($1,024.99 \text{ kg m}^{-3}$) for ocean water.

Molecular diffusion (Fickian) of a solute is driven by concentration gradients in the fluid and may take place in the absence of ground-water flow. Molecular diffusion of a solute in a fluid is characterized by the molecular diffusivity, which was assigned a value of $1.1 \times 10^{-8} \text{ ft}^2/\text{s}$ ($1.0 \times 10^{-9} \text{ m}^2/\text{s}$) in the model.

Aquifer Properties

For the numerical model, aquifer properties were assigned values based on published estimates. Matrix compressibility was assigned a value of $1.2 \times 10^{-7} \text{ ft}^2 \text{ lb}^{-1}$ ($2.5 \times 10^{-9} \text{ Pa}^{-1}$) (Souza and Voss, 1987). For all aquifers, the values of effective porosity (and of specific yield for the top onshore nodes of the mesh) used in the model were 0.15 (table 5). The effective porosity values used in the model are within the range of previously estimated values for basaltic-rock aquifers on Oʻahu (Souza and Voss, 1987) but greater than values used in the simulation of the Pearl Harbor aquifer (Oki, 2005b). The larger values improved the match between measured and simulated salinity profiles and the historical shallowing of the transition zone. Smaller values of effective porosity caused the simulated transition zone to rise much faster than was measured in the Waiehu Deep Monitor Well (5430-05). One possible explanation for a higher effective porosity of basaltic rocks on Maui than on Oʻahu is that the rocks on Maui are younger (< 1.5 Ma for Maui compared to 2.6–1.8 Ma for Oʻahu) and therefore less exposed to weathering which typically reduces the rock porosity.

For all basalt units the transverse dispersivity was assigned a value of 0.66 ft (0.20 m), and for sedimentary and valley-fill deposits the value was 3.3 ft (1.0 m) (Souza and Voss, 1987) (table 5). Longitudinal dispersivity was assigned a value of 250 ft (76 m) in the horizontal direction (corresponding to the major and semi-major axes of the permeability tensor) (Souza and Voss, 1987) and 25 ft (7.6 m) in the vertical direction (corresponding to the minor axis of the permeability tensor).

The hydraulic-conductivity values for the different geologic features initially were estimated on the basis of published information (Rotzoll and others, 2007) and were adjusted in the numerical model to provide a better match

Table 5. Aquifer-property values used in the construction of the numerical ground-water model of central and west Maui, Hawai'i.[ft, feet; ft/d, feet per day; ft²/lb, feet squared per pound]

Parameter	Estimated value		
	Vertical	Horizontal, transverse	Horizontal, longitudinal
Hydraulic conductivity (ft/d)			
Wailuku Basalt, 'Īao	0.38	200	300
Wailuku Basalt, Kānoa	2.62	699	2,097
Wailuku Basalt, Lahaina	10.49	699	2,097
Wailuku Basalt, Mā'alaea	9.72	2,593	7,778
Honolua Volcanics	0.08	0.08	0.08
Honomanū/Kula Basalt	13.85	3,694	11,083
Sedimentary deposits	0.38	17	17
Valley-fill barriers	0.69	6.9	6.9
Dispersivity (ft)	Transverse	Longitudinal, minimum	Longitudinal, middle and maximum
All volcanic units	0.66	25	250
Sedimentary and valley-fill deposits	3.30	25	250
Porosity (and specific yield)	0.15		
Solid-matrix compressibility (ft²/lb)	1.2x10 ⁻⁷		

to measured water levels and salinity profiles from selected wells in the study area. Horizontal hydraulic-conductivity values used in the model ranged between 0.08 ft/d for Honolua Volcanics and 11,083 ft/d for the volcanic-rock aquifers of Haleakalā (table 5). Horizontal hydraulic-conductivity values for the volcanic-rock aquifers in the model were highest along the assumed longitudinal axis of the surficial lava flows (approximately perpendicular to the existing topographic contours) and generally one-third as much along the transverse axis. Vertical hydraulic conductivity of the volcanic-rock aquifers in the model was 0.00125 to 1 times lower than the longitudinal hydraulic conductivity. Horizontal hydraulic conductivity of the sedimentary caprock is 17 ft/d and vertical hydraulic conductivity is 0.69 ft/d. The valley-fill barriers were modeled using a horizontal hydraulic conductivity of 6.9 ft/d and a vertical hydraulic conductivity 10 times lower.

Simulated Historical Conditions 1926–2006

Transient historical conditions were simulated using 15-day time steps during 1926–2006 and initial conditions derived from the steady-state simulation. Withdrawal rates varied monthly, recharge rates were steady for each of the six recharge periods, and specified pressures representing the ocean varied monthly after 1970. Hydraulic properties used in the model were initially based mainly on previous estimates but were adjusted in the model to obtain better agreement between simulated and measured water levels and measured salinity profiles. The main hydrologic parameters controlling flow in the Wailuku Aquifer Sector are the hydraulic con-

ductivity of the valley-filling deposits and the sedimentary caprock and the effective porosity of the basalt aquifer. The high initial water levels (greater than 30 ft) could only be simulated by creating barriers to the eastward flow of ground water toward the isthmus and the north/south flow of ground water toward the coast at Waihe'e and Mā'alaea.

The final distribution of hydrologic parameters was determined through an extensive trial and error process to determine the most likely values. The trial and error fitting process included matching long-term water level changes throughout the system over tens of years, matching short-term changes over a few months at individual wells, matching hydrologic gradients from well to well and from wells to the coast, matching salinity profile changes over tens of years, and matching salinities at individual pumped wells. Aquifer properties were adjusted in a wide range of reasonable values and a suitable combination of property values was found that produced a reasonable match between simulated heads, gradients, and salinities to the historic hydrologic data.

Water Levels

Simulated water levels generally are in agreement with measured water levels from representative wells in the modeled area (fig. 25). Measured and simulated water levels in the Wailuku Aquifer Sector decline beginning about 1950 after pumping in this area began. Although measured water levels in the Central and Lahaina Aquifer Sectors are scarce, the simulated water levels match their relatively smaller declines throughout the simulated period near areas of higher withdrawal. Where

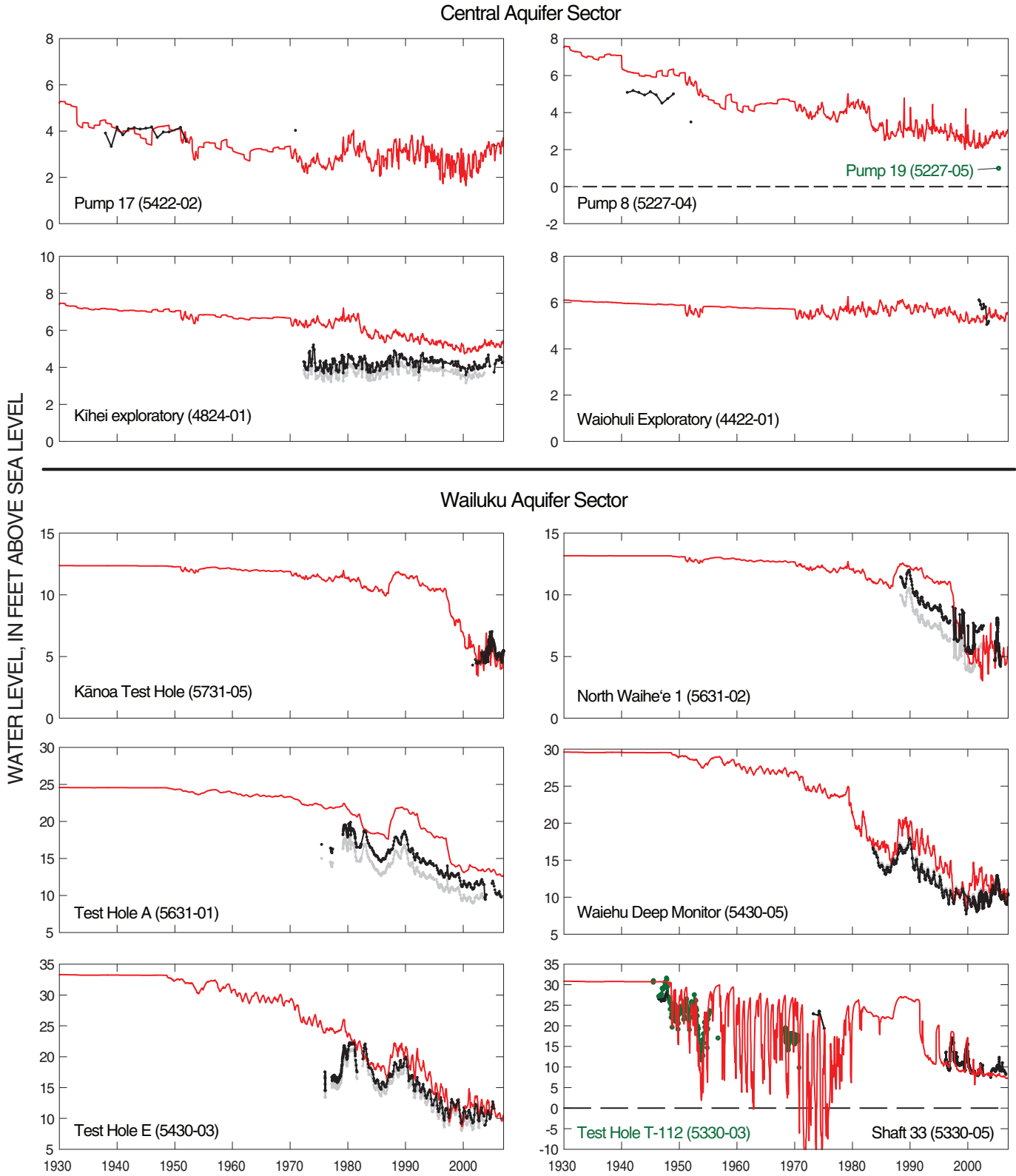
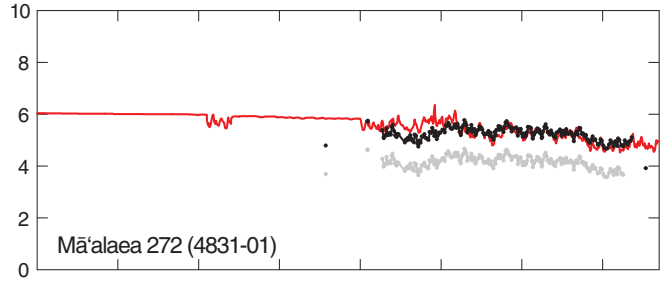
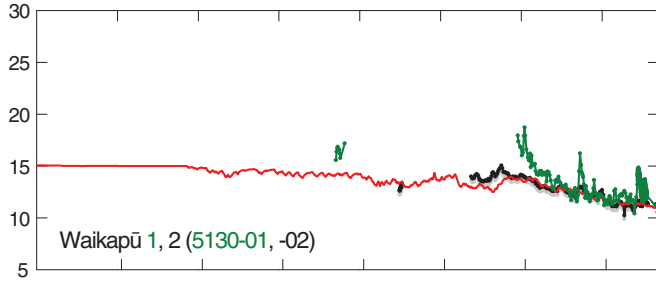
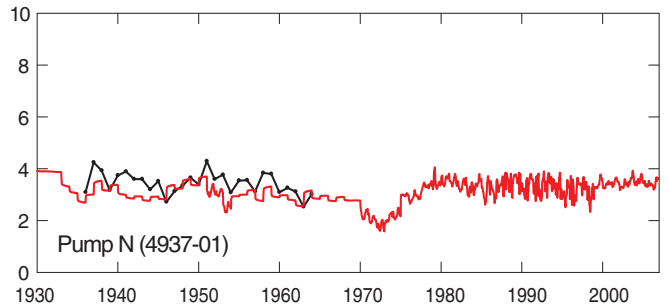
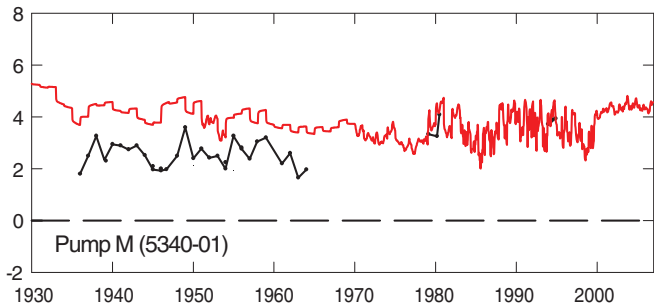
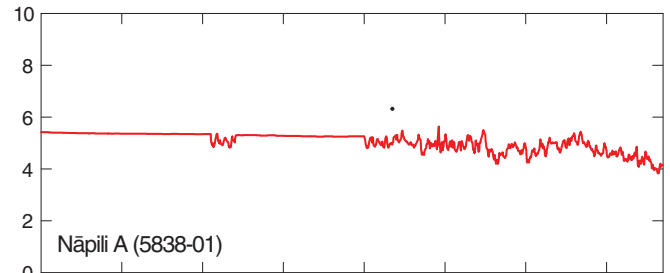
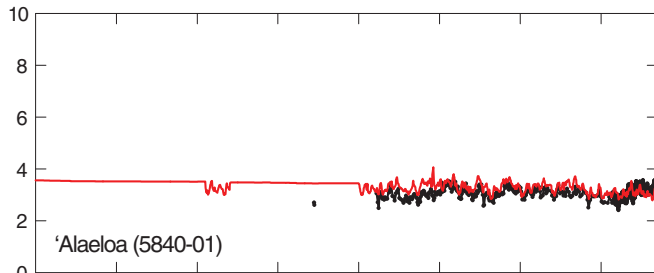


Figure 25. Measured (black and green lines) and simulated (red lines) water levels in selected wells in central and west Maui, Hawai'i. Well number shown in parentheses after well name.



Lahaina Aquifer Sector



EXPLANATION

MEASURED WATER LEVEL

- BASED ON ORIGINAL MEASURING POINT
- BASED ON REVISED MEASURING POINT AFTER 2003 RESURVEY (U.S. Geological Survey, 2006)
- SIMULATED WATER LEVEL

Figure 25.—Continued.

original and revised measuring points are available, the historic water levels are plotted using both measuring points, because the timing of the measuring-point changes is unknown.

Because recharge in the historical model was based on average estimates over 53 years during 1926–79 and for 5-yr periods afterward, interannual variations in water levels caused by interannual variations in recharge were not simulated. Some interannual variability in water levels was simulated, however, because of withdrawal variations. The match of simulated and measured water levels improves after 1979, when the recharge periods are reduced to 5-yr increments.

The effects of including ocean-level variations in the historical simulation are most apparent at wells near the coast and away from areas of relatively lower permeability sedimentary deposits. Simulated water levels at the Kihei Exploratory well (4824-01), Mā'alaea 272 (4831-01), and 'Alaeloa well (5840-01) reasonably match short- and long-period observed water-level variations. For example, the increase in ocean level of about 0.5 ft during 2000–04 (fig. 25) is reflected by the increase in water levels in these three wells during a time when recharge rates were relatively lower and withdrawal near these wells was not decreasing.

Within the Wailuku Aquifer Sector, simulated water levels generally match measured water levels, especially after 2000 (fig. 26). Within the Central and Lahaina Aquifer Sectors, simulated water levels are slightly higher than measured water levels in some areas and slightly lower in others, with no apparent bias to a particular area.

Some of the discrepancy between measured and simulated water levels can be attributed to uncertainties in the estimated distribution of hydraulic properties in the numerical model. Some discrepancy also may be related to other factors including: (1) few reported predevelopment water levels are available in the 'Īao area and none are available north of Waihe'e River, (2) temporally coarse 5-yr recharge estimates may not reflect conditions antecedent to the day when water levels were measured, (3) reported ground-water withdrawal information may be inaccurate, (4) some of the measured water levels are from pumping wells and therefore may reflect only local aquifer conditions near the well, (5) model spatial discretization may be too coarse in some areas to accurately simulate local water level changes.

During 1926–2006, simulated ground-water levels decline the most in the Wailuku Aquifer Sector because of increased withdrawal and decreased recharge (fig. 27). Simulated water levels have declined more than 25 ft near the Waihe'e (5431-02, -03, -04) and Waiehu Heights (5430-01, -02) wells. Beneath the isthmus in the Central Aquifer Sector, simulated water levels declined 1–4 ft, mainly because of decreased recharge. Simulated water levels declined 1–2 ft in parts of the Lahaina Aquifer Sector.

Salinity Profiles

Before about 1985, useful salinity profiles from deep monitor wells in the study area were limited to only one well,

the Fairground well (5328-24), where a single profile is available from 1936 (fig. 20). Salinity profiles have been collected quarterly in the Waiehu Deep Monitor well (5430-05) since 1985 and the Māhinahina Deep Monitor well (5739-03) since 2002. A few profiles from the new 'Īao Deep Monitor well (5230-02) between 'Īao and Waikapū Streams are available, but only since 2005, and so they are not compared with results from the historical simulation. Measured salinity profiles in the Waiehu Deep Monitor well indicate a shallowing of the brackish-water transition zone over time, and simulated salinity profiles are consistent with this trend (fig. 28). The simulated trend of the depth where the water is 50-percent seawater fits the measured values best for the more recent data, rising a little more than about 6 ft/yr during 1995–2006. The simulated trend of the depth where the water is 2-percent seawater shows a more rapid shallowing than was measured in the Waiehu Deep Monitor well. The shapes of the simulated salinity profiles also generally are consistent with the measured profiles. At the Waiehu Deep Monitor well, simulated and measured depths where salinity is 50 percent that of seawater are within about 16 feet of each other at the end of the historical simulation. At the Māhinahina Deep Monitor well (5739-03), the simulated depth where salinity is 50 percent that of seawater is about 80 ft deeper than the measured depth at the end of 2006 (fig. 29). At the Fairgrounds Test Hole (5328-24), the simulated 50-percent depth is about 150 ft lower than the measured depth. These wells are in areas where water-level data are scarce; therefore, the modeled water levels and thickness of the freshwater lens may be too high and too large, respectively. The scarce data and the lower priority interest of these areas in this study, little effort was spent adjusting aquifer properties in the model to improve the agreement between these simulated and measured profiles.

Some of the discrepancy between measured and simulated salinity profiles can be attributed to (1) uncertainties in the estimated distribution of hydraulic properties in the model, (2) possible borehole flow in the deep monitor wells (Paillet and others, 2002), (3) insufficient vertical discretization in the numerical model mesh, and (4) additional factors described above for simulated water levels. Borehole flow in the deep monitor wells can cause a lack of agreement between the simulated and measured profiles. The simulated profile is computed using the freshwater head near the transition zone, whereas the measured profile is influenced by the water level in the open well or borehole, which (because of the vertical hydraulic communication created by the open borehole and the accompanying intra-borehole flow) represents a composite head in the interval of aquifer penetrated by the well. Near the coast, the head at depth tends to be greater than at the water table, so the water level in an open well near the coast that penetrates a large interval of the aquifer will tend to be lower than that of the surrounding aquifer at the water table. Hence, the midpoint of the measured salinity profile in the well will tend to be shallower than in the aquifer.

The simulated depth where water in the aquifer has 50-percent seawater salinity is deeper than 700 ft below sea

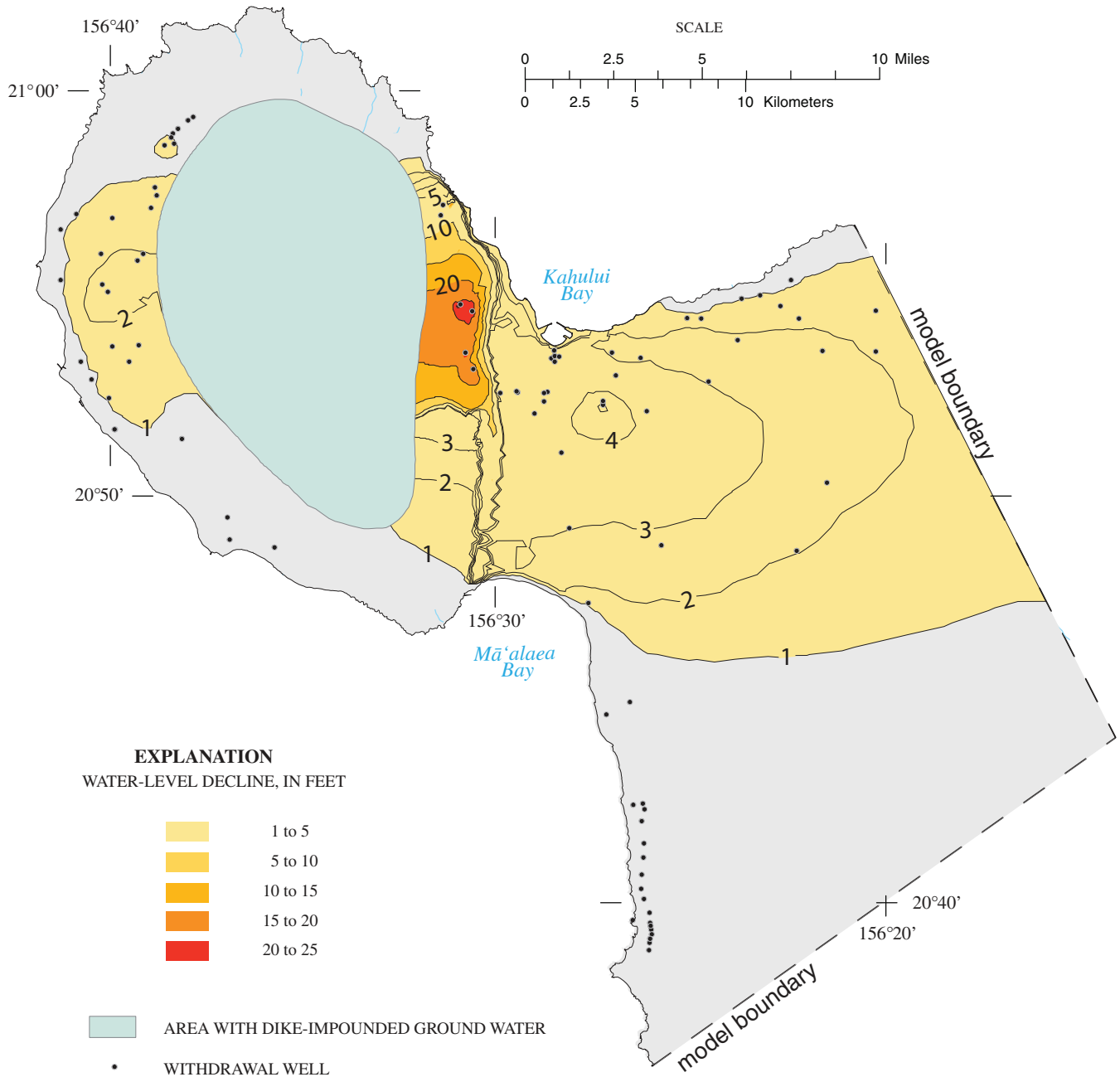


Figure 27. Simulated water-level changes between 1926 and 2006 in central and west Maui, Hawai'i.

level in part of the Wailuku Aquifer Sector (fig 30). The 50-percent salinity contours generally follow the pattern of the simulated water-level map (fig. 26), being deeper inland where water levels are higher. Withdrawal wells that are drilled deeper than the CWRM's recommended well depth guidelines compared to simulated salinity are shown in red in figure 26. The CWRM recommends that new wells be drilled no deeper than $\frac{1}{4}$ of the depth to 50-percent seawater salinity (State of Hawai'i, 2004).

Simulated Future Scenarios

The numerical model constructed for this study was used to quantify changes in ground-water level and salinity with continued ground-water withdrawal under various withdrawal and recharge scenarios (table 6). Scenarios included ground-water withdrawal at 2006 rates and locations with 2000–04 land use and 1926–2006 rainfall (scenario 1), withdrawal at 1996 rates and locations with 2000–04 land use and 1926–2006 rainfall (scenario 2), and withdrawal at redistributed rates and locations using various recharge scenarios (scenarios 3–7). Scenarios 1–3 and 5–7 were simulated for 2007–2157 and scenario 4 for 2007–2037. Most of the scenarios were contin-

ued for 150 years to reach equilibrated hydrologic conditions, when no significant water-level or salinity changes are apparent. Scenario 2, with 1996 withdrawal rates and locations, represents the historical condition with the highest withdrawal rates from the fewest wells in the 'Āao Aquifer System. In this scenario, withdrawal after 1996 was maintained at the 1996 rates through the end of the 150-yr scenario. The simulated initial conditions for all other scenarios were the final conditions from the 1926–2006 historical simulation.

For each simulation, the simulated salinity at selected pumping wells is classified as: (1) acceptable, salinity less than 1.0 percent seawater; (2) cautionary, salinity between 1.0 and 2.5 percent seawater; and (3) threatened, salinity greater than 2.5 percent seawater. Wells with simulated salinity in the cautionary class have the potential to produce water with salinity higher than is acceptable for drinking. Wells with simulated salinity in the threatened class are likely to produce water unacceptable for drinking. This classification was developed cooperatively with the DWS to provide a basis for comparing the various scenarios investigated in this study. At several sites, the simulated water levels and salinities are shown for the location in the model representing the deepest well (or representative well if depths are similar) in the group of closely spaced wells (referred to hereafter as a well field). The Kānoa Test Hole

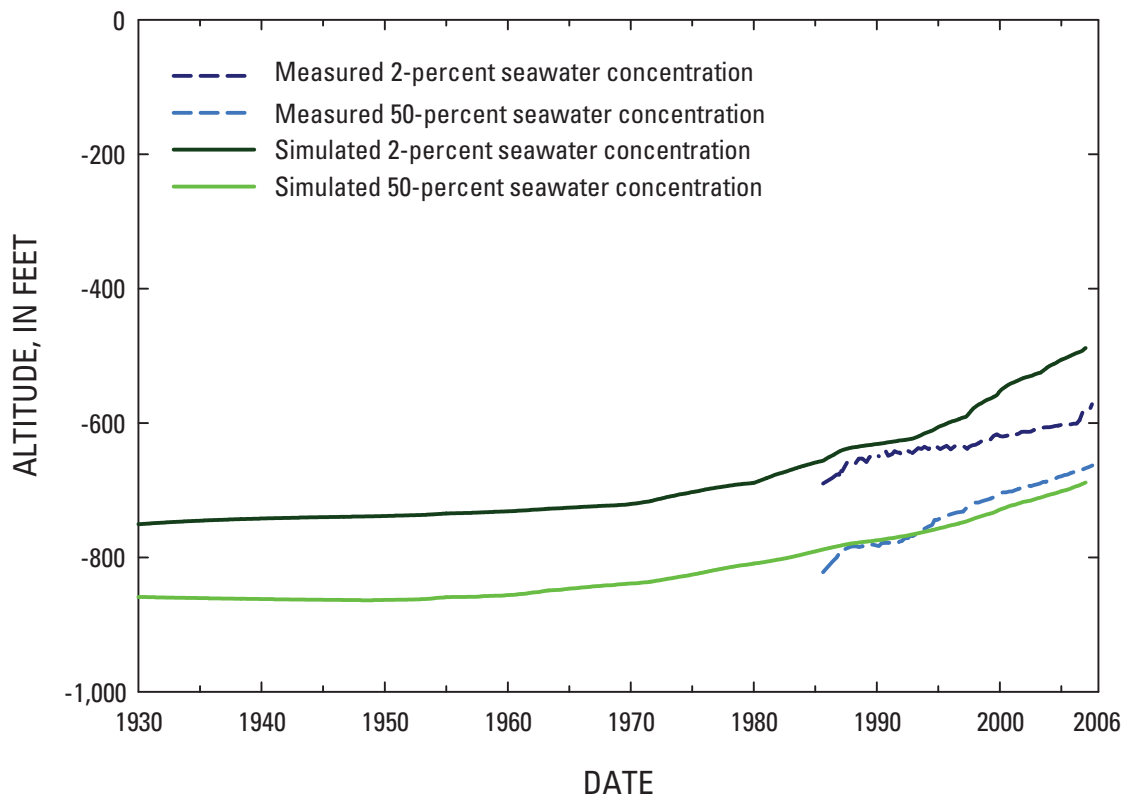


Figure 28. Measured and simulated altitude of the top (2-percent seawater) and middle (50-percent seawater) of the transition zone in the Waiehu Deep Monitor well (5430-05), Maui, Hawai'i.

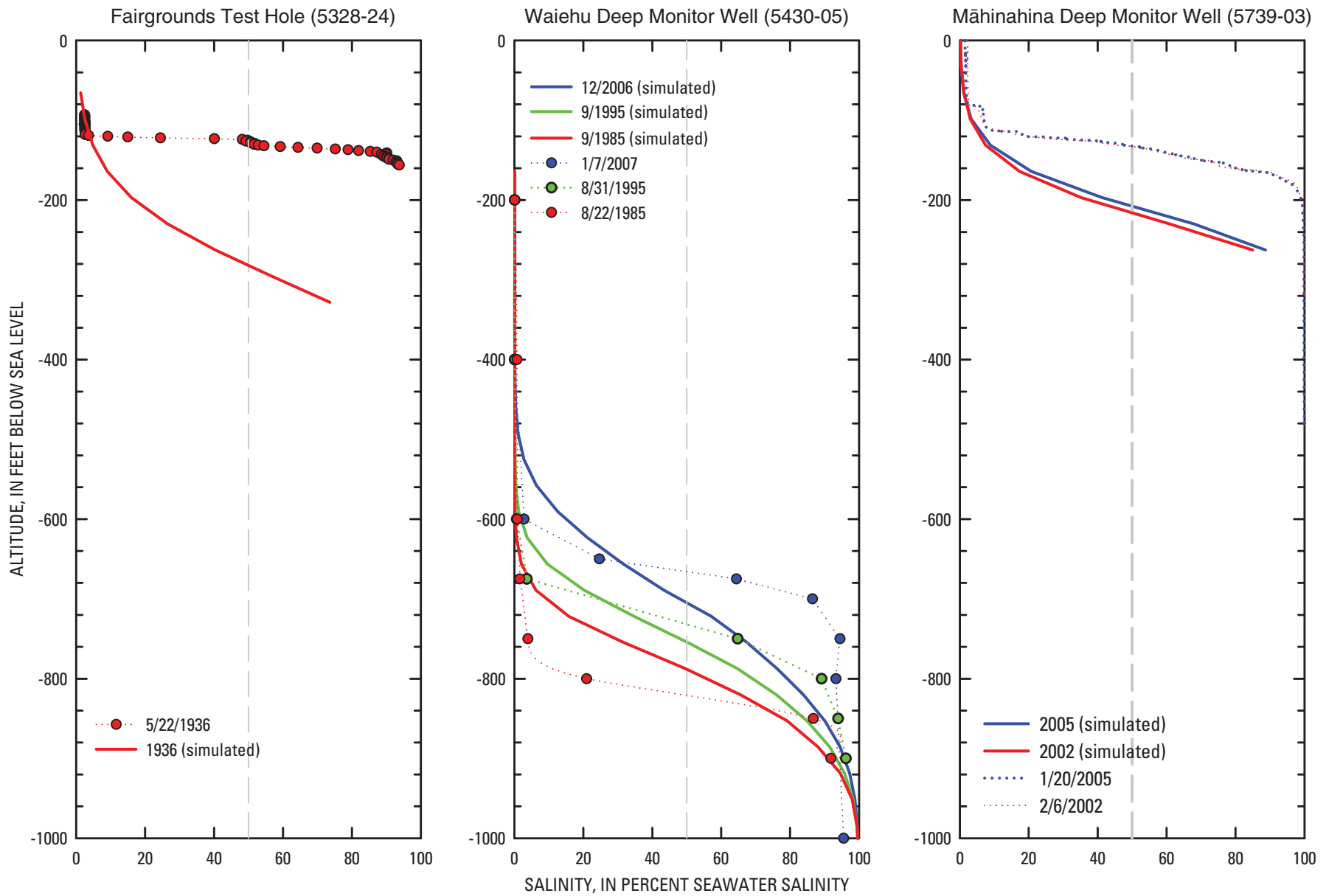


Figure 29. Measured and simulated salinity profiles in selected wells in central and west Maui, Hawai'i.

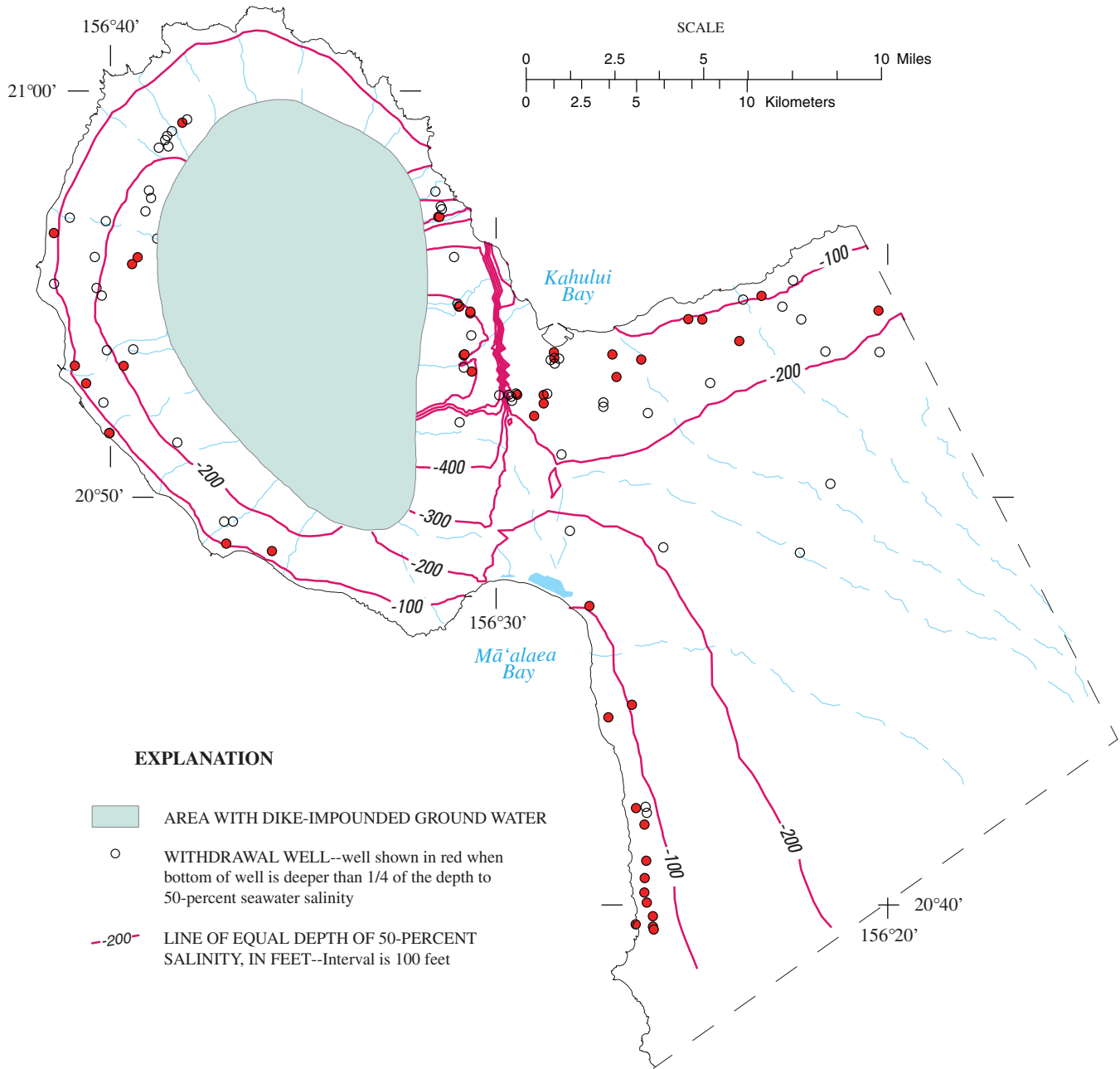


Figure 30. Simulated depth of 50-percent seawater salinity at end of historical simulation (2006) and locations of wells penetrating deeper than 1/4 of the simulated depth to 50-percent seawater salinity in central and west Maui, Hawai'i.

Table 6. Withdrawal and recharge used in various simulation scenarios, central and west Maui, Hawai'i.

[All simulations are from 2007–2157, except scenario 4 from 2007–2037; Mgal/d, million gallons per day]

Scenario	Recharge condition	Pumping condition in Wailuku Aquifer Sector Management Area
1	350 Mgal/d: 2000–04 land use with 1926–2004 rainfall	21.4 Mgal/d: 2006 withdrawal rates
2	350 Mgal/d: 2000–04 land use with 1926–2004 rainfall	20.1 Mgal/d: 1996 withdrawal rates
3	350 Mgal/d: 2000–04 land use with 1926–2004 rainfall	27.1 Mgal/d: Redistributed withdrawal
4	251 Mgal/d during drought: 2000–04 land use with 1926–2004 rainfall with worst historic drought (1998–2002 rainfall) during 2017–2022	27.1 Mgal/d: Redistributed withdrawal
5	362.3 Mgal/d: 2000–04 land use with 1926–2004 rainfall plus 12.3 Mgal/d of recharge from four 'īao/Waihe'e area streams	27.1 Mgal/d: Redistributed withdrawal
6	354.1 Mgal/d: 2000–04 land use with 1926–2004 rainfall plus 4.1 Mgal/d of recharge from four 'īao/Waihe'e area streams	27.1 Mgal/d: Redistributed withdrawal
7	274 Mgal/d: Natural land use with 1926–2004 rainfall plus 12.3 Mgal/d of recharge from four 'īao/Waihe'e area streams	27.1 Mgal/d: Redistributed withdrawal

(5731-05) represents the Kānoa well field of Kānoa 1 (5731-02) and Kānoa 2 (5731-04); North Waihe'e well field includes North Waihe'e 1 (5631-02 [deepest]) and North Waihe'e 2 (5631-03) wells; Waihe'e well field includes Waihe'e 1 (5431-02 [deepest]), Waihe'e 2 (5431-03), and Waihe'e 3 (5431-04); Waiehu Heights well field includes Waiehu Heights 1 (5430-01 [deepest]) and Waiehu Heights 2 (5430-02); Mokuahau well field includes Mokuahau pump 2 (5330-09), Mokuahau pump 1 (5330-10), and Mokuahau pump 3 (5330-11).

Scenario 1—2006 Withdrawal Rates and Locations with 2000–04 Land Use and 1926–2006 Rainfall

In scenario 1, the most likely future average recharge and most recent withdrawal estimates were used to simulate the effects of continuing the current conditions over the next 150 years. Assigned total recharge over the model domain was 350 Mgal/d, based on 2000–04 land use and 1926–2006 rainfall (table 6). Total withdrawal was simulated in two ways on the basis of reported 2006 withdrawal rates using (1) monthly rates and (2) average annual rates. This approach was used to determine whether using average annual rates, which provide faster and slightly more stable model solutions versus using monthly rates, was acceptable. Total withdrawal averaged 69 Mgal/d throughout the modeled area, with about 21.4 Mgal/d from the Wailuku Aquifer Sector (16.8 Mgal/d from 'īao and 4.6 Mgal/d from Waihe'e Aquifer Systems).

Model results indicate that for most wells, average annual withdrawal rates provide the same long-term trends computed using monthly withdrawal rates (fig. 31). For each well shown, the simulated water level is the average of the water levels of the nodes representing the well and the simulated salinity is for the deepest node representing the well. The exception to this is the Waiehu Deep Monitor well (5430-05), where the simulated

water level is determined nearer the top of the well's open interval at -138 ft. The depths of the nodes used are shown under each well name and number. Simulated seasonal water-level fluctuations, caused as pumping varies throughout the year, are centered about the water levels at annual average rates for all of the wells pictured. The largest seasonal fluctuations, about 4 ft/yr, are near the Waihe'e and Mokuahau well fields (as indicated by Waihe'e 1 (5431-02) and Mokuahau 2 (5330-09) wells, respectively). Long-term average water-level differences are 2–3 ft lower than the starting water levels after 150 years in many of the wells. Simulated salinity values are the same for both withdrawal methods in the wells with the freshest water but slightly higher for the simulated monthly withdrawals in the wells where salinity is increasing over time. This result is consistent with the understanding that cyclical withdrawal from a freshwater-lens system tends to increase mixing of water in the aquifer. The largest long-term simulated salinity increases are at the Kūpa'a well (5731-03) and Kānoa well field (as indicated by Kānoa Test Hole (5731-05)), where the salinity increases by about 1-percent seawater salinity over 150 years. The largest seasonal fluctuations, at the Kānoa well field, are about 0.5-percent seawater salinity. Near the Waiehu Heights well field, the model develops a numerical instability, when monthly pumping rates are used, most likely because of numerical dispersion near the top of the transition zone enhanced by the monthly change in withdrawal rates in the well. This instability goes away when yearly pumping rates are used.

The simulated depths of the bottom of freshwater and the middle of the transition zone at the Waiehu deep monitor well continue to shallow and are about 250 ft shallower after 150 years (fig. 32). These results are identical for both simulated withdrawal methods. Regional changes of average water levels in the aquifer after 150 years, presented relative to conditions at the end of the 1926–2006 historical simulation, are greatest

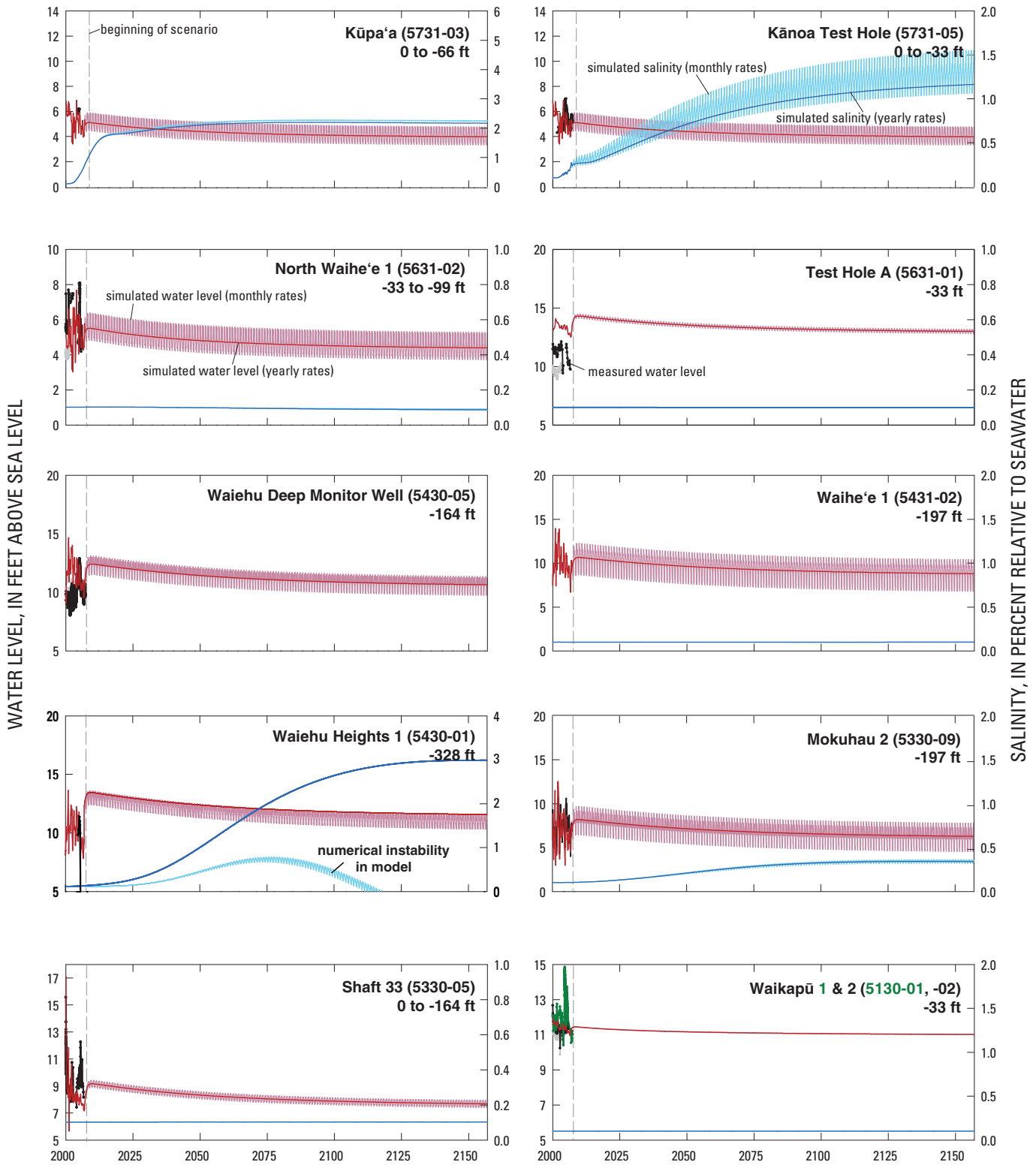


Figure 31. Measured (black and green lines) and simulated water-level (red lines) and simulated salinity data (blue lines) for Scenario 1 using monthly and yearly pumping rates at selected wells in the Wailuku Aquifer Sector, 2000–2157, Maui, Hawai‘i. For each well shown, the simulated water level is the average of the water levels of the nodes representing the well and the simulated salinity is for the deepest node representing the well. The exception to this is the Waiehu Deep Monitor well (5430-05), where the simulated water is determined nearer the top of the well’s open interval at -138 ft. The depths of the nodes used are shown under each well name and number.

inland of the four main well fields in the 'Āao Aquifer System, where average water-level differences are 1–3 ft lower (fig. 33). Near the well fields in the Waihe'e Aquifer System, average water-level differences are higher by less than a foot. However, this apparent rise results because water levels at the end of the historical simulation are available only at the time in the yearly pumping pattern when withdrawal is highest, whereas the water levels at the end of the 150 years are from a time when the withdrawal is lowest. Even though average water levels are about 1 ft lower, the monthly low water level at the beginning of the simulation is lower than the monthly high water level at the end of the simulation, giving an apparent rise of the water table in figure 33. The freshwater body has thinned, mainly in the 'Āao Aquifer System, as the depths of the bottom of the freshwater and the middle of the transition zone are higher in a broad area by more than 200 ft.

As the freshwater body thins, the simulated salinity at the Waiehu Heights well field moves into the cautionary salinity class (1.0–2.5 percent seawater) after 30 years (fig. 34). After 150 years, the simulated salinity at the Waiehu Heights well field is in the threatened class (greater than 2.5 percent seawater salinity) and the simulated salinity at the Kānoa well field is in the cautionary class. The Waiehu Heights wells are more vulnerable to increased salinities because they penetrate deeper below sea level than other withdrawal wells; Waiehu Heights 1 (5430-01) is open to the aquifer down to 338 ft below sea level. The Kānoa wells are more vulnerable to increased salinities because they are near the northern limit of the sedimentary caprock where the freshwater lens is thinner and less isolated from the ocean.

For this scenario, withdrawal of 4.6 Mgal/d from Waihe'e Aquifer System results in 2.83 Mgal/d of cautionary yield after 150 years (table 7). Withdrawal of 16.8 Mgal/d from 'Āao Aquifer System results in 1.51 Mgal/d of cautionary yield after 30 years and 1.51 Mgal/d of threatened yield after 150 years. No withdrawal was simulated from the Waikapū aquifer system.

Scenario 2—1996 Withdrawal Rates and Locations with 2000–04 Land Use and 1926–2006 Rainfall

In 1996, 20.1 Mgal/d were withdrawn from four well fields in the 'Āao Aquifer System, before withdrawal was spread north into the Waihe'e Aquifer System (fig. 13). By simulating this withdrawal condition during 1996–2006 and then 150 years into the future, the long-term effects of ground-water withdrawal near the CWRM's sustainable yield estimate from four well fields in the 'Āao Aquifer System can be investigated. Assigned total recharge over the model domain was 350 Mgal/d based on 2000–04 land use and 1926–2006 rainfall (table 6). Total withdrawal averaged 77 Mgal/d throughout the modeled area, with 20.1 Mgal/d from the 'Āao Aquifer System, and was simulated using monthly rates.

Several well fields show significant water-level declines and salinity increases when the 1996 rates are maintained for 150 years (fig. 35). Average water levels decline as much as 5 ft at the Mokuhau well field and simulated salinity values increase to 2–3 percent seawater salinity (as indicated by Mokuhau 2 (5330-09)). Salinities at Waiehu Heights well field increase to about 15-percent seawater salinity, and salinities increase to about 1.5-percent seawater salinity at Waihe'e well field. These results indicate that the 1996 pumping distribution would cause several well fields to produce nonpotable water in the future. Water levels at wells in the Waihe'e Aquifer System increase and salinity decreases because these wells were not pumped in this simulation. The simulated depths of the bottom of freshwater and the middle of the transition zone at the Waiehu deep monitor well are about 300 ft shallower after 150 years (fig. 36). Regional changes of water levels and freshwater depths in the aquifer after 150 years, presented relative to conditions at the end of the historical simulation, are greatest inland of the Waiehu Heights and Mokuhau well fields. Water levels decrease more than 3 ft and the depths of the bottom of

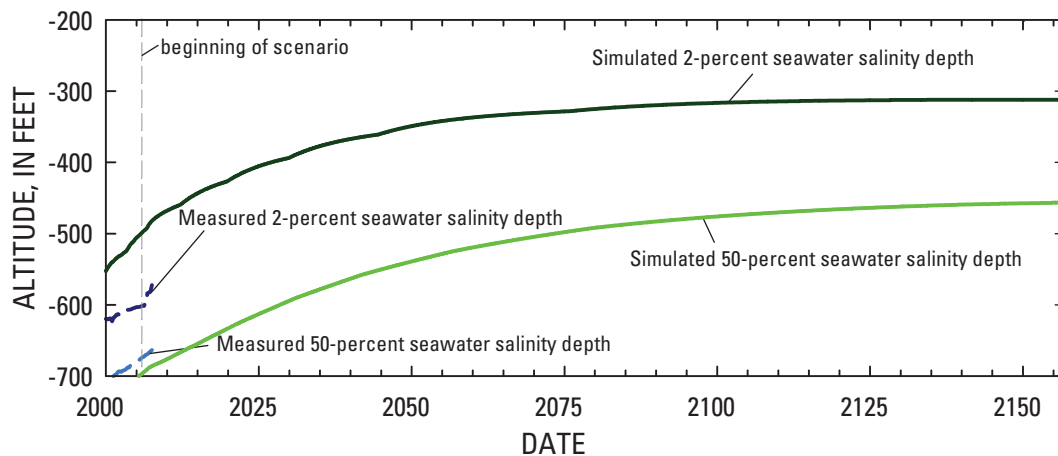


Figure 32. Measured and simulated positions of the bottom of freshwater (2-percent seawater salinity) and middle of the transition zone (50-percent seawater salinity) for Scenario 1 at the Waiehu Deep Monitor well (5430-05), 2000–2157, Maui, Hawaii.

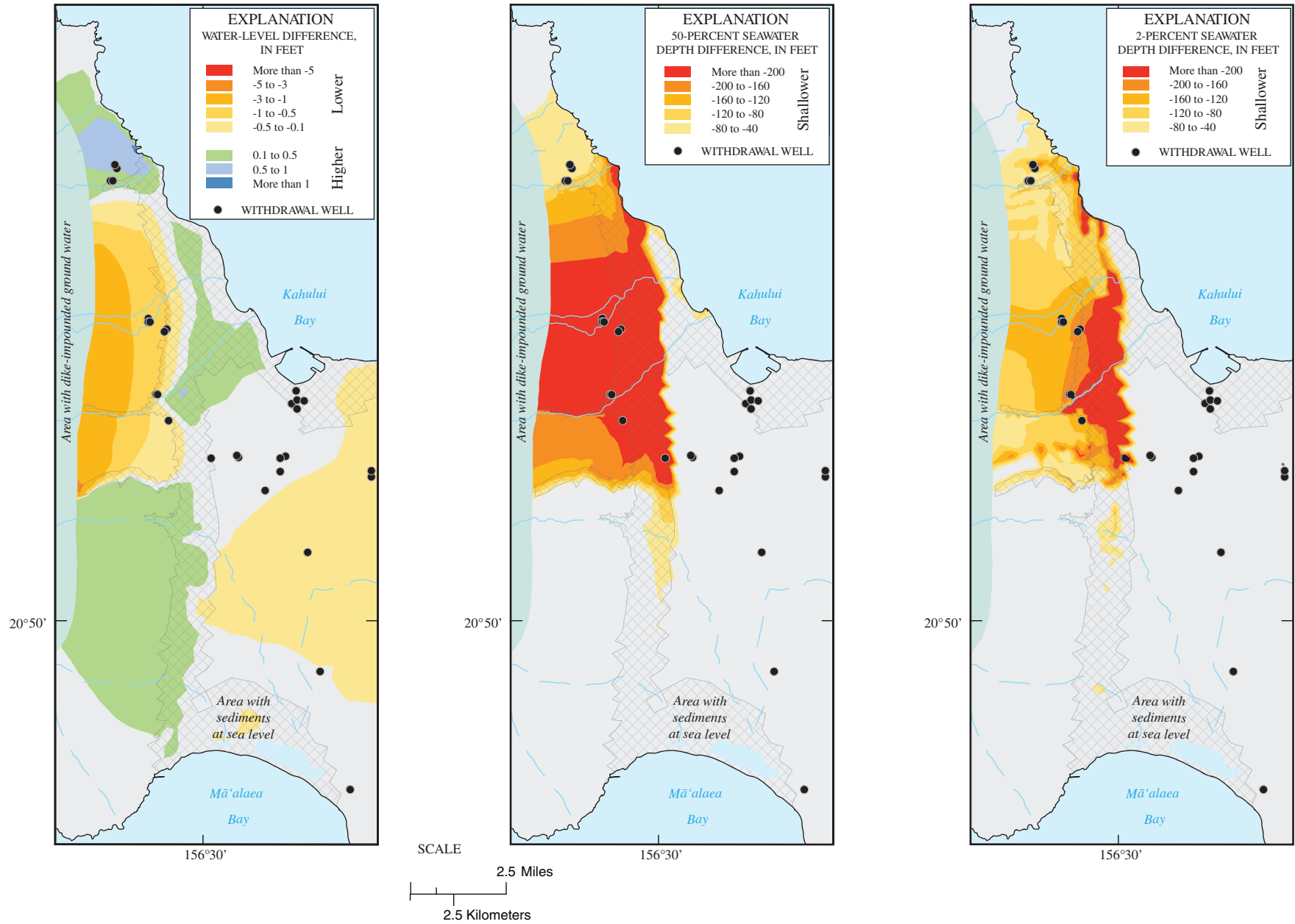


Figure 33. Simulated change (relative to end of historical simulation) in water level, 50-percent seawater salinity depth, and 2-percent seawater salinity depth after 150 years of withdrawal at 2006 rates with long-term average recharge (1926–2006) [scenario 1], central Maui, Hawai'i.

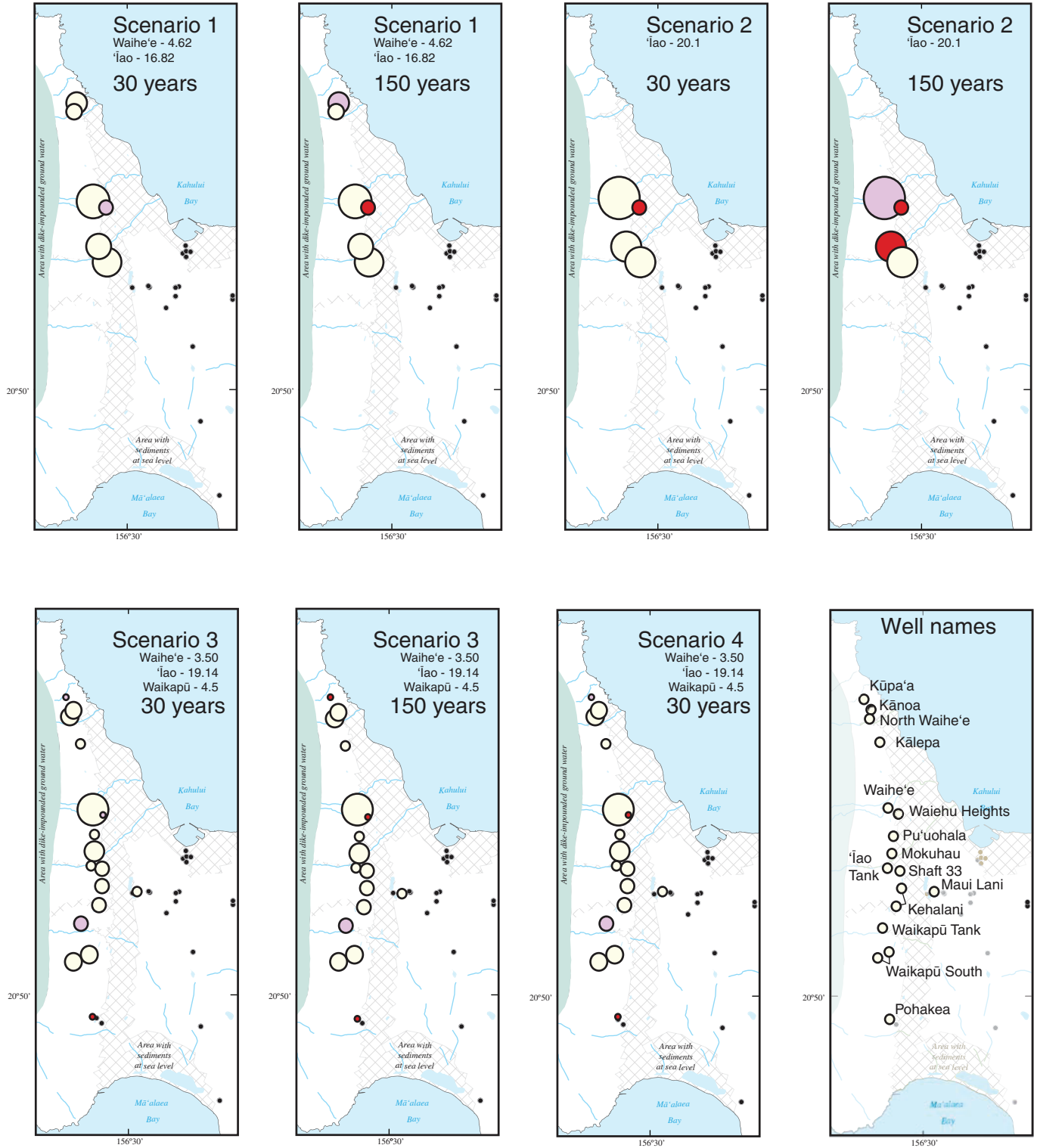


Figure 34. Predicted salinities in wells included in scenarios 1–7, central Maui, Hawai'i.

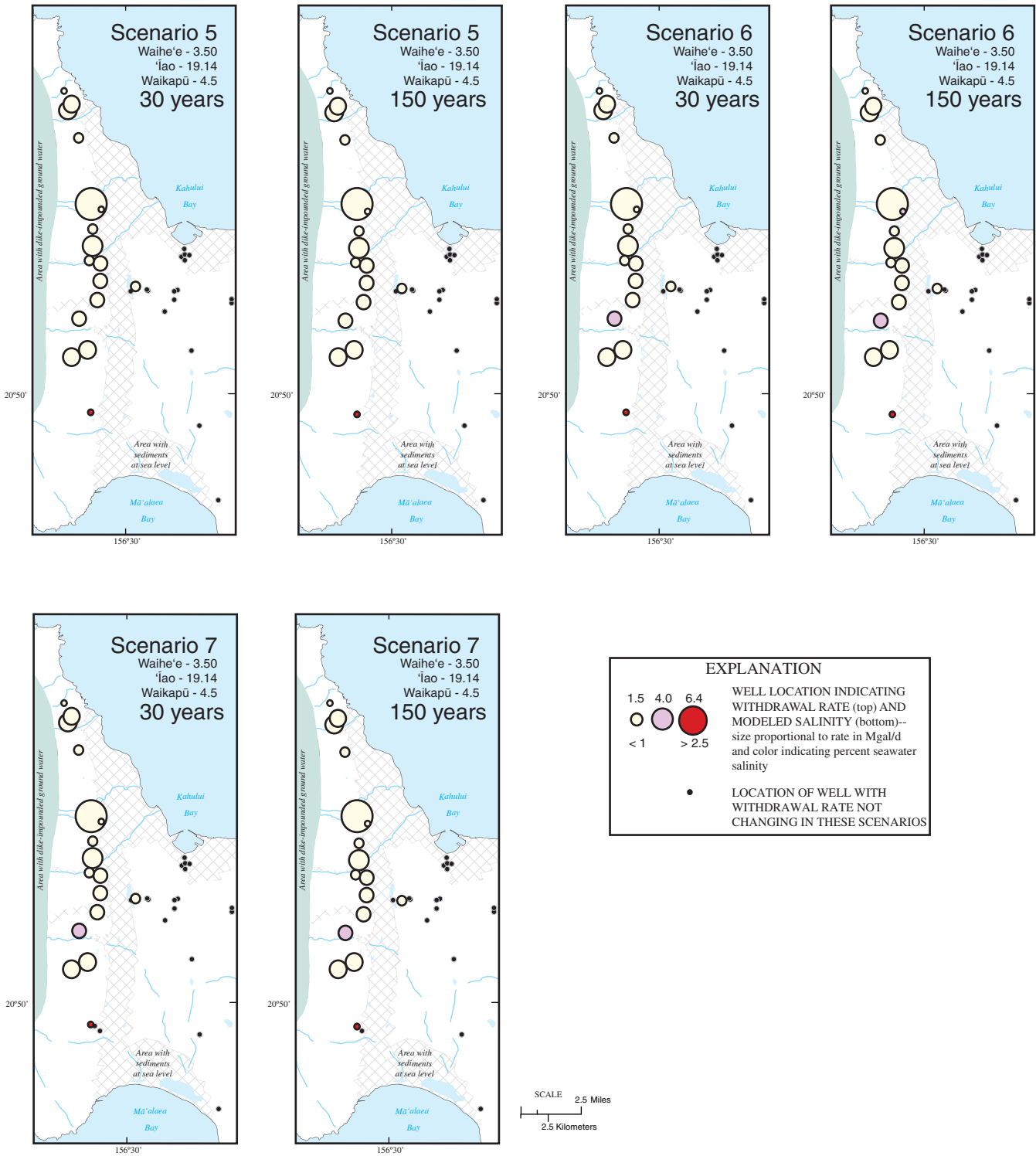


Figure 34.—Continued.

Table 7. Classification of withdrawal for simulated scenarios, Wailuku Aquifer Sector, Maui, Hawai'i.

[All results in million gallons per day; CWRM, State of Hawai'i Commission on Water Resource Management; na, not applicable]

Aquifer system	CWRM sustainable yield	Total simulated withdrawal	After 30 years		After 150 years	
			Cautionary withdrawal	Threatened withdrawal	Cautionary withdrawal	Threatened withdrawal
Scenario 1—2006 withdrawal						
Waihe'e	8	4.6	0.0	0.0	2.83	0.0
Īao	20	16.8	1.51	0.0	0.0	1.51
Waikapū	2	0.0	0.0	0.0	0.0	0.0
Scenario 2—1996 withdrawal						
Waihe'e	8	0.0	0.0	0.0	0.0	0.0
Īao	20	20.1	8.23	1.56	0.0	14.94
Waikapū	2	0.0	0.0	0.0	0.0	0.0
Scenario 3—redistributed withdrawal						
Waihe'e	8	3.5	0.5	0.0	0.0	0.5
Īao	20	19.14	2.1	0.0	1.5	0.6
Waikapū	2	4.5	0.0	0.5	0.0	0.5
Scenario 4—5-yr drought						
Waihe'e	8	3.5	0.5	0.0	na	na
Īao	20	19.14	1.5	0.6	na	na
Waikapū	2	4.5	0.0	0.5	na	na
Scenario 5—restored streamflow (12.3 Mgal/d)						
Waihe'e	8	3.5	0.0	0.0	0.0	0.0
Īao	20	19.14	0.0	0.0	0.0	0.0
Waikapū	2	4.5	0.0	0.5	0.0	0.5
Scenario 6—restored streamflow (4.1 Mgal/d)						
Waihe'e	8	3.5	0.0	0.0	0.0	0.0
Īao	20	19.14	1.5	0.0	2.1	0.0
Waikapū	2	4.5	0.0	0.5	0.0	0.5
Scenario 7—no irrigation						
Waihe'e	8	3.5	0.0	0.0	0.0	0.0
Īao	20	19.14	1.5	0.0	1.5	0.0
Waikapū	2	4.5	0.0	0.5	0.0	0.5

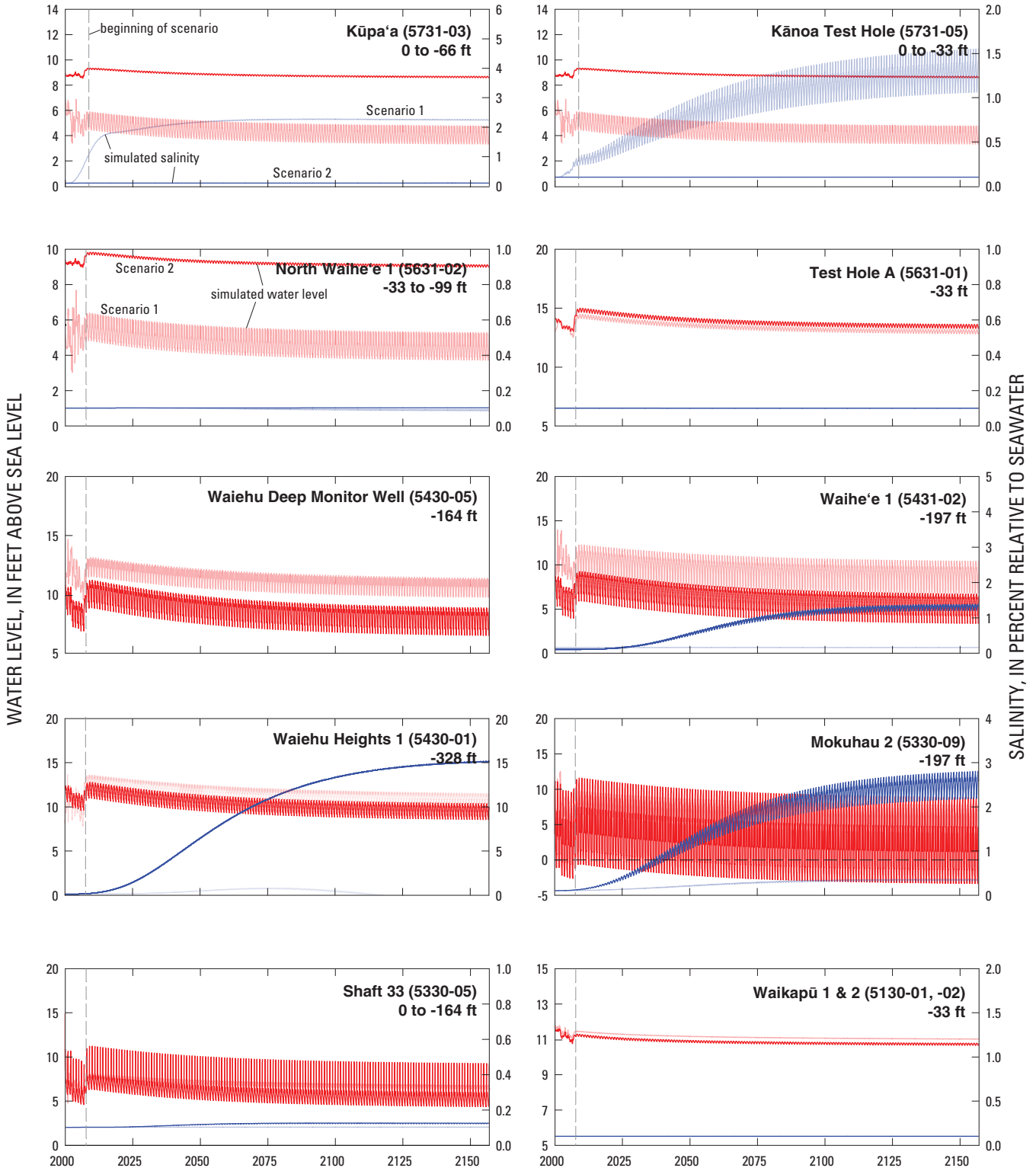


Figure 35. Simulated water-level (red lines) and salinity (blue lines) data for Scenario 2 (dark lines) compared with Scenario 1 (light lines) at selected wells in the Wailuku Aquifer Sector, 2000–2157, Maui, Hawai'i. For each well shown, the simulated water level is the average of the water levels of the nodes representing the well and the simulated salinity is for the deepest node representing the well. The exception to this is the Waiehu Deep Monitor well (5430-05), where the simulated water is determined nearer the top of the well's open interval at -138 ft. The depths of the nodes used are shown under each well name and number.

the freshwater are shallower by more than 200 ft over a large area near the Waihe'e and Waiehu Heights well fields (fig. 37).

As the freshwater body thins the simulated salinity at the Waiehu Heights well field increases into the threatened range after 30 years (fig. 34). The simulated salinity at the Waihe'e well field becomes cautionary after 30 years and threatened after 150 years. Also after 150 years, the simulated salinity at the Mokuhau well field is in the threatened class. For this scenario, withdrawal of 20.1 Mgal/d from 'Āo Aquifer System results in 9.79 Mgal/d of cautionary and threatened yield after 30 years and 14.94 Mgal/d of threatened yield after 150 years. No withdrawal was simulated from the Waihe'e or Waikapū Aquifer systems (table 7).

Scenario 3—Redistributed Withdrawals with 2000–04 Land Use and 1926–2006 Rainfall

In scenario 3, ground-water withdrawal was redistributed to maximize withdrawal and minimize salinities in the pumped water. Reduced rates at existing wells were combined with withdrawal from potential new well sites that, in consultation with the Maui DWS, were determined reasonable locations for future water-system expansion. Rates and locations were adjusted in an iterative process, and the results of the various realizations were evaluated for acceptable conditions. A formal optimization procedure was not feasible because of the complexities and length of time required in simulating variable density ground-water flow. Assigned total recharge over the model domain was 350 Mgal/d, based on 2000–04 land use and 1926–2006 rainfall (table 6). Total withdrawal was simulated using annual rates, and the wells not included in the adjustment process were maintained at 2006 withdrawal rates. In the final redistributed condition, withdrawal was 75 Mgal/d throughout the modeled area, with about 27.1 Mgal/d from the Wailuku Aquifer Sector (table 7). Potential new withdrawal

locations in the Wailuku Aquifer Sector include existing but currently unused DWS wells at Kūpa'a (5731-03), 'Āo Tank (5230-03), and Waikapū Tank (5131-01), a set of private Pōhākea wells (4930-01 to -03), and new locations at Kālepa, Pu'uohala, Kehalani (2 wells), and Waikapū South (2 wells) (fig. 34; table 8). The Shaft 33 replacement well represents a vertical well drilled at the same location as the shaft. Also included is planned withdrawal from the Maui Lani wells (5229-04 to -06) in the Kahului Aquifer System.

Most wells have water-level declines and salinity increases after 150 years when compared to the end of the historical simulation when the redistributed rates and locations are maintained for 150 years, but the changes are less than observed after 150 years at the withdrawal wells in scenario 1 (fig. 38). Maximum water-level declines are 3–6 ft near the new wells. After 150 years, the simulated depths of the bottom of freshwater and the middle of the transition zone at the Waiehu Deep Monitor well are about 240–250 ft shallower than the end of the historical simulation but very similar to the depths at the end of scenario 1 (fig. 39). Regional differences of water levels and freshwater depths in the aquifer after 150 years, relative to conditions at the end of scenario 1, are largest around the new well fields, where water levels are more than 5 ft lower (fig. 40). Where withdrawal was reduced at some of the existing wells, water levels are as much as 1 ft higher relative to the end of scenario 1.

As the freshwater body thins, the simulated salinities at the Waiehu Heights well field, Waikapū Tank (5131-01), and Kūpa'a wells (5731-03) increase to cautionary after 30 years and the salinity at the Pōhākea wells (4930-01) becomes threatened (fig. 34). After 150 years, the simulated salinities at the Waiehu Heights well field and Kūpa'a well (5731-03) increase to threatened. The Waiehu Heights wells are more vulnerable to increased salinities because they penetrate deeper below sea level than other withdrawal wells; Waiehu Heights 1 (5430-01) is open to the aquifer down to 338 ft

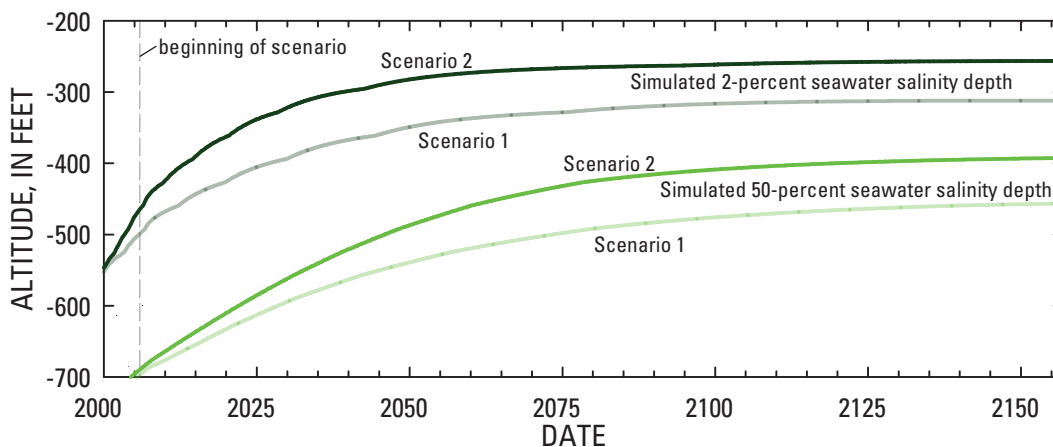


Figure 36. Simulated positions of the bottom of freshwater (2-percent seawater salinity) and middle of the transition zone (50-percent seawater salinity) for Scenario 2 at the Waiehu Deep Monitor well (5430-05), 2000–2157, Maui, Hawaii.

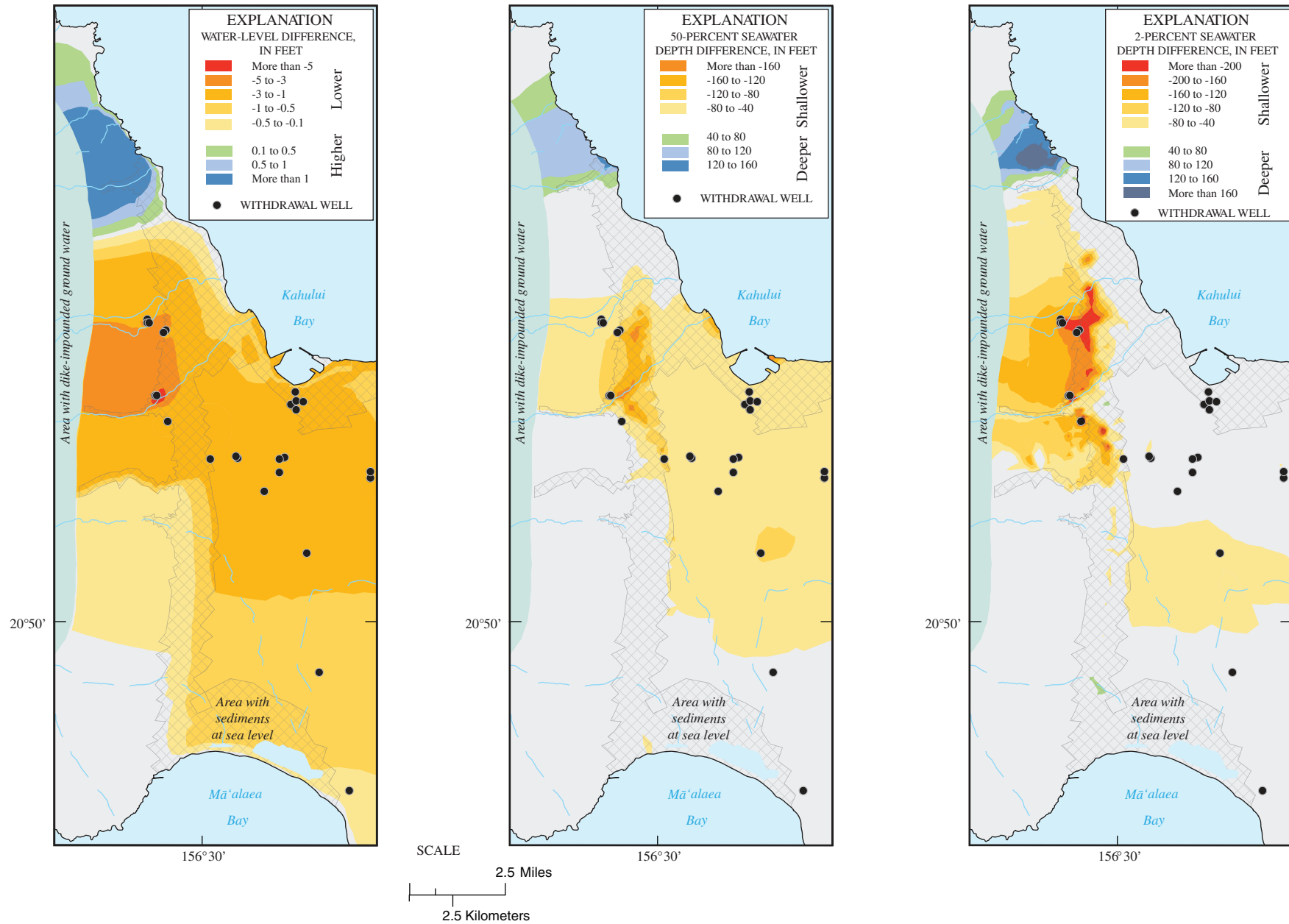


Figure 37. Simulated change (relative to end of historical simulation) in water level, 50-percent seawater salinity depth, and 2-percent seawater salinity depth after 150 years of withdrawal at 1996 rates with long-term average recharge (1926–2006) [scenario 2], central Maui, Hawai'i.

Table 8. Selected wells and rates used in redistributed withdrawal scenarios, central and west Maui, Hawai'i.

[All other wells remain at 2006 withdrawal rates]

Well name	Well number	Withdrawal rate (million gallons per day)
Waihe'e aquifer system		
North Waihe'e	5631-02,-03	1.57
Kānoa	5731-01,-02	1.43
Kūpa'a	5731-03	0.5
Total		3.5
Īao aquifer system		
Kālepa	new	1.0
Waiehu Heights	5430-01,-02	0.6
Waihe'e	5431-02,-03,-04	6.39
Pu'uohala	new	1.0
Mokuhau	5330-09,10,11	3.15
Īao Tank	5230-03	1.0
Shaft 33 replacement well	new	1.5
Waikapū Tank	5131-01	1.5
Kehalani 2	new	1.5
Kehalani 3	new	1.5
Total		19.14
Waikapū aquifer system		
Waikapū South	new	4.0
Pōhākea	4930-01,-02,-03	0.5
Total		4.5
Total Wailuku aquifer management area		27.14
Kahului aquifer system		
Maui Lani	5229-04,-05,-06	0.96

below sea level. The Kānoa wells are more vulnerable to increased salinities because they are near the northern limit of the sedimentary caprock and where the freshwater lens is thinner and less isolated from the ocean. Therefore, in the process of determining the desired redistributed withdrawal conditions, the simulated salinities at these well sites received less importance as, because of their depth and location, there was less concern whether the salinities increased. For this scenario, withdrawal of 3.5 Mgal/d from the Waihe'e Aquifer system results in 0.5 Mgal/d of cautionary yield after 30 years and 0.5 Mgal/d of threatened yield after 150 years (table 7). Withdrawal of 19.14 Mgal/d from Īao Aquifer System results in 2.10 Mgal/d of cautionary yield after 30 years and 2.10 Mgal/d of threatened and cautionary yield after 150 years. Withdrawal of 4.50 Mgal/d from Waikapū Aquifer System results in 0.5 Mgal/d of threatened yield after 30 and after 150 years.

Scenario 4—Effects of Drought on Redistributed Withdrawals

The effects of drought and the redistributed withdrawal were investigated in scenario 4. Assigned total recharge over the model domain was 350 Mgal/d, based on 2000–04 land use and 1926–2006 rainfall during simulation periods 2007–16 and 2022–37. A 5-yr drought in the middle of the 30-yr simulation was represented during simulation period 2017–21 using historical recharge conditions estimated with 2000–04 land use and 1998–2002 rainfall (Engott and Vana, 2007, table 11). The recharge during this period was 251 Mgal/d. In the redistributed withdrawal condition, withdrawal was 75 Mgal/d throughout the modeled area, with about 27.1 Mgal/d from the Wailuku Aquifer Sector. This scenario is considered a worst-case scenario, because the 5-yr drought is not balanced by

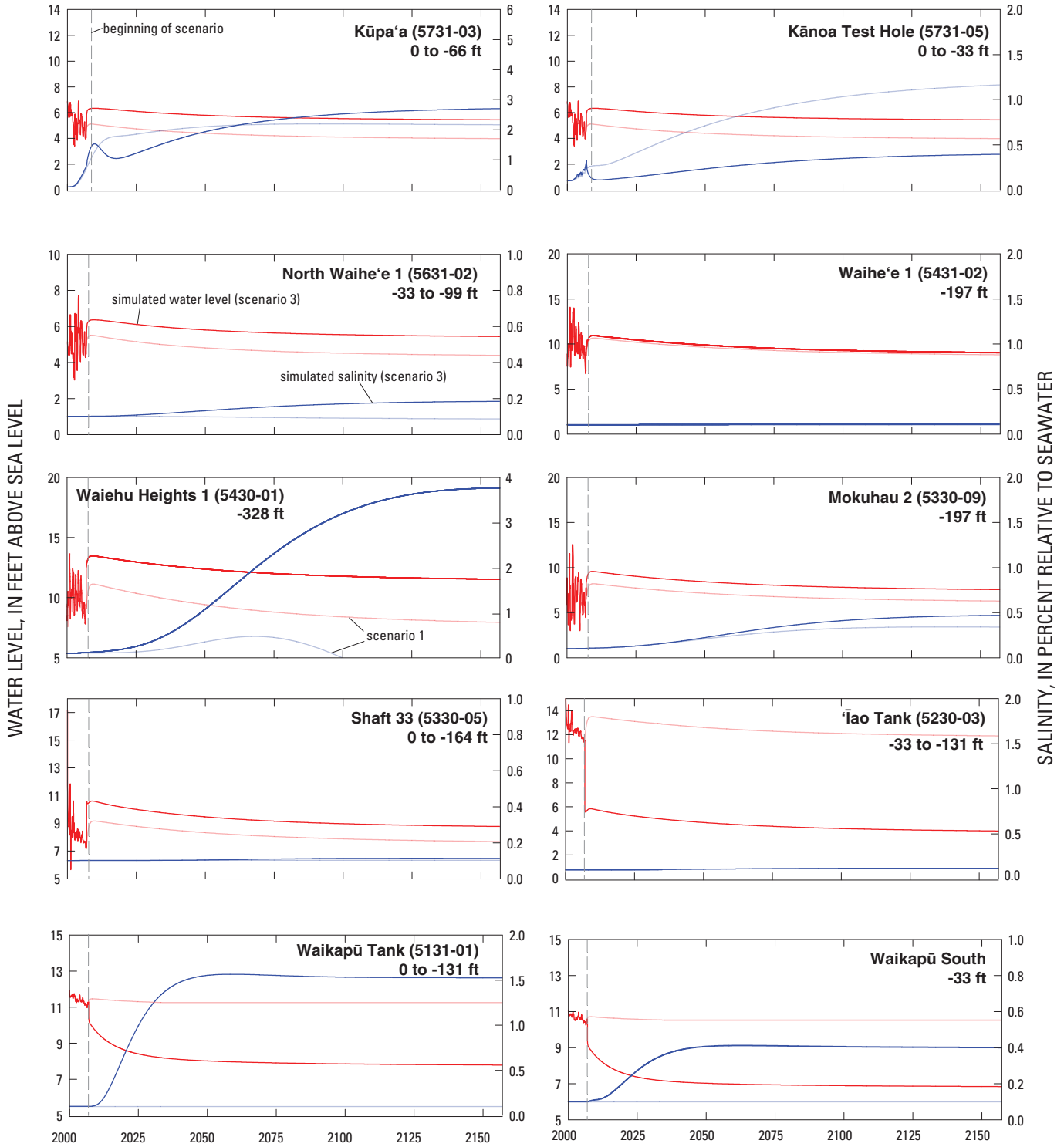


Figure 38. Simulated water-level (red lines) and salinity (blue lines) data for Scenario 3 (dark lines) compared with Scenario 1 (light lines) at selected wells in the Wailuku Aquifer Sector, 2000–2157, Maui, Hawai'i. For each well shown, the simulated water level is the average of the water levels of the nodes representing the well and the simulated salinity is for the deepest node representing the well. The depths of the nodes used are shown under each well name and number.

some compensating wet years that would typically occur to balance out the long-term average during a 30-yr period.

Differences in water levels between the drought and the nondrought scenario are insignificant after 30 years (fig. 41). Water levels are 2–5 ft lower by the end of the 5-yr drought but recover relatively quickly to the same water levels as the non-drought conditions by the end of the 30-yr simulation. Simulated salinities increase in several wells during the drought and do not return to the same salinities as during the prior nondrought conditions after 30 years. The most significant salinity increases are at the Waiehu Heights well field and Kūpa‘a well (5731-03), where the salinities are about 2 and 1 percent higher, respectively, relative to the nondrought scenario after 30 years. This demonstrates that movement of the transition zone can commonly lag behind head changes at the water table, because it takes longer for the stresses to propagate downward through the aquifer. The simulated depths of the bottom of freshwater and the middle of the transition zone at the Waiehu Deep Monitor well are shallower relative to the nondrought scenario after 30 years (fig. 42). The middle of the transition zone is about 10 ft shallower and the bottom of the freshwater is about 50 ft shallower at the end of the 30-yr simulation.

Because of the drought, the simulated salinities at the Waiehu Heights wells (5430-01) increase to threatened after 30 years (fig. 34). In scenario 3, the simulated salinities in this well were lower, in the cautionary class. For this scenario, withdrawal of 3.5 Mgal/d from the Waihe‘e Aquifer system results in 0.5 Mgal/d of cautionary yield after 30 years (table 7). Withdrawal of 19.14 Mgal/d from ‘Īao Aquifer System results in 2.10 Mgal/d of cautionary and threatened yield after 30 years. Withdrawal of 4.50 Mgal/d from Waikapū Aquifer System results in 0.5 Mgal/d of threatened yield after 30 years.

Scenarios 5 and 6—Effects of Restoring Streamflow on Redistributed Withdrawals

The effects of restoring all or a portion of currently diverted streamflow to four streams overlying the Wailuku Aquifer Sector were investigated in scenarios 5 and 6. Assigned total recharge over the model domain was based on 2000–04 land use, 1926–2006 rainfall, and an additional 12.3 Mgal/d (scenario 5) or 4.1 Mgal/d (scenario 6) of recharge distributed along Waikapū, ‘Īao, and Waiehu Streams and Waihe‘e River (table 6). The additional recharge for scenario 5 was estimated assuming no stream diversions and that all seepage loss measured in these streams (table 1) recharges the aquifer at sea level. Scenario 6 represents a case where one-third of the diverted streamflow is restored to the streams and seepage losses are proportionally lower. Neither scenario 5 nor 6 was simulated ideally, because no recharge distribution is available that includes removal of just the irrigation provided by these four streams. However, between Waihe‘e River and Waikapū Stream, there is very little land use in the 2000–04 period that includes irrigation (fig. 2), so the change between the available recharge distribution used for these scenarios and a recharge distribution with irrigation water from these four streams removed would be insignificant. Therefore, these scenarios provide an adequate representation of conditions for the area of interest. Scenarios 5 and 6 represent possible future conditions but are not posed as recommendations or suggestions for future stream management. Ground-water withdrawal in scenario 5 and 6 was the same as in scenario 3, in which withdrawal was 75 Mgal/d throughout the modeled area, with about 27.1 Mgal/d from the Wailuku Aquifer Sector.

All Wailuku Aquifer Sector well fields show significant water-level increases and salinity decreases relative to scenario 3

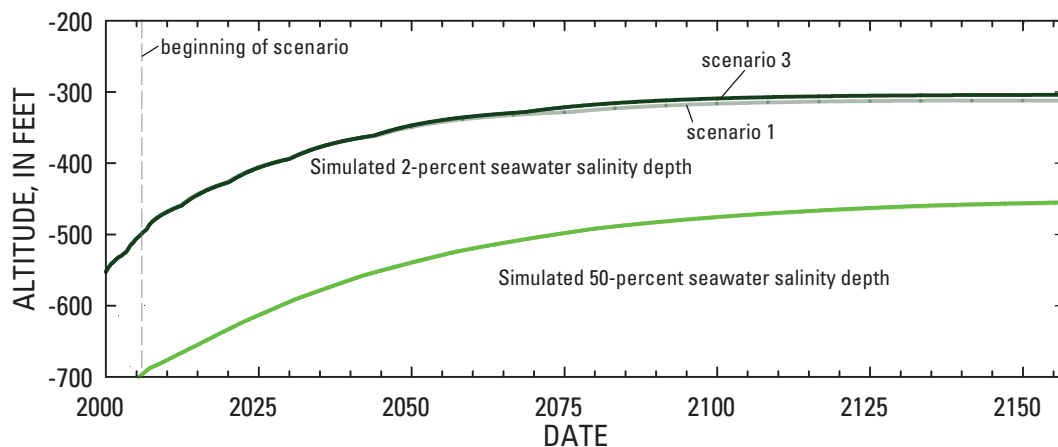


Figure 39. Simulated positions of the bottom of freshwater (2-percent seawater salinity) and middle of the transition zone (50-percent seawater salinity) for Scenario 3 compared with Scenario 1 at the Waiehu Deep Monitor well (5430-05), 2000–2157, Maui, Hawai‘i.

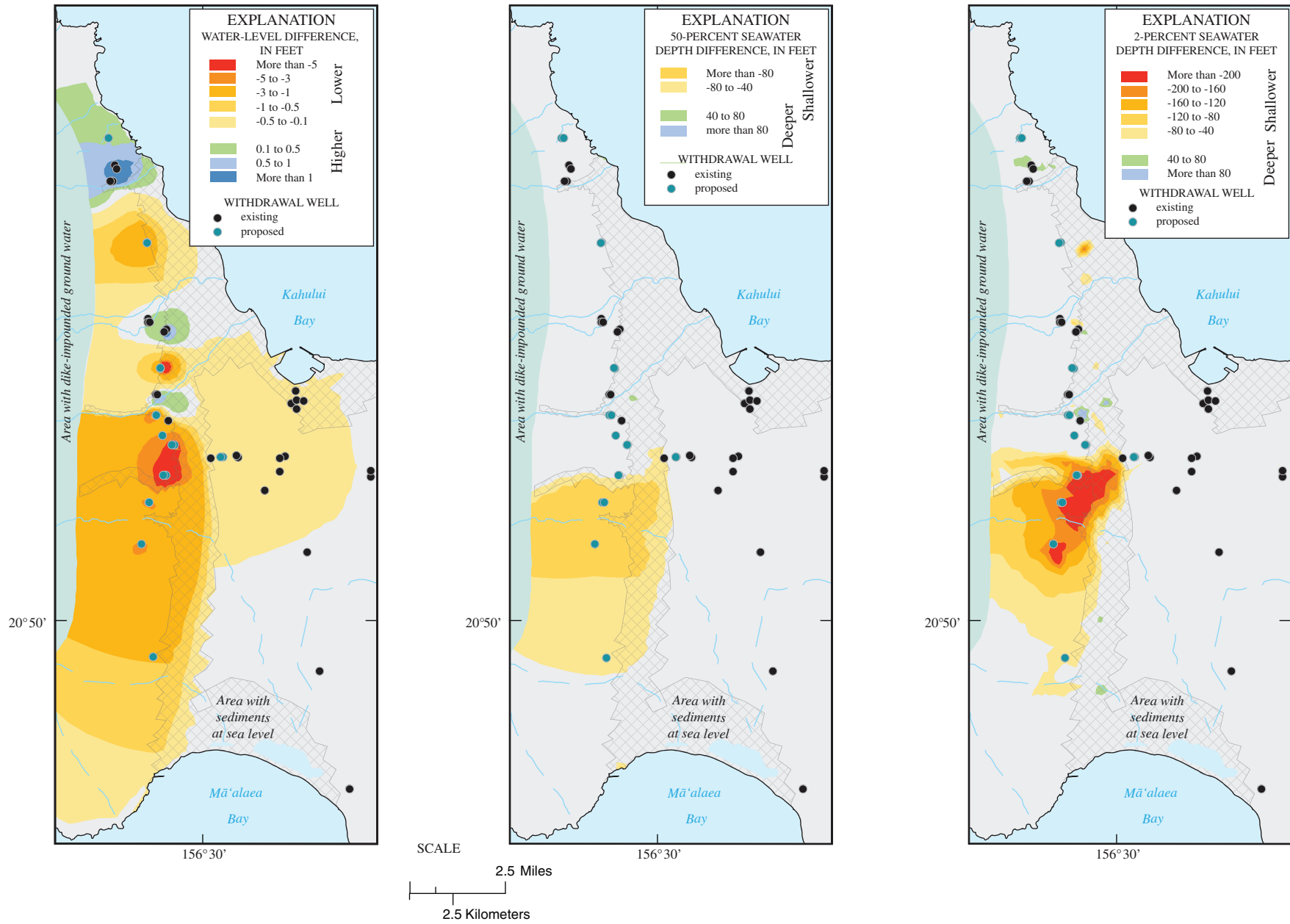


Figure 40. Simulated change (relative to scenario 1) in water level, 50-percent seawater salinity depth, and 2-percent seawater salinity depth after 150 years of withdrawal at redistributed rates with long-term average recharge (1926–2006) [scenario 3], Maui, Hawai'i.

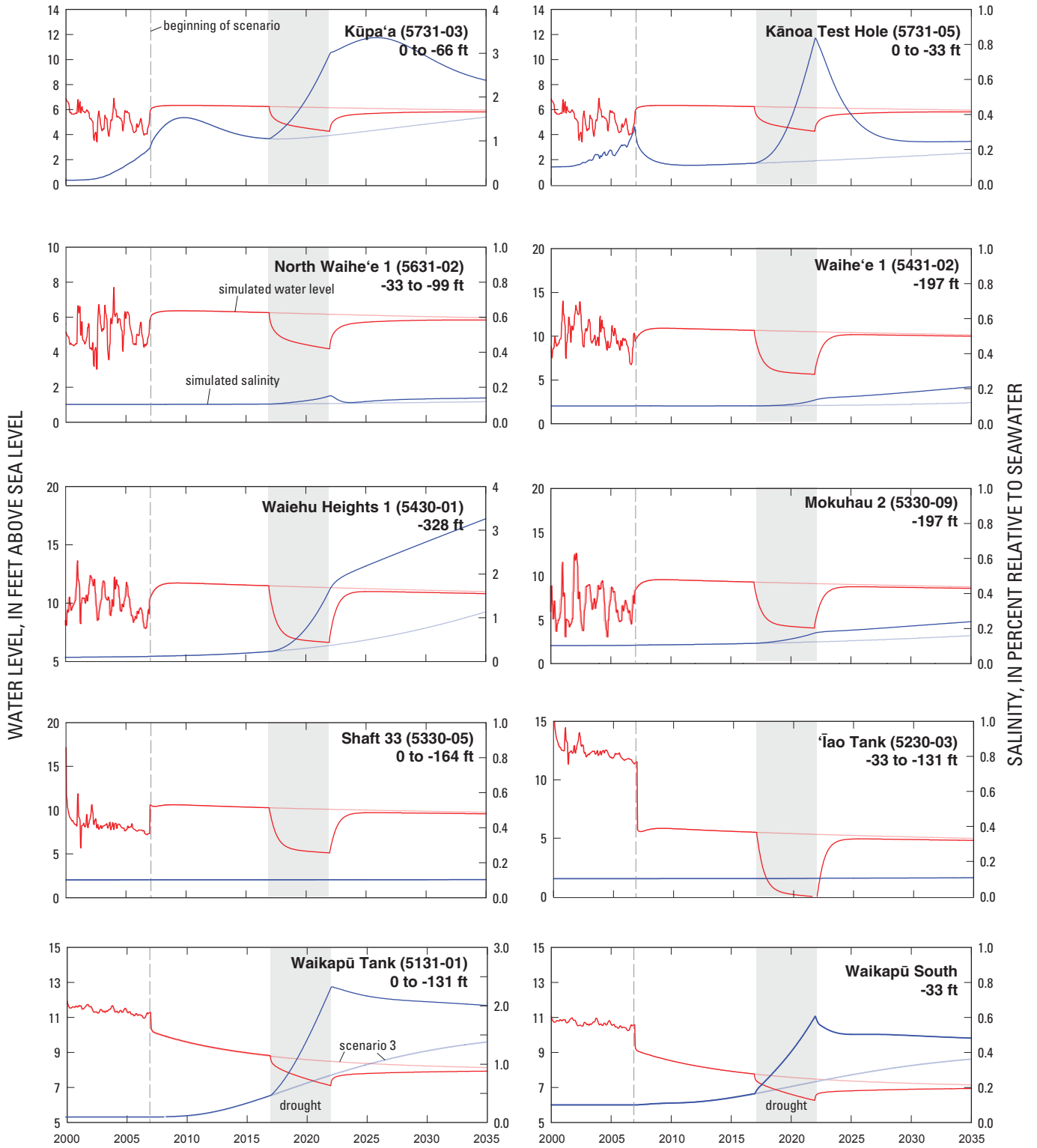


Figure 41. Simulated water-level (red lines) and salinity (blue lines) data for Scenario 4 (dark lines) compared with Scenario 3 (light lines) at selected wells in the Wailuku Aquifer Sector, 2000–35, Maui, Hawai‘i. The gray band represents the drought period. For each well shown, the simulated water level is the average of the water levels of the nodes representing the well and the simulated salinity is for the deepest node representing the well. The depths of the nodes used are shown under each well name and number.

after 150 years when the additional recharge is added beneath the streams (fig. 43). Average water levels are 1–5 ft higher for scenario 5 relative to the water levels at the end of scenario 3, with the largest differences at Waihe'e, Waiehu Heights, and Mokuhau well fields. Average water levels are 0.5–2 ft higher for scenario 6 relative to the water levels at the end of scenario 3. Simulated salinity values are lower at all of the well fields, with the largest differences at Waiehu Heights well field and Kūpa'a well (5731-03) (fig. 43). The simulated depths of the bottom of freshwater and the middle of the transition zone at the Waiehu Deep Monitor well from scenario 5 are about 160–170 ft deeper relative to scenario 3 after 150 years (fig. 44). For scenario 6, the simulated depths of the bottom of freshwater and the middle of the transition zone are about 100 ft deeper relative to scenario 3.

Regional changes of water levels and freshwater depths in the aquifer after 150 years, relative to conditions at the end of scenario 3, are greatest around 'Īao and Waiehu Streams where most of the additional recharge is located. In scenario 5, water levels are more than 5 ft higher and the depths of the bottom of the freshwater are deeper by more than 200 ft (fig. 45). In scenario 6, water levels are 1–3 ft higher and the depths of the bottom of the freshwater are deeper by 40–80 ft (fig. 46).

The additional recharge causes the freshwater body to thicken; therefore, some of the wells that were potentially or likely to produce water unacceptable for drinking in scenario 3 have lower simulated salinities in scenarios 5 and 6 (fig. 34). For scenario 5, the simulated salinities in all of the selected wells, with the exception of the Pōhākea wells in the Waikapū aquifer system, are in the acceptable class, even after 150 years. For scenario 6, the simulated salinity at Waikapū Tank well (5131-01) increases to cautionary after 30 years and remains cautionary after 150 years. For scenario 5, withdrawal of 3.5 Mgal/d from the Waihe'e Aquifer system results in no cautionary or threatened yield after 150 years (table 7). With-

drawal of 19.14 Mgal/d from 'Īao Aquifer System results in no cautionary or threatened yield after 150 years. Withdrawal of 4.50 Mgal/d from Waikapū Aquifer System results in 0.5 Mgal/d of threatened yield after 30 and 150 years. For scenario 6, withdrawal of 3.5 Mgal/d from the Waihe'e Aquifer system results in no cautionary or threatened yield after 150 years (table 7). Withdrawal of 19.14 Mgal/d from 'Īao Aquifer System results in 1.50 Mgal/d of cautionary yield after 30 years and 2.10 Mgal/d of cautionary yield after 150 years. Withdrawal of 4.50 Mgal/d from Waikapū Aquifer System results in 0.5 Mgal/d of threatened yield after 30 and after 150 years.

Scenario 7—Effects of No Agricultural Irrigation or Stream Diversions

The effects of removing agricultural irrigation in the study area were investigated in scenario 7. Recharge was based on the hypothetical Land Use III condition of Engott and Vana (2007, table 11) which represented 2000–04 land use, 1926–2004 rainfall, and no agricultural irrigation. Assigned recharge was 274 Mgal/d, which included 12.3 Mgal/d of additional recharge assuming no stream diversions for agricultural irrigation. Scenario 7 represents a hypothetical condition, the results of which can be informative about the hydrologic system, and it is not posed as a recommendation or suggestion for future land use. Ground-water withdrawal in scenario 7 was the same as in scenario 3, in which withdrawal was 75 Mgal/d throughout the modeled area, with about 27.1 Mgal/d from the Wailuku Aquifer Sector.

Most Wailuku Aquifer Sector well fields show significant water-level increases and salinity decreases relative to scenario 3 after 150 years (fig. 47). Near these withdrawal wells, the effect of the additional recharge beneath the streams is greater than the effects from the loss of recharge beneath the central

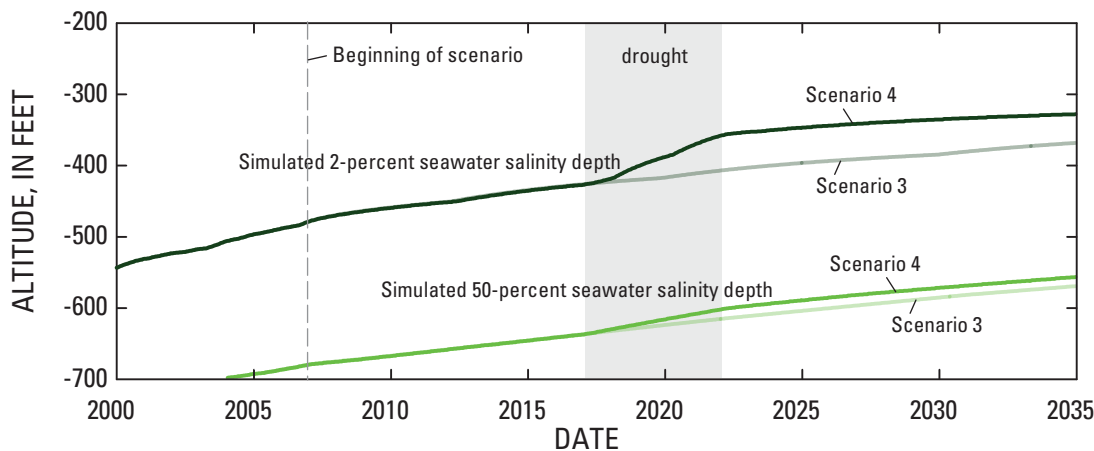


Figure 42. Simulated positions of the bottom of freshwater (2-percent seawater salinity) and middle of the transition zone (50-percent seawater salinity) for Scenario 4 compared with Scenario 3 at the Waiehu Deep Monitor well (5430-05), 2000–35, Maui, Hawai'i.

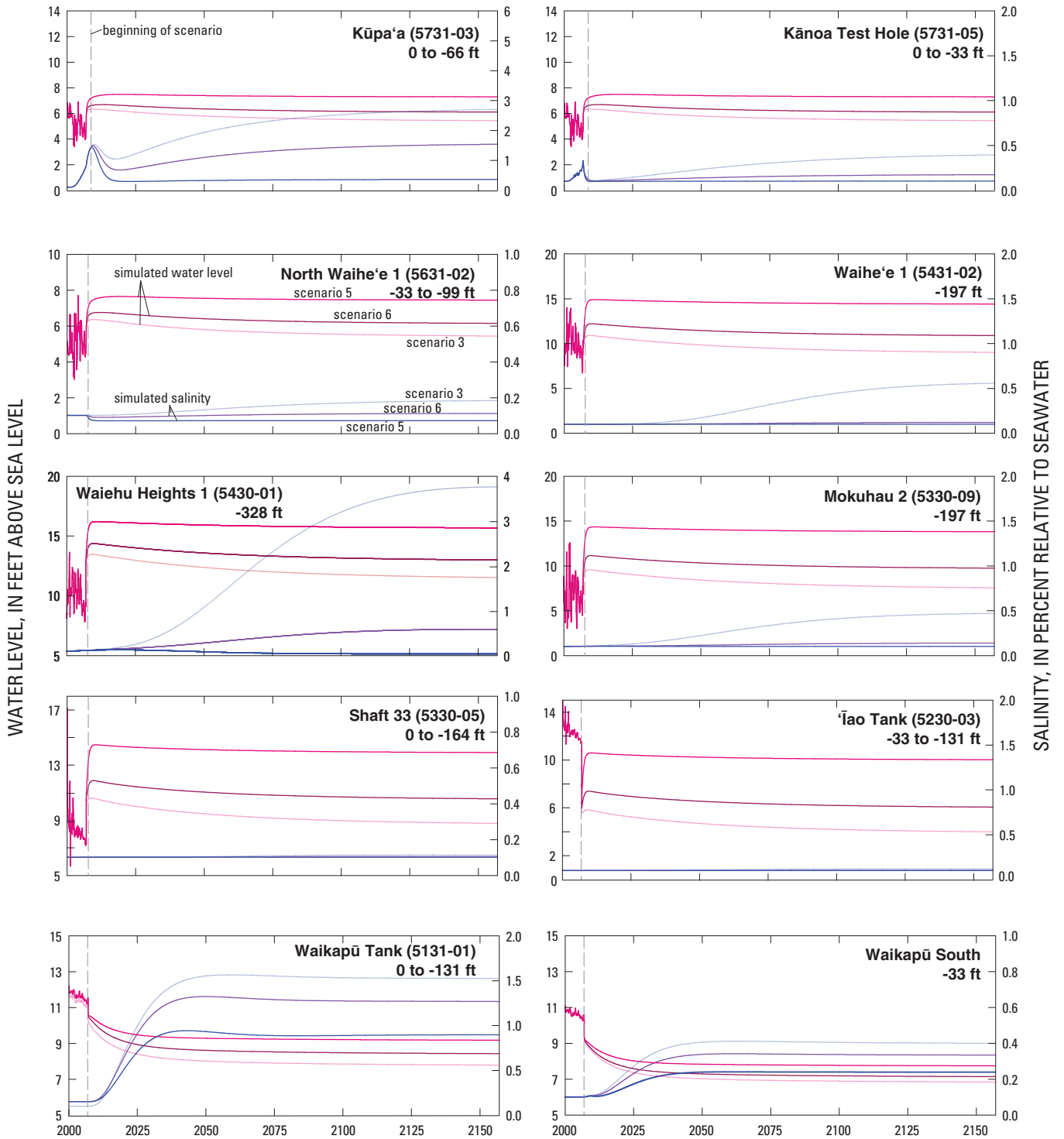


Figure 43. Simulated water-level (red lines) and salinity (blue lines) data for Scenarios 5 and 6 compared with Scenario 3 at selected wells in the Wailuku Aquifer Sector, 2000–2157, Maui, Hawai‘i. For each well shown, the simulated water level is the average of the water levels of the nodes representing the well and the simulated salinity is for the deepest node representing the well. The depths of the nodes used are shown under each well name and number.

isthmus. Average water levels are 1–5 ft higher for scenario 7 relative to the water levels at the end of scenario 3, with the largest differences at Waihe'e, Waiehu Heights, and Moku-hau well fields. At wells near and south of Waikapū Stream, the water level differences are smaller relative to scenario 5, because this area has reduced irrigation recharge that balances the gains from the additional stream recharge (compare figs. 45 and 49). Simulated salinity values are lower compared to scenario 3 at most of the well fields, with the largest differences at Waiehu Heights well field and Kūpa'a well (5731-03) (fig. 47). Salinity is slightly higher at Waikapū South because of some reduced irrigation recharge. The simulated depths of the bottom of freshwater and the middle of the transition zone at the Waiehu Deep Monitor well from scenario 7 are about 150–160 ft deeper relative to scenario 3 after 150 years (fig. 48).

Regional changes of water levels and freshwater depths in the aquifer after 150 years, relative to conditions at the end of scenario 3, are greatest around 'Īao and Waiehu Streams, where most of the additional recharge occurs. In scenario 7, water levels are more than 5 ft higher and the depths of the bottom of the freshwater are deeper by more than 160 ft (fig. 49). Reduced irrigation in the isthmus leads to water levels that are more than 1 ft lower and broad areas where the depths of the bottom of the freshwater and the middle of the lens are more than 40 ft shallower.

As in scenario 5, for the selected wells in the Wailuku Aquifer Sector, only the simulated salinity in the Waikapū Tank well (5131-01) increases to cautionary after 30 years (fig. 34). For scenario 7, withdrawal of 3.5 Mgal/d from the Waihe'e Aquifer system results in no cautionary or threatened yield after 150 years at the DWS wells or well fields (table 7). Withdrawal of 19.14 Mgal/d from 'Īao Aquifer System results in 1.50 Mgal/d of cautionary yield after 30 and after 150 years. Withdrawal of 4.50 Mgal/d from Waikapū

Aquifer System results in 0.5 Mgal/d of threatened yield after 30 and after 150 years.

Additional withdrawal locations

As part of the iterative process used in developing the redistributed pumping distribution used in scenarios 3–7, additional withdrawal sites were considered around the northern and southern coasts of west Maui (fig. 50). Six sites were tested in the Waihe'e Aquifer System north of the Kūpa'a well, each with a withdrawal rate of 0.5 Mgal/d for 30 years using 2000–04 land use, 1926–2004 rainfall, and the redistributed pumping distribution of scenario 3. Four of the six sites (Waiokila, Wailena, Waipili, and Waihalo) had final simulated salinity values ranging between 3 and 4-percent of seawater salinity and another (Kahakuloa) was more than 1-percent seawater. Only the Po'elua site, farthest to the north, had a simulated salinity below 1 percent of seawater salinity. Salinity at this well was higher at the end of the historical simulation mainly because of lower recharge during 2000–2004 than in the future scenario with average conditions. The model mesh in this northern area was not constructed with fine discretization, nor were there any measured water-level or salinity values for comparison, so the results are considered less reliable. However, the results are sufficient to indicate that it is less likely that a series of wells, each withdrawing 0.5 Mgal/d of potable water, could be developed in this area. Although this area receives ample recharge under average conditions, the relatively high aquifer permeability coupled with the lack of a low-permeability capping layer at the coast lead to the development of a relatively thin freshwater lens that is more susceptible to seawater intrusion.

Two potential well sites in the southern part of the Waikapū Aquifer System were considered because of their

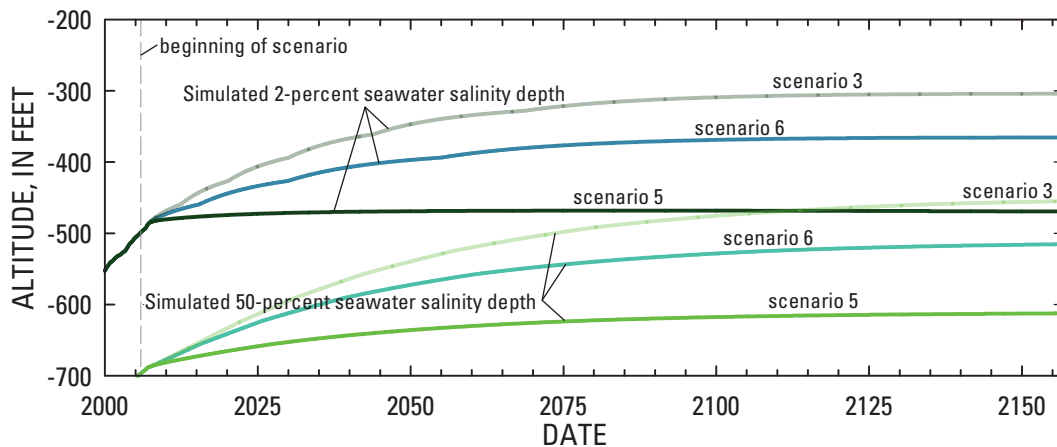


Figure 44. Simulated positions of the bottom of freshwater (2-percent seawater salinity) and middle of the transition zone (50-percent seawater salinity) for Scenarios 5 and 6 compared with Scenario 3 at the Waiehu Deep Monitor well (5430-05), 2000–2157, Maui, Hawai'i.

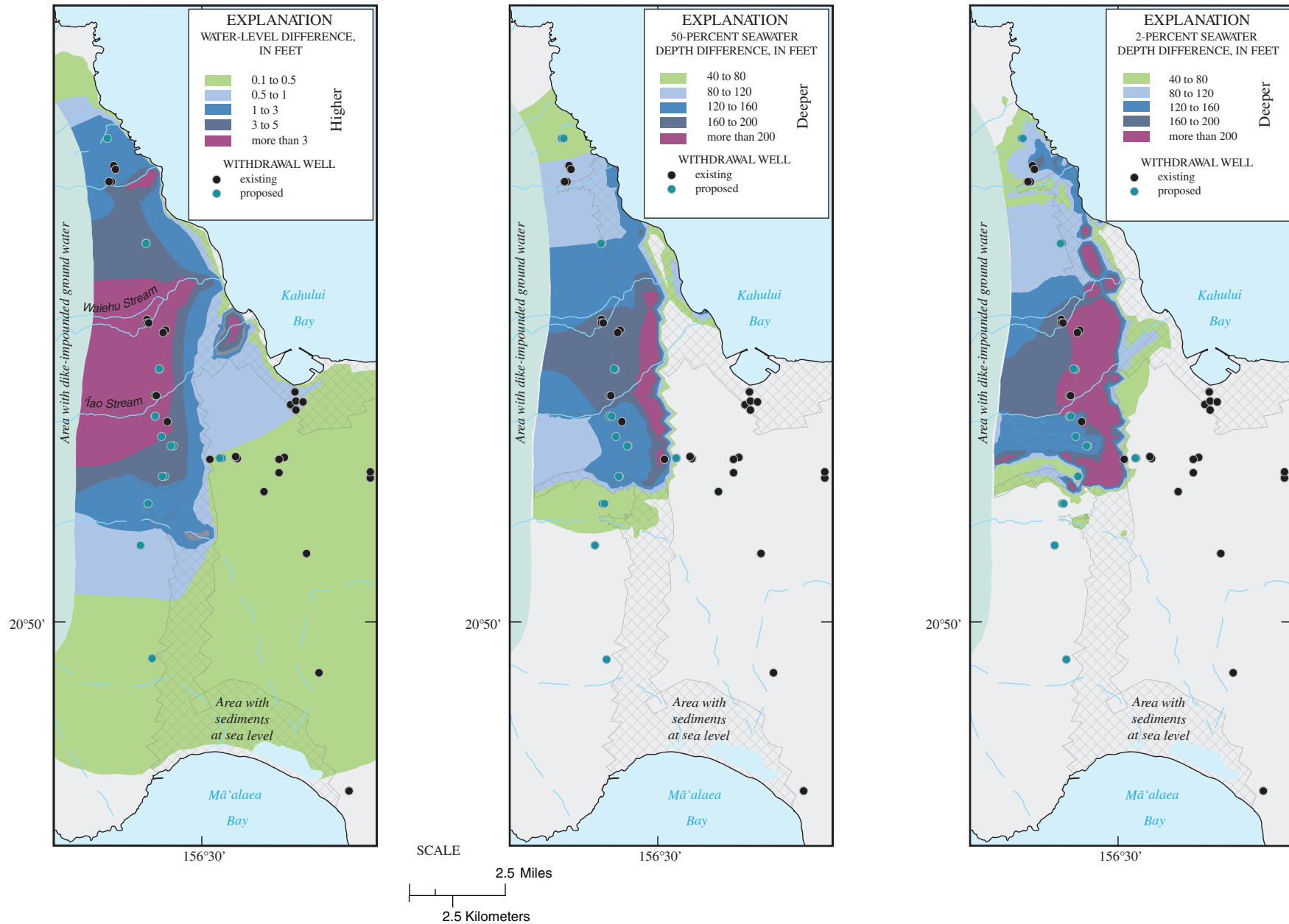


Figure 45. Simulated change (relative to scenario 3) in water level, 50-percent seawater salinity depth, and 2-percent seawater salinity depth after 150 years of withdrawal at redistributed rates with 12.3 Mgal/d of additional stream recharge [scenario 5], Maui, Hawai'i.

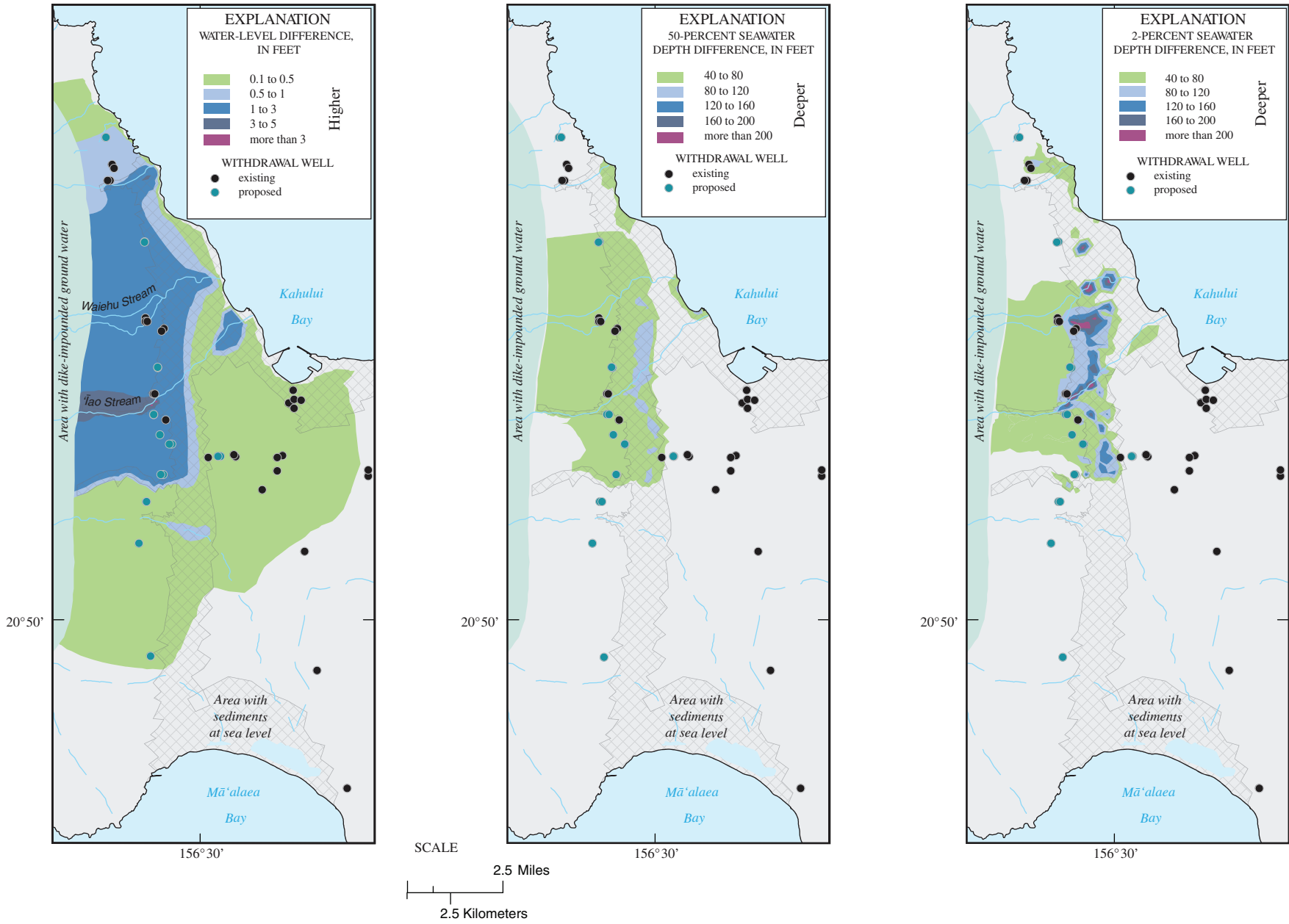


Figure 46. Simulated change (relative to scenario 3) in water level, 50-percent seawater salinity depth, and 2-percent seawater salinity depth after 150 years of withdrawal at redistributed rates with 4.1 Mgal/d of additional stream recharge [scenario 6], Maui, Hawai'i.

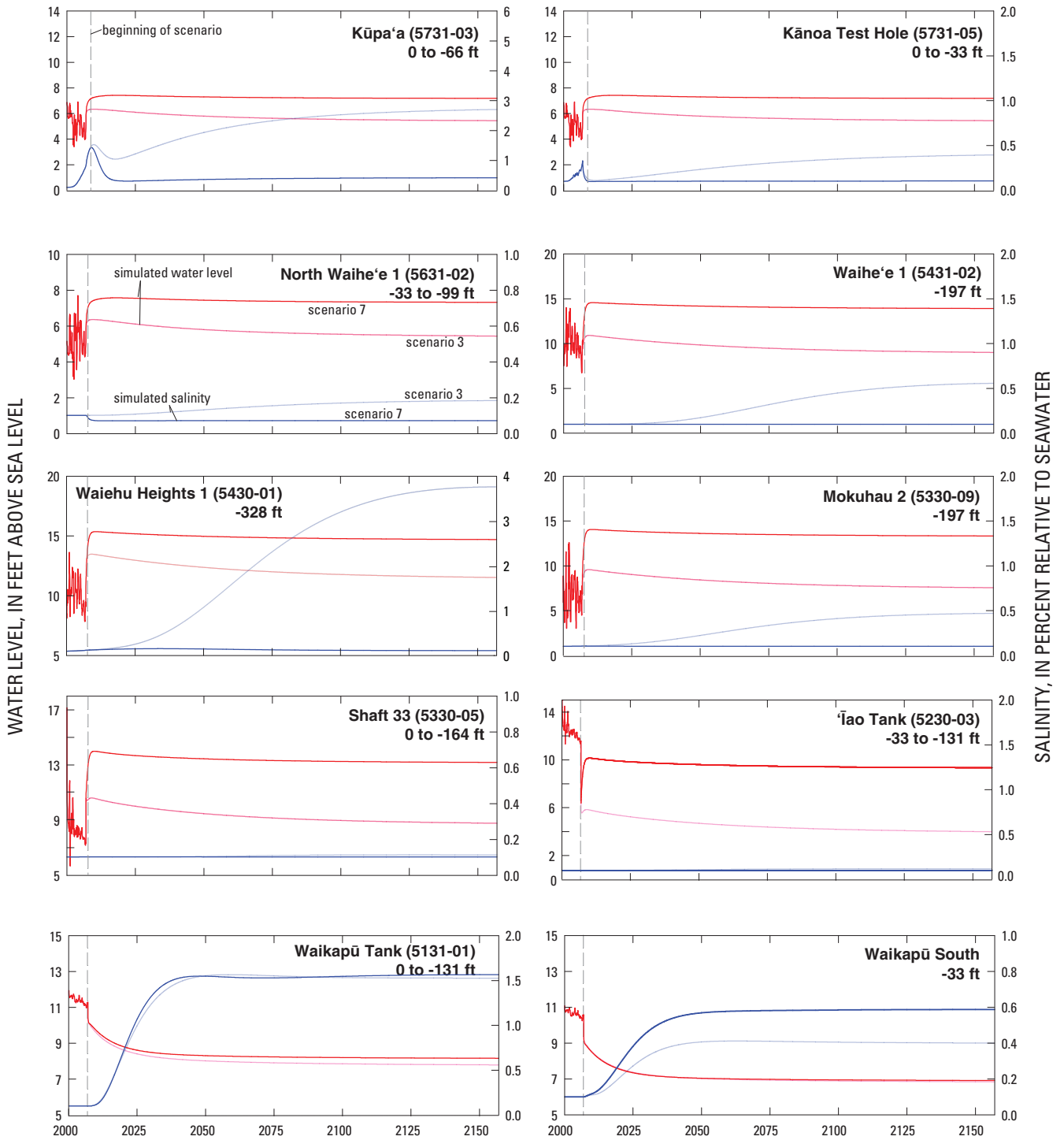


Figure 47. Simulated water-level (red lines) and salinity (blue lines) data for Scenario 7 compared with Scenario 3 at selected wells in the Wailuku Aquifer Sector, 2000–2157, Maui, Hawai'i. For each well shown, the simulated water level is the average of the water levels of the nodes representing the well and the simulated salinity is for the deepest node representing the well. The depths of the nodes used are shown under each well name and number.

proximity to existing water-supply infrastructure, but even without ground-water withdrawal at these sites, simulated salinities increased to nonpotable levels as a result of withdrawal elsewhere in the aquifer (fig. 50). The simulated salinity at the Pu'u Hona site increased from about 1-percent to nearly 2.5-percent seawater salinity after 30 years. Measured salinity data during 1939–60 from monitoring well 4931-01 at the Pu'u Hona site ranged between 112 and 316 mg/L chloride (about 0.6–1.6-percent seawater salinity), indicating that the simulated salinity values are a reasonable approximation of field conditions (unpublished chloride data in files of USGS Pacific Island Water Science Center). Simulated salinities at the Mā'alaea Tank site increased from about 8-percent to nearly 15-percent seawater salinity, indicating a lack of fresh-water resource in this area.

Model Limitations

The numerical model developed for this study simulates water levels and salinity on a regional scale and may not accurately predict either the pumping water level at an individual well or the salinity of water pumped from that well. Salinity of water pumped from a well may be controlled by local heterogeneities in the aquifer that are not represented in the model, and the level of model discretization affects the numerical accuracy with which transport mechanisms are simulated. The model has several other limitations for predictive purposes because of the various assumptions used and possible uncertainties in input data. These limitations are discussed below.

Differences between measured and simulated water levels and salinity profiles are greater in some areas than others, which may reflect uncertainties in the recharge or withdrawal estimates, boundary conditions, assigned parameter values in

the model, or representations of the different hydrogeological features in the model. Recharge estimates are based on water-budget computations that could be improved with a better understanding of the spatial distributions of rainfall, evapotranspiration, runoff, and land-cover characteristics. Improved recharge estimates in the study area will lead to improved estimates for parameter values in the numerical ground-water model and greater confidence in model results. Withdrawals represented in the model were based on available information. Unreported withdrawals and uncertainties in reported withdrawals that cannot be quantified also affect the accuracy of model results.

For this study, no-flow boundaries were assigned in the east at the rift zones of Haleakalā, which precludes ground-water movement across these boundaries. Although some flow likely takes place across these boundaries, the amount is probably small and cannot be quantified without expanding the modeled area.

The distributions of parameter values assigned in the model were kept simple to avoid creating an overly complex model that could not be justified on the basis of existing information. Heterogeneity in the ground-water system likely exists but is poorly understood. Values assigned to model parameters initially were based on existing estimates and subsequently adjusted to simulate historical head and salinity observations. However, some of these parameter values, particularly dispersion coefficients, may be poorly known.

Most of the modeling effort focused on matching the hydrologic response in the Wailuku Aquifer Sector. Although simulated water levels generally match measured data in the Central and Lahaina Aquifer Sectors, more effort is needed to refine these areas, especially if concerns about these areas need to be addressed further.

The geometrical representation of the valley-fill barriers, caprock, and contact between West Maui Volcano and

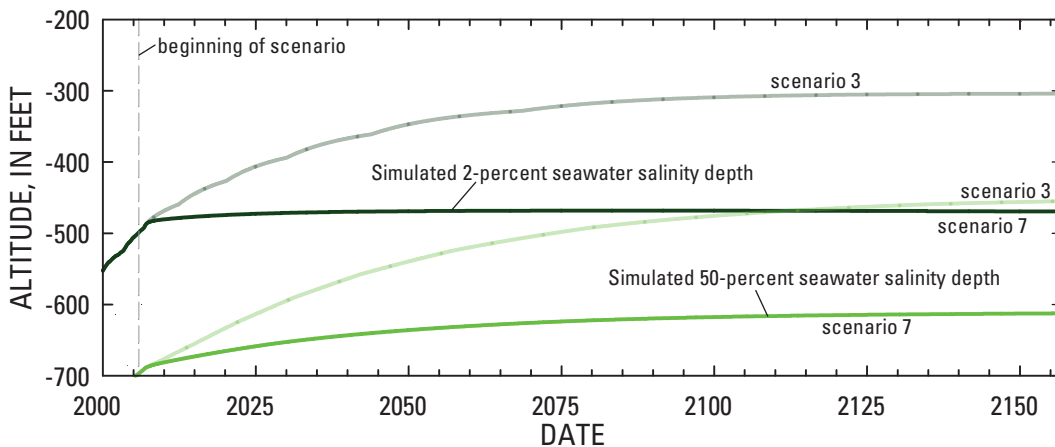


Figure 48. Simulated positions of the bottom of freshwater (2-percent seawater salinity) and middle of the transition zone (50-percent seawater salinity) for Scenario 7 compared with Scenario 3 at the Waiehu Deep Monitor well (5430-05), 2000–2157, Maui, Hawai'i.

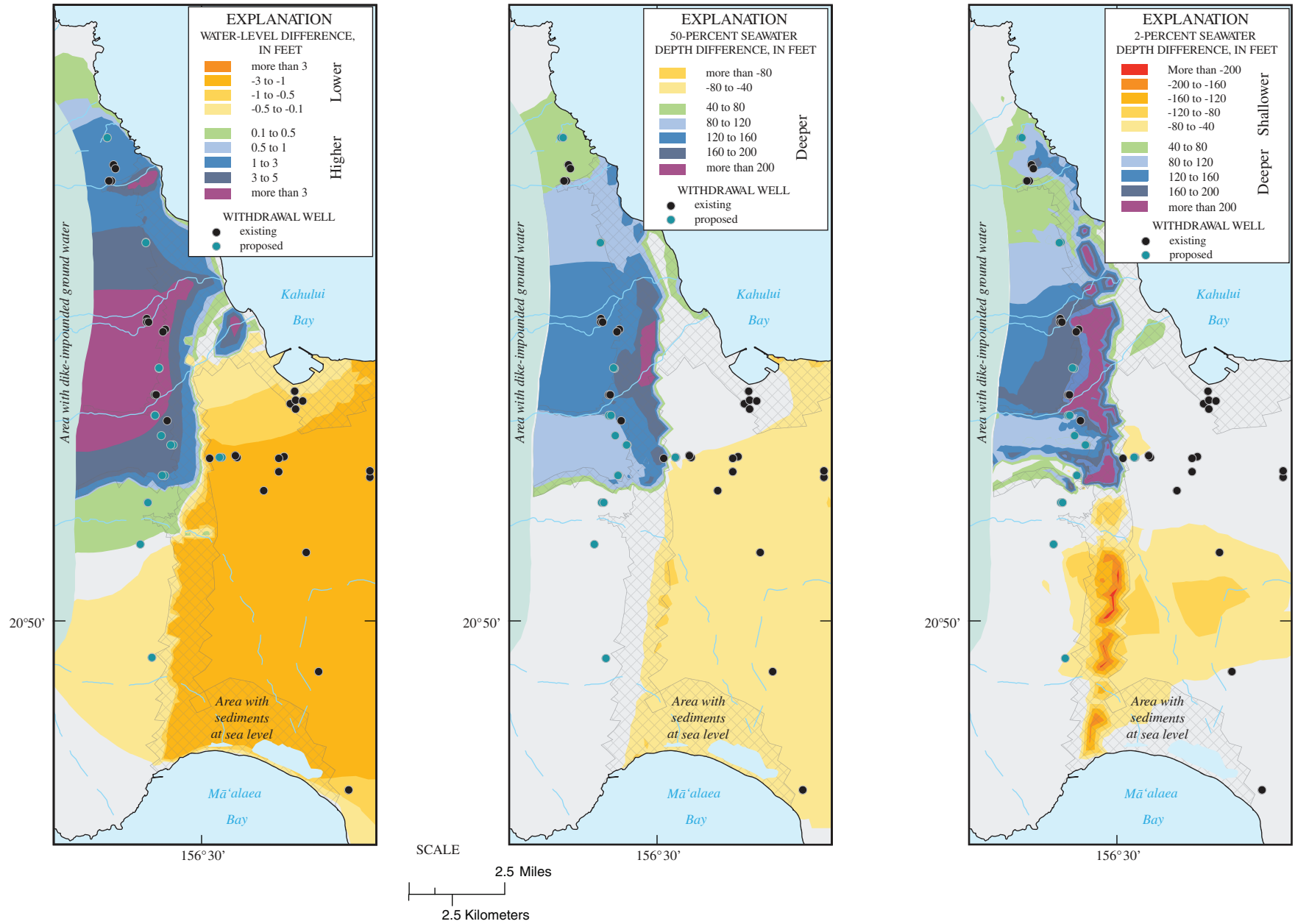


Figure 49. Simulated change (relative to scenario 3) in water level, 50-percent seawater salinity depth, and 2-percent seawater salinity depth after 150 years of withdrawal at redistributed rates with no recharge from agriculture irrigation [scenario 7], Maui, Hawai'i.

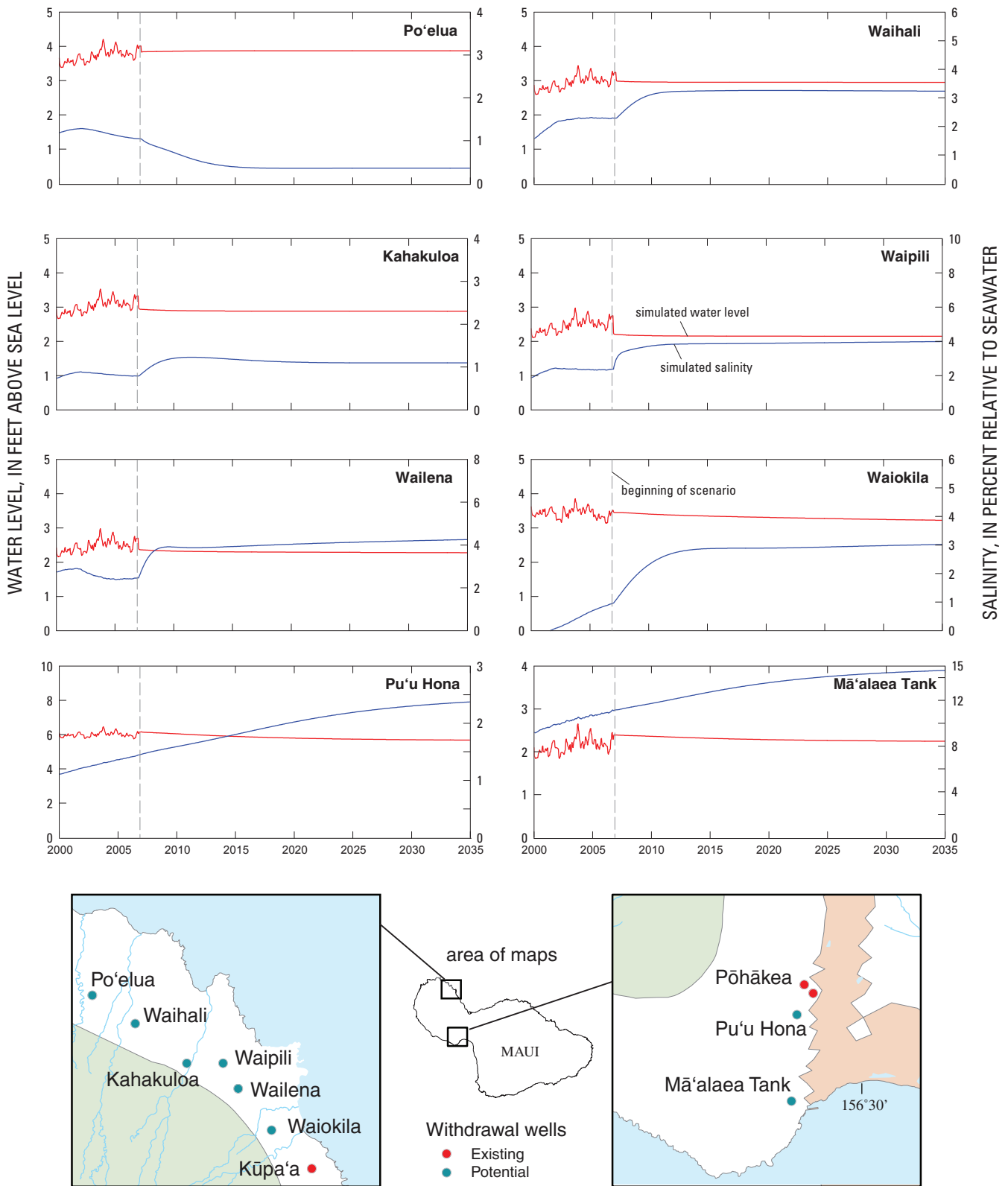


Figure 50. Simulated water-level (red lines) and salinity (blue lines) data for potential additional withdrawal sites in the Wailuku Aquifer Sector, 2000–2035, Maui, Hawai'i.

Haleakalā also were simplified for the model. The geometric definition of the valley-fill barriers can be improved using surface geophysical techniques in conjunction with drilling additional monitor wells within the valleys. For this study, the coastal caprock was represented as a homogeneous zone of relatively low permeability. High-permeability zones likely exist in the caprock, but they are poorly understood and were not represented in the model. Confidence in model results can be improved by addressing the limitations described in this section. In particular, improved estimates of the distribution of model parameters likely will lead to better model reliability. Despite these limitations, the model presented here does an adequate job for the purposes of this study.

Summary

Most of the public water supply in Maui, Hawai‘i, is from a freshwater lens in the Wailuku area of the island. Because of population increase, ground-water withdrawals from wells in this area increased from less than 10 Mgal/d during 1970 to about 23 Mgal/d during 2006. In response to increased withdrawals from the freshwater-lens system, water levels declined, the transition zone between freshwater and saltwater became shallower, and the chloride concentrations of water pumped from wells increased.

To aid in prudent management of ground-water resources and plan for sustainable growth on the island, the Maui County Department of Water Supply (DWS) entered into a cooperative agreement in 2003 with the U.S Geological Survey (USGS) to conduct a study of the ground-water availability in central and west Maui. The objectives of this 4.5-year study are to (1) obtain a better understanding of the regional ground-water flow system in the study area, (2) estimate ground-water recharge in the study area, and (3) use a numerical ground-water flow and transport model to estimate the effects of selected withdrawal and recharge scenarios on water levels and on the transition zone between fresh water and ocean water.

Irrigation rates in the study area have been steadily decreasing since the 1970s. Decreasing irrigation coincided recently with periods of below-average rainfall, leading to substantially reduced recharge rates in many areas. Recharge was determined for six periods (Engott and Vana, 2007). The period 1926–79 had the highest estimated recharge. Recharge from irrigation during this period was at least 50 percent higher than in any other period considered. Estimated recharge for central and west Maui declined 44 percent during 1979–2000. The period 2000–04 had the lowest estimated recharge. Recharge from irrigation during this period was 46 percent lower than during 1926–79, and rainfall was the lowest of any period.

Average withdrawals in 2000–06 were 21.4 Mgal/d in the Wailuku Aquifer Sector. Average withdrawals from the Central Aquifer Sector were about 68 Mgal/d and average withdrawals from the Lahaina Aquifer Sector during 2000–06 were about 4

Mgal/d. Most streams on West Maui Volcano receive ground-water discharge from the dike-impounded water body. Total average base flow at gaging stations operated on the largest 14 gaged streams on West Maui Volcano is about 101 Mgal/d.

A three-dimensional numerical ground-water model capable of simulating density-dependent solute transport was developed as part of this study. The model used published estimates for most of the permeability, storage, and dispersivity values. Simulated water levels and salinity profiles generally were in agreement with measured water levels and salinity profiles from representative wells in the modeled area during the period 1926–2006. Measured salinity profiles in the Waiehu deep monitor well indicate a shallowing of the brackish-water transition zone over time, and simulated salinity profiles are consistent with this trend.

The numerical model constructed for this study was used to quantify changes in ground-water level and salinity with ground-water withdrawal under various withdrawal and recharge scenarios. Scenarios included ground-water withdrawal at 2006 and 1996 rates and locations with average recharge, and withdrawal at redistributed rates and locations with several different recharge scenarios. Simulation results from the two scenarios that include the former withdrawal distributions indicate the following for the Wailuku Aquifer Sector: (1) average recharge rates and the 2006 withdrawal distribution (21.4 Mgal/d from 6 well fields) cause average water levels at wells to decrease 2–3 ft and the transition zone to become more than 200 ft shallower after 150 years, and (2) average recharge rates and the 1996 withdrawal distribution (20.1 Mgal/d from 4 well fields) cause average water levels at wells to decrease by more than 3 ft and the transition zone to become more than 300 ft shallower after 150 years. With the 2006 distribution, two of the six well fields have simulated salinity values that increase into the range of concern after long-term withdrawal. With the 1996 distribution, three of the four well fields have simulated salinity values that increase into the range of concern after long-term withdrawal.

A condition in which ground-water withdrawal was redistributed to maximize withdrawal and minimize salinities was determined using the numerical model in an iterative manner. Reduced rates at existing wells were combined with withdrawal from potential new well sites that, in consultation with the Maui DWS, were determined reasonable locations for future water-system expansion. The redistribution simulates 27.1 Mgal/d of withdrawal from 14 wells or well fields in the Wailuku Aquifer Sector. Simulation results from the five scenarios that include redistributed withdrawal conditions indicate the following for the Wailuku Aquifer Sector: (1) average recharge rates cause average water levels to decrease 2–3 ft and the transition zone to become more than 200 ft shallower after 150 years; (2) a 5-yr drought condition similar to the 1998–2002 drought causes additional salinity increases after 30 years but only one well has salinity increases of concern; (3) additional recharge from restored streamflow significantly increases water levels, thickens the freshwater body, and decreases salinity at withdrawal sites; and (4) a complete removal of irrigation recharge

decreases water levels and increases salinity in the central isthmus, but recharge through streams still significantly increases water levels, thickens the freshwater body, and decreases salinity at withdrawal sites in the Wailuku Aquifer Sector.

The numerical model developed for this study simulates water levels and salinity on a regional scale and may not accurately predict either the pumping water level at an individual well or the salinity of water pumped from that well. Salinity of water pumped from a well may be controlled by local heterogeneities in the aquifer that are not represented in the model. The model has several other limitations for predictive purposes, because of the various assumptions used and possible uncertainties in input data. Model reliability can be improved as understanding of ground-water recharge, the distribution of model parameter values, and the geometry of the sedimentary layers and valley-fill barriers improves.

References Cited

- Blumenstock, D.I., and Price, Saul, 1967, *Climates of the States-Hawaii*: U.S. Department of Commerce, *Climatology of the United States*, no. 60-51, 27 p.
- Bowles, S.P., 1970, Storm runoff disposal wells at Kahului, Maui: A report for Kahului Development Co., July 1970.
- Burnham, W.L., Larson, S.P., and Cooper, H.H., Jr., 1977, Distribution of injected wastewater in the saline lava aquifer, Wailuku-Kahului wastewater treatment facility, Kahului, Maui, Hawaii: U.S. Geological Survey Open-File Report no. 77-469, 58 p.
- C. Takumi Engineering Inc., 1999, Preliminary engineering report for new potable water source Kanoa Well No. 1 (State Well No. 5731-02), Waihee, Maui, Hawaii: Prepared for Department of Water Supply, County of Maui.
- Chen, C.-Y., Frey, F.A., Garcia, M.O., Dalrymple, G.B., and Hart, S.R., 1991, The tholeiite to alkalic basalt transition at Haleakala Volcano, Maui, Hawaii: *Contributions to Mineralogy and Petrology*, v. 106, p. 183–200.
- Cox, D.C., 1951, Lowland ground-water development prospects in and north of Iao Valley, Wailuku, Maui: Honolulu, Hawaii, Hawaii Sugar Planter's Association, 12 p.
- Engott, J.A., and Vana, T.T., 2007, Effects of agricultural land-use changes and rainfall on ground-water recharge in central and west Maui, Hawai'i, 1926–2004: U.S. Geological Survey Scientific Investigations Report 2007-5103, 56 p.
- Freeze, R.A., and Cherry, J.A., 1979, *Groundwater*: Englewood Cliffs, N.J., Prentice-Hall, Inc., 604 p.
- Giambelluca, T.W., and Nullet, Dennis, 1991, Influence of the trade-wind inversion on the climate of a leeward mountain slope in Hawaii: *Climate Research*, v. 1, p. 207–216.
- Giambelluca, T.W., Nullet, M.A., and Schroeder, T.A., 1986, *Rainfall atlas of Hawaii*: State of Hawaii, Department of Land and Natural Resources, Division of Water and Land Development, Report R76, 267 p.
- Gingerich, S.B., and Oki, D.S., 2000, Ground water in Hawaii: U.S. Geological Survey Fact Sheet FS126-00, 6 p.
- Gingerich, S.B., and Voss, C.I., 2005, Three-dimensional variable-density flow simulation of a coastal aquifer in southern Oahu, Hawaii, USA: *Hydrogeology Journal*, v. 13, p. 436–450.
- Harbaugh, A.W., 1990, A computer program for calculating subregional water budgets using results from the U.S. Geological Survey modular three-dimensional ground-water flow model: U.S. Geological Survey Open-File Report 90-392, 46 p.
- Harbaugh, A.W., Banta, E.R., Hill, M.C., and McDonald, M.G., 2000, MODFLOW-2000, the U.S. Geological Survey modular ground-water model—user guide to modularization concepts and the ground-water flow process: U.S. Geological Survey Open-File Report 00-92, 121 p.
- Huber, R.D., and Adams, W.M., 1971, Density logs from underground gravity surveys in Hawaii: University of Hawaii Water Resources Research Center Technical Report no. 45, 39 p.
- Hunt, C.D., Jr., 2007, Ground-water nutrient flux to coastal waters and numerical simulation of wastewater injection at Kihei, Maui, Hawaii: U.S. Geological Survey Scientific Investigations Report 2006–5283, 69 p.
- Ishizaki Kenneth, Burbank, N.C., Jr., and Lau, L.S., 1967, Effects of soluble organics on flow through thin cracks of basaltic lava: University of Hawaii Water Resources Research Center Technical Report no. 16, 56 p.
- Langenheim, V.A.M., and Clague, D.A., 1987, The Hawaiian-Emperor volcanic chain, part II, stratigraphic framework of volcanic rocks of the Hawaiian Islands, chap. 1 of Decker, R.W., Wright, T.L., and Stauffer, P.H., eds., *Volcanism in Hawaii*: U.S. Geological Survey Professional Paper 1350, v. 1, p. 55–84.
- Liu, C.C.K., 2005, Completion report of a research project on analytical groundwater flow and transport modeling for the estimation of the sustainable yield of Pearl Harbor Aquifer for Hawaii Department of Land and Natural Resources State Commission on Water Resource Management (unedited manuscript), 58 p.
- Macdonald, G.A., Abbott, A.T., and Peterson, F.L., 1983, *Volcanoes in the sea, the geology of Hawaii* (2d ed.): Honolulu, Hawaii, University of Hawai'i Press, 517 p.
- McCandless, J.S., 1936, Development of artesian well water in

- the Hawaiian Islands, 1880–1936: Honolulu, Hawaii, 79 p.
- McDougall, Ian, 1964, Potassium-argon ages from lavas of the Hawaiian Islands: *Geological Society of America Bulletin*, v. 75, p. 107–128.
- Meyer, C.F., Kleinecke, D.C., Todd, D.K., and Ewing, L.E., 1974, Mathematical modeling of freshwater aquifers having saltwater bottoms: Final technical completion report GE74TMP-43, General Electric Co., TEMPO, Center for Advanced Studies, Santa Barbara, California, 176 p. + app.
- Meyer, William, and Presley, T.K., 2001, The response of the Iao aquifer to ground-water development, rainfall, and land-use practices between 1940 and 1998, island of Maui, Hawaii: U.S. Geological Survey Water-Resources Investigations Report 00-4223, 60 p.
- Meyer, William, and Souza, W.R., 1995, Factors that control the amount of water that can be diverted to wells in a high-level aquifer, in Hermann, Raymond, Back, William, Sidle, R.C., and Johnson, A.I., eds., *Water resources and environmental hazards: emphasis on hydrologic and cultural insight in the Pacific Rim: Proceedings of the American Water Resources Association Annual Summer Symposium, Honolulu, Hawaii, June 25-28, 1995*, p. 207-216.
- Miller, M.E., 1987, Hydrogeologic characteristics of central Oahu subsoil and saprolite; implications for solute transport: University of Hawaii at Manoa M.S. thesis, 231 p.
- Mink, J.F., and Lau, L.S., 1980, Hawaiian groundwater geology and hydrology, and early mathematical models: University of Hawaii Water Resources Research Center Technical Memorandum Report no. 62, 74 p.
- Mink, J.F., and Lau, L.S., 1990, Aquifer identification and classification for Maui: groundwater protection strategy for Hawaii: Honolulu, Hawaii, University of Hawaii Water Resources Research Center, Technical Report no. 185, 47 p.
- National Geophysical Data Center, 2004, NGDC Coastal Relief Model: National Oceanic and Atmospheric Administration Web page Carla J. Moore, webmaster [<http://www.ngdc.noaa.gov/mgg/coastal/coastal.html>. last accessed July 28, 2006]
- National Oceanic and Atmospheric Administration, 2007, Historic tide data: [http://tidesandcurrents.noaa.gov/data_menu.shtml?stn=1615680%20Kahului,%20HI&type=Historic+Tide+Data. Last accessed June 16, 2007].
- Naughton, J.J., Macdonald, G.A., and Greenberg, V.A., 1980, Some additional potassium-argon ages of Hawaiian rocks; the Maui Volcanic Complex of Molokai, Maui, Lanai, and Kahoolawe: *Journal of Volcanology and Geothermal Research*, v. 7, p. 339–355.
- Nichols, W.D., Shade, P.J., and Hunt, C.D., 1996, Summary of the Oahu, Hawaii regional aquifer-system analysis: U.S. Geological Survey Professional Paper 1412-A, 61 p.
- Oki, D.S., 1998, Geohydrology of the central Oahu, Hawaii, ground-water flow system and numerical simulation of the effects of additional pumping: U.S. Geological Survey Water-Resources Investigations Report 97-4276, 132 p.
- Oki, D.S., 2005a, Trends in streamflow characteristics at long-term gaging stations, Hawaii: U.S. Geological Survey Scientific Investigations Report 2004-5080, 120 p.
- Oki, D.S., 2005b, Numerical simulation of the effects of low-permeability valley-fill barriers and the redistribution of ground-water withdrawals in the Pearl Harbor Area, Oahu, Hawaii: U.S. Geological Survey Scientific Investigations Report 2005-5253, 111 p.
- Oki, D.S., Souza, W.R., Bolke, E.L., and Bauer, G.R., 1998, Numerical analysis of the hydrogeologic controls in a layered coastal aquifer system, Oahu, Hawaii, USA: *Hydrogeology Journal*, v. 6, no. 2, p. 243-263.
- Paillet, F.L., Williams, J.H., Oki, D.S., and Knutson, K.D., 2002, Comparison of formation and fluid-column logs in a heterogeneous basalt aquifer: *Ground Water*, v. 40, no. 6, p. 577-585.
- Peterson, F.L., and Hargis, D.R., 1971, Effect of storm runoff disposal and other artificial recharge to Hawaiian Ghyben-Herzberg aquifers: University of Hawaii, Water Resources Research Center Technical Report no. 54, 51 p.
- Peterson, F.L., and Sehgal, M.M., 1974, Determining porosity with neutron logs from Hawaiian basaltic aquifers: University of Hawaii Water Resources Research Center Technical Report no. 80, 37 p.
- R.M. Towill Corporation, 1978, Feasibility study, surface water impoundment/recharge Pearl Harbor basin Oahu, Hawaii, variously paginated.
- Rotzoll, K., El-Kadi, A.I., and Gingerich, S.B., 2007, Estimating hydraulic properties of volcanic aquifers using constant-rate and variable-rate aquifer tests: *Journal of the American Water Resources Association* v. 43, no. 2, p. 334–345.
- Sherrod, D.R., Nishimitsu, Yoshitomo, and Tagami, Takahiro, 2003, New K-Ar ages and the geologic evidence against rejuvenated-stage volcanism at Haleakalā, East Maui, a postshield-stage volcano of the Hawaiian island chain: *Geological Society of America Bulletin*, v. 115, no. 6, p. 683-694.
- Soroos, R.L., 1979, Test monitoring of prototype injection well, Waiale, Maui, Hawaii: U.S. Geological Survey Open-File Report no. 79-274, 31 p.

- Souza, W.R., 1981, Ground-water status report, Lahaina District, Maui, Hawaii: U.S. Geological Survey Open-File Report 81-549, 2 sheets.
- Souza, W.R., and Voss, C.I., 1987, Analysis of an anisotropic coastal aquifer system using variable-density flow and solute transport simulation: *Journal of Hydrology*, v. 92, p. 17-41.
- State of Hawaii, 1961, Summary of drilling logs and pumping test for Exploratory Well No. 1, Waikapu, Maui, Hawaii: Department of Land and Natural Resources Division of Water and Land Development Circular C4.
- State of Hawaii, 1965, Summary of drilling log and pumping test for Alaeloa Well 318, Alaeloa, Maui, Hawaii: Department of Land and Natural Resources Division of Water and Land Development Circular C35.
- State of Hawaii, 1967, Summary of drilling log and pumping test for Maalaea Well 272, Maalaea, Maui, Hawaii: Department of Land and Natural Resources Division of Water and Land Development Circular C43.
- State of Hawaii, 1990, Water resources protection plan, volumes I and II, June 1990: Commission on Water Resource Management, Department of Land and Natural Resources, variously paginated.
- State of Hawaii, 2000, The State of Hawaii data book 2000, a statistical abstract: State of Hawaii, Department of Business, Economic Development, and Tourism [<http://www.hawaii.gov/dbedt/db00>. accessed June 10, 2002].
- State of Hawaii, 2003, Public Notice of Iao Ground-Water Management Area Designation, Island of Maui: State of Hawaii Department of Land and Natural Resources Commission on Water Resource Management [<http://hawaii.gov/dlnr/cwrm/current/iao/nt030721.pdf>].
- State of Hawaii, 2004, Hawaii well construction and pump installation standards: State of Hawaii Department of Land and Natural Resources Commission on Water Resource Management 2nd edition, variously paginated.
- Stearns, H.T., 1976, Second supplement to the central Maui water study of March 1974, unpublished report to Waiehu Heights Association in U.S. Geological Survey files.
- Stearns, H.T., and Macdonald, G.A., 1942, Geology and ground-water resources of the island of Maui, Hawaii: Hawaii Division of Hydrography Bulletin 7, 344 p.
- Takasaki, K.J., 1972, Preliminary report on the water resources of Central Maui: State of Hawaii, Department of Land and Natural Resources, Division of Water and Land Development, Circular C62, 59 p. plus appendixes.
- Tenorio, P.A., Young, R.H.F., Burbank, N.C., Jr., and Lau, L.S., 1970, Identification of irrigation return water in the sub-surface, phase III Kahuku, Oahu and Kahului and Lahaina, Maui: University of Hawaii, Water Resources Research Center Technical Report no. 44, 53 p.
- U.S. Geological Survey, 2006a, Synoptic water-level survey, Central Maui, Hawaii: [http://hi.water.usgs.gov/projects/cmaui_gw/synoptic_cmaui_data.htm. accessed June 16, 2006].
- U.S. Geological Survey, 2006b, Revised measuring-point elevations for selected wells in the Waihee and Iao Aquifer areas on the Island of Maui: [http://hi.water.usgs.gov/studies/cmaui_gw/project_cmaui_mp.html]. , accessed June 16, 2006].
- U.S. Geological Survey, 2006c, Recent hydrologic conditions, Iao and Waihee aquifer areas, Maui, Hawaii: [http://hi.water.usgs.gov/iao/iao_summary.htm. accessed November 27, 2006].
- Voss, C. I., and Provost, A.M., 2003, SUTRA, a model for saturated-unsaturated variable-density ground-water flow with solute or energy transport: U.S. Geological Survey Water-Resources Investigations Report 02-4231, 250 p.
- Wahl, K.L., and Wahl, T.L., 1995, Determining the flow of Comal Springs at New Braunfels, Texas: Proceedings of Texas Water '95, A Component Conference of the First International Conference on Water Resources Engineering, American Society of Civil Engineers, August 16-17, 1995, San Antonio, Texas, p. 77-86.
- Wentworth, C.K., 1938, Geology and ground water resources of the Palolo-Waiialae District; Honolulu, Hawaii: Honolulu Board of Water Supply, 274 p.
- Wentworth, C.K., 1951, Geology and ground-water resources of the Honolulu-Pearl Harbor area, Oahu, Hawaii: Honolulu Board of Water Supply, 111 p.
- Western Region Climate Center, 2007, Climatological Data Summaries: [<http://www.wrcc.dri.edu/summary/Climsmhi.html>. accessed July 24, 2007].
- Winston, R.B., and Voss, C.I., 2003, SutraGUI, a graphical-user interface for SUTRA, a model for ground-water flow with solute or energy transport: U.S. Geological Survey Open-File Report 03-285, 114 p., [<http://water.usgs.gov/nrp/gwsoftware/sutra.html>].
- Yamanaga, George, and Huxel, C.J., 1969, Preliminary report on the water resources of the Lahaina District, Maui: State of Hawaii, Department of Land and Natural Resources, Division of Water and Land Development, Circular C51, 47 p.
- Yamanaga, George, and Huxel, C.J., 1970, Preliminary report on the water resources of the Wailuku area, Maui: State of Hawaii, Department of Land and Natural Resources, Division of Water and Land Development, Circular C61, 43 p.

Appendixes A–C

Appendix A. Wells in the central Maui study area with stratigraphic information, Hawai'i

Table A1. Information for wells with stratigraphic information in the central Maui study area, Hawai'i.

[Altitude relative to mean sea level; ft; feet; --, not applicable; CWRM, State of Hawai'i Department of Land and Natural Resources Commission on Water Resource Management; USGS, U.S. Geological Survey Pacific Islands Water Science Center; TH, test hole]

Well number	Local well name	Altitude of top of Wailuku Basalt (ft)	Altitude of top of Honomanū Basalt / Kula Volcanics (ft)	Reference
4829-01	Keālia Pond	--	-26	CWRM well completion report
4829-02	Mā'ālaea Power Plant	--	-38	do
4829-03	Mā'ālaea Back-Up	--	-15	do
4829-04	Mā'ālaea M-17	--	-53	do
4830-01	Mā'ālaea Triangle	16	--	do
4831-01	Mā'ālaea 272	130	--	State of Hawaii (1967)
4928-02	Pu'unēnē Airport Shaft	--	45	Stearns and Macdonald (1942)
4929-01	Field 910	--	24	do
4931-01	Near Pu'u Hele	264	--	do
4936-01	Olowalu 'Elua	135	--	CWRM well completion report
5028-01	Waikapū Shaft TH	--	61	Stearns and Macdonald (1942)
5028-02	Waikapū Shaft TH	--	25	do
5128-01	Waikapū Shaft TH	--	-40	do
5130-01	Waikapū 1	383	--	State of Hawaii (1961)
5130-02	Waikapū 2	210	--	unpublished driller's log in USGS files
5138-01	Launiupoko 1	566	--	do
5227-06	Tmk 3-8-09-24	--	14	do
5228-08	Tmk 3-8-23-18	--	-6	do
5228-14	Tmk 3-8-19-29	--	24	do
5228-15	Moloka'i Street Disposal	--	9	Peterson and Hargis (1971)
5228-17	Luana II-1	--	42	CWRM well completion report
5228-18	Luana III-2	--	47	do
5228-19	Kahului	--	36	do
5228-20	'Elima Irrigation	--	43	do
5229-01	Wai'ale Prototype	--	80	Soroos (1979)
5229-02	Maui Lani 1	--	85	CWRM well completion report
5229-03	Maui Lani 2	--	30	do
5230-01	Ka Hale A Ke Ola	--	141	do
5240-04	Lahaina	-45	--	unpublished driller's log in USGS files
5327-10	Kanahā Pond	--	-35	do
5328-01	Cannery Shaft	--	15	do
5328-02	Cannery	--	-50	Peterson and Hargis (1971)
5328-22	Kahiki Street	--	-65	do

Table A1. Information for wells with stratigraphic information in the central Maui study area, Hawai'i.—Continued

[Altitude relative to mean sea level; ft; feet; --, not applicable; CWRM, State of Hawai'i Department of Land and Natural Resources Commission on Water Resource Management; USGS, U.S. Geological Survey Pacific Islands Water Science Center; TH, test hole]

Well number	Local well name	Altitude of top of Wailuku Basalt (ft)	Altitude of top of Honomanū Basalt / Kula Volcanics (ft)	Reference
5328-23	Kahiki Street	--	-14	do
5328-24	Fair Grounds	--	-52	Stearns and Macdonald (1942)
5328-26	Cannery	--	-48	Peterson and Hargis (1971)
5328-27	Cannery	--	-30	do
5328-28	Cannery	--	-20	do
5328-30	Tmk 3-8-18-9	--	-8	unpublished driller's log in USGS files
5328-31		--	-5	do
5328-32	Tmk 3-8-23-1	--	-14	do
5328-33	Tmk 3-8-19-14	--	-12	do
5328-34	Tmk 3-8-22-1	--	-9	do
5328-35	Tmk 3-8-15-1	--	-23	do
5328-36	Tmk 3-8-23-35	--	-21	do
5328-37	Tmk 3-8-23-45	--	13	do
5328-38	Tmk 3-8-19-37	--	-1	do
5328-39	Tmk 3-8-12-60	--	-26	do
5328-40	Tmk 3-8-16-31	--	-19	do
5328-41	Tmk 3-8-19-51	--	2	do
5328-42	Kaua'i Street	--	-16	Peterson and Hargis (1971)
5328-43	Kahului	--	2	unpublished driller's log in USGS files
5328-45	Kahului	--	4	Soroos (1979)
5328-48	Hale Mahaolu II	--	4	CWRM well completion report
5328-49	Kahului Community Park	--	26	do
5329-01	Tmk 3-8-35-70	--	43	unpublished driller's log in USGS files
5329-06	Baldwin High TH	--	16	Stearns and Macdonald (1942)
5329-08	Tmk 3-8-40-5	--	44	unpublished driller's log in USGS files
5329-09	Tmk 3-8-30-39	--	21	do
5329-10	Tmk 3-8-39-30	--	33	do
5329-11	218 Hōlua Avenue	--	48	Peterson and Hargis (1971)
5329-12	Hōlua Avenue	--	88	do
5329-13	Kunu Place	--	40	do
5329-18	Wai'ale Observation	--	38	Soroos (1979)
5329-19	Maui Central Park 1	--	10	CWRM well completion report
5329-20	Maui Central Park 2	--	14	do
5329-21	Maui Central Park 3	--	3	do
5330-03	TH-112	68	--	unpublished geologist log in USGS files
5330-04	Wailuku Mill TH	--	-16	do

Table A1. Information for wells with stratigraphic information in the central Maui study area, Hawai'i.—Continued

[Altitude relative to mean sea level; ft; feet; --, not applicable; CWRM, State of Hawai'i Department of Land and Natural Resources Commission on Water Resource Management; USGS, U.S. Geological Survey Pacific Islands Water Science Center; TH, test hole]

Well number	Local well name	Altitude of top of Wailuku Basalt (ft)	Altitude of top of Honomanū Basalt / Kula Volcanics (ft)	Reference
5330-05	Wailuku Shaft 33	68	--	do
5330-06	Mokuhau TH 1	-150	--	do
5330-07	Mokuhau TH 2	3	--	do
5330-08	Mokuhau TH 3	-25	--	do
5330-09	Mokuhau 1	-58	--	unpublished driller's log in USGS files
5330-12	Pu'uohala TH-C	-151	--	Stearns (1976)
5331-01	TH-102	303	--	Stearns and Macdonald (1942)
5427-01	Kahului PP A	--	-88	unpublished driller's log in USGS files
5427-08	Injection Test	--	-58	do
5429-02	Pāpōhaku Park	--	-55	CWRM well completion report
5430-01	Waiehu Heights 1	187	--	Stearns (1976)
5430-03	TH-E	-76	--	do
5430-04	TH-D	89	--	do
5430-05	Waiehu Deep Monitor well	99	--	unpublished driller's log in USGS files
5431-01	TH-B	463	--	Stearns (1976)
5431-04	Waihe'e 3	413	--	CWRM well completion report
5530-02	Waiehu TH		-97	Stearns and Macdonald (1942)
5631-02	North Waihe'e 1	250	--	CWRM well completion report
5731-02	Kānoa 1	60	--	C. Takumi Engineering Inc. (1999)
5731-03	Kūpa'a 1	564	--	do
5731-05	Kānoa TH	57	--	do
5840-01	'Alaeloa	175	--	State of Hawaii (1965)
5841-03	Shoemaker	4	--	CWRM well completion report
GS-5		--	-50	Burnham and others (1977)
GS-7		--	-5	do
GS-4		--	-65	do

Appendix B. Monthly ground-water withdrawals during 1900–2006 from wells in central and west Maui, Hawai‘i

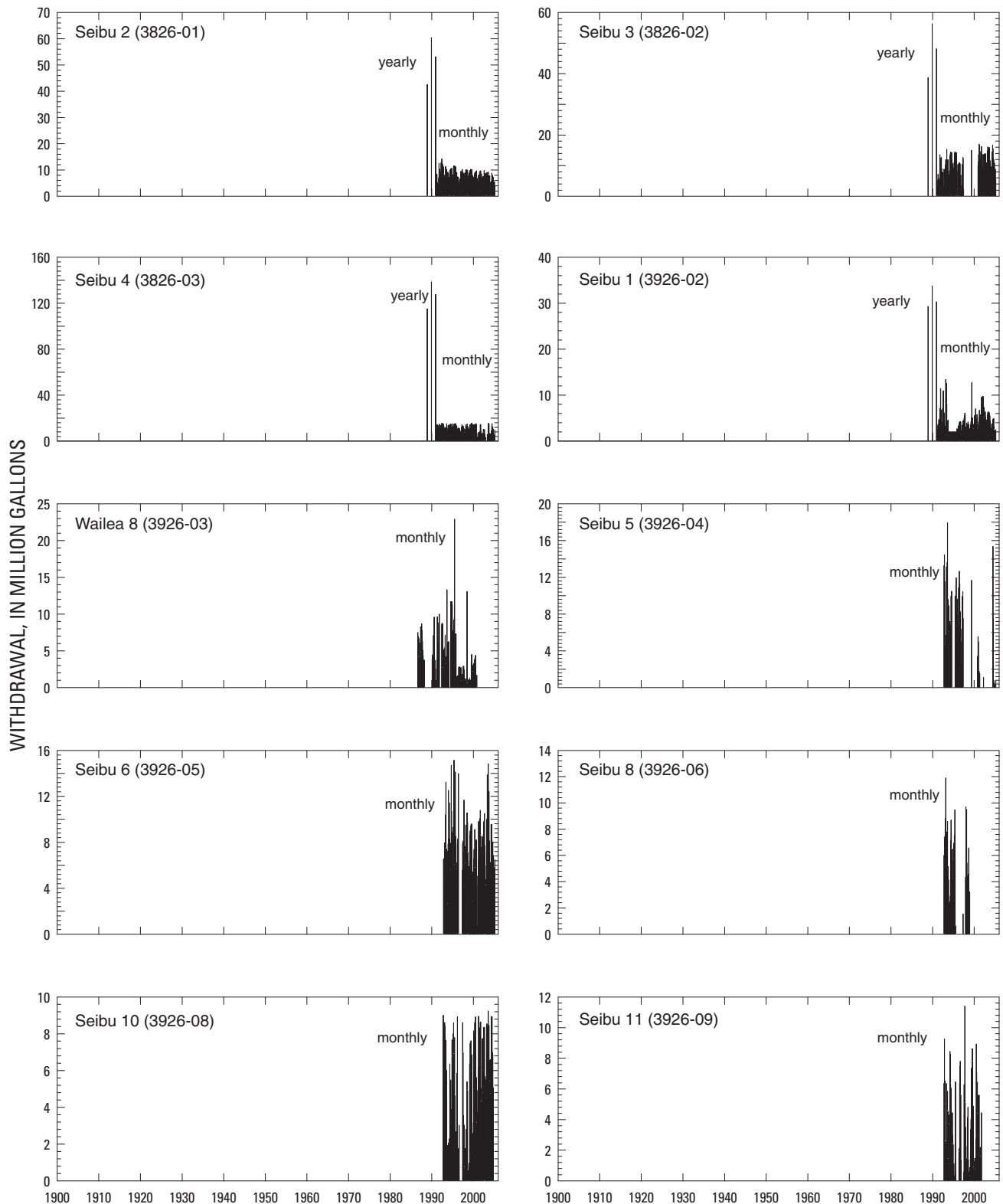


Figure B1. Monthly ground-water withdrawals during 1900–2006 from wells in central and west Maui, Hawai‘i.

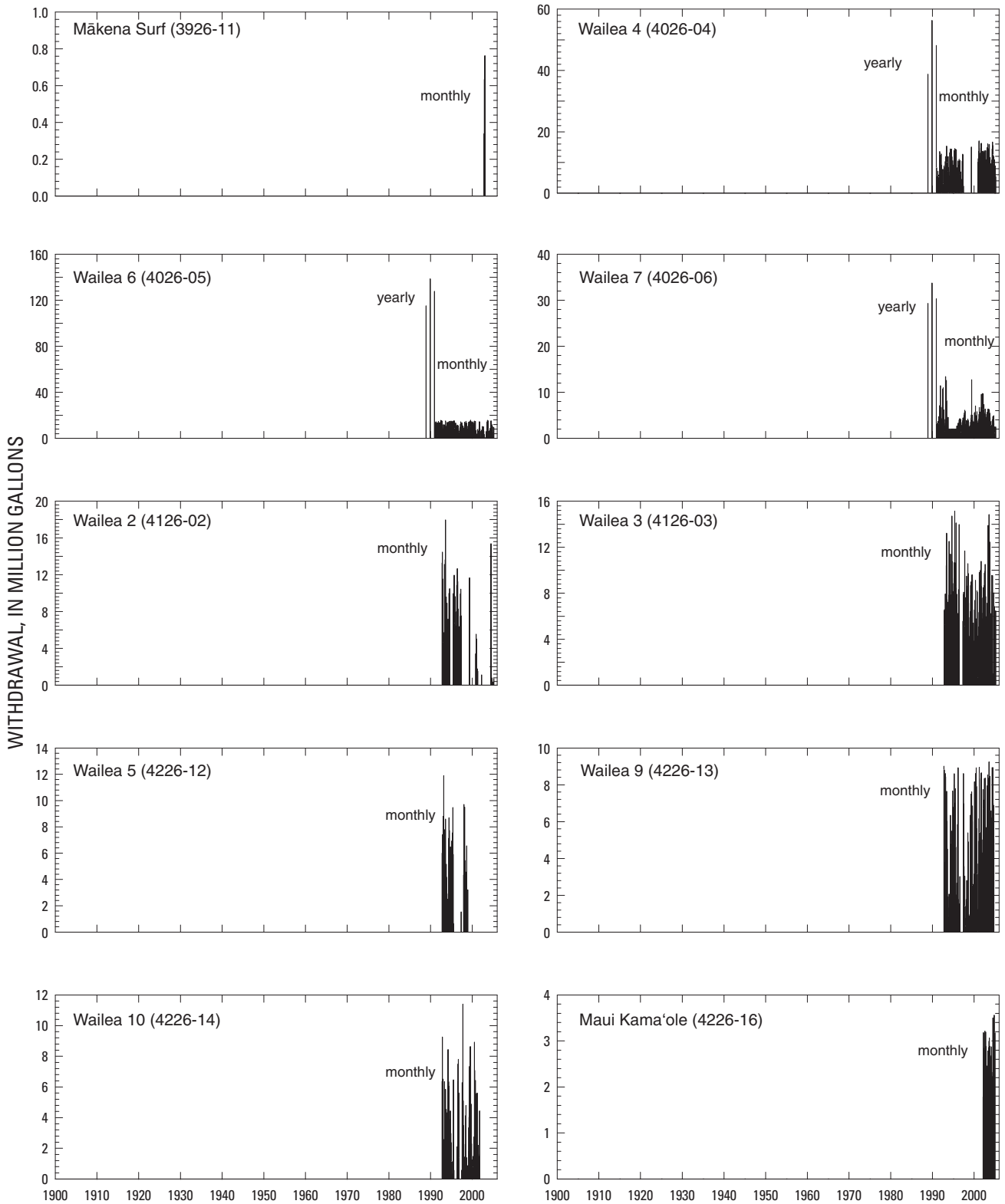


Figure B1.—Continued.

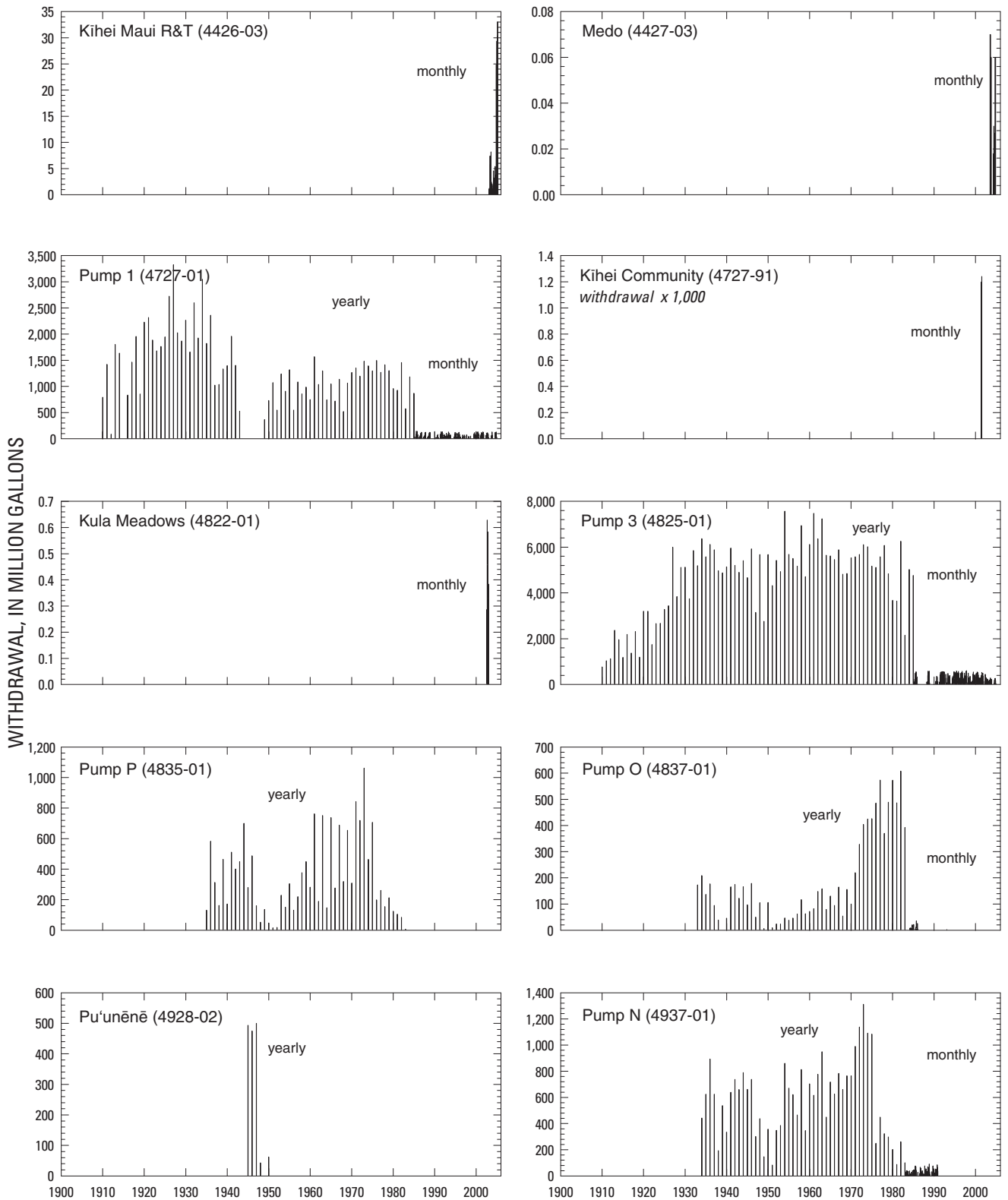


Figure B1.—Continued.

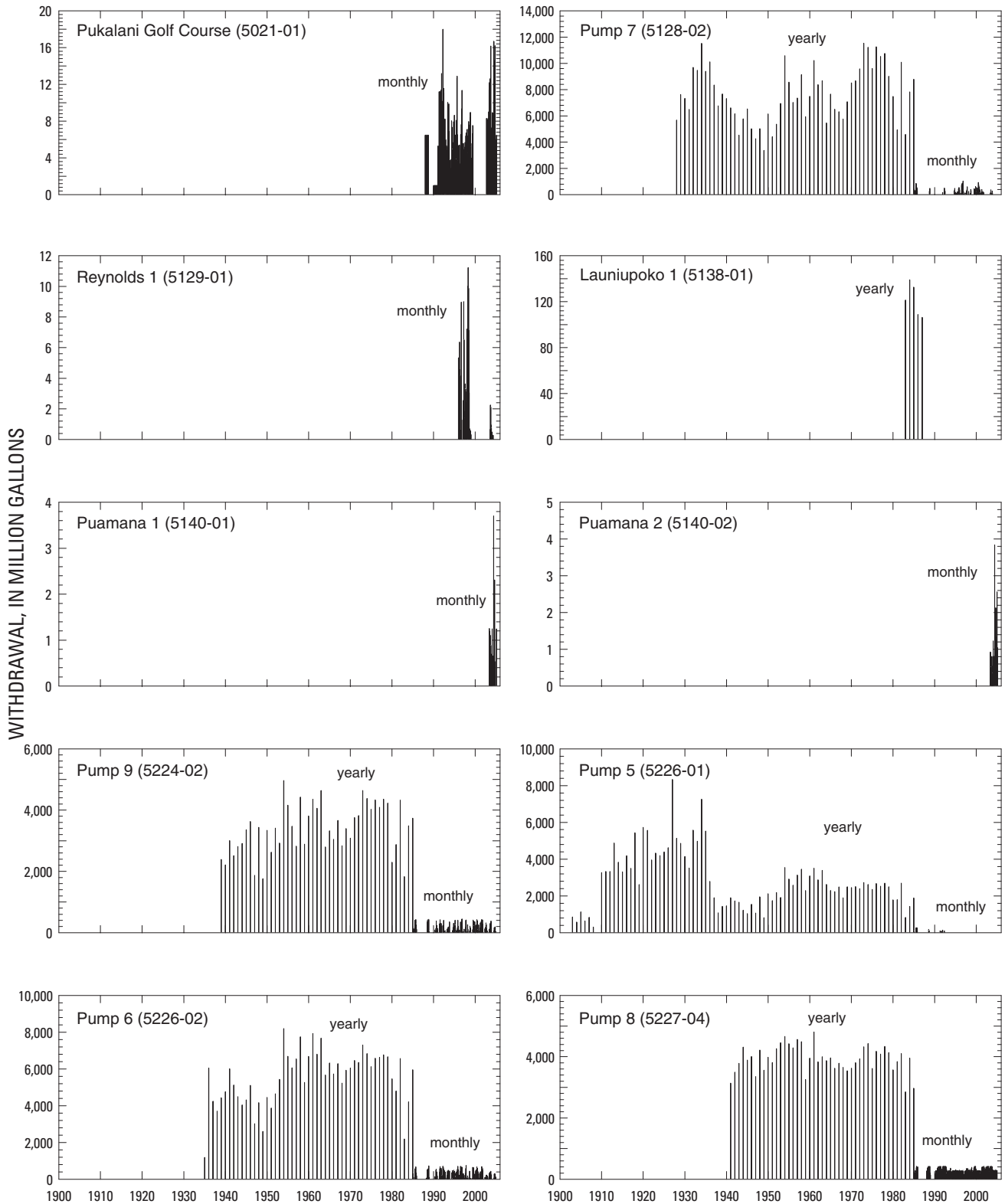


Figure B1.—Continued.

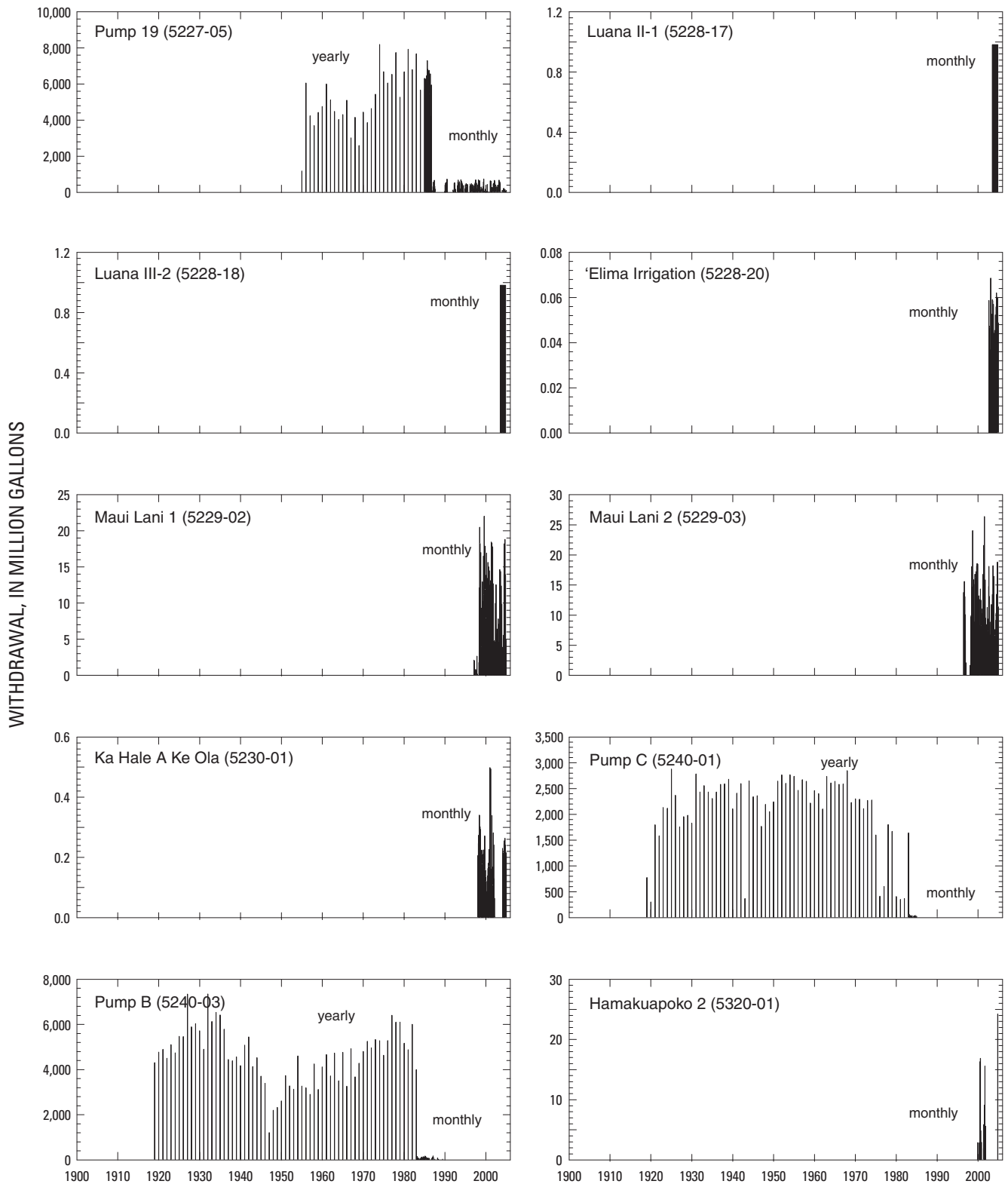


Figure B1.—Continued.

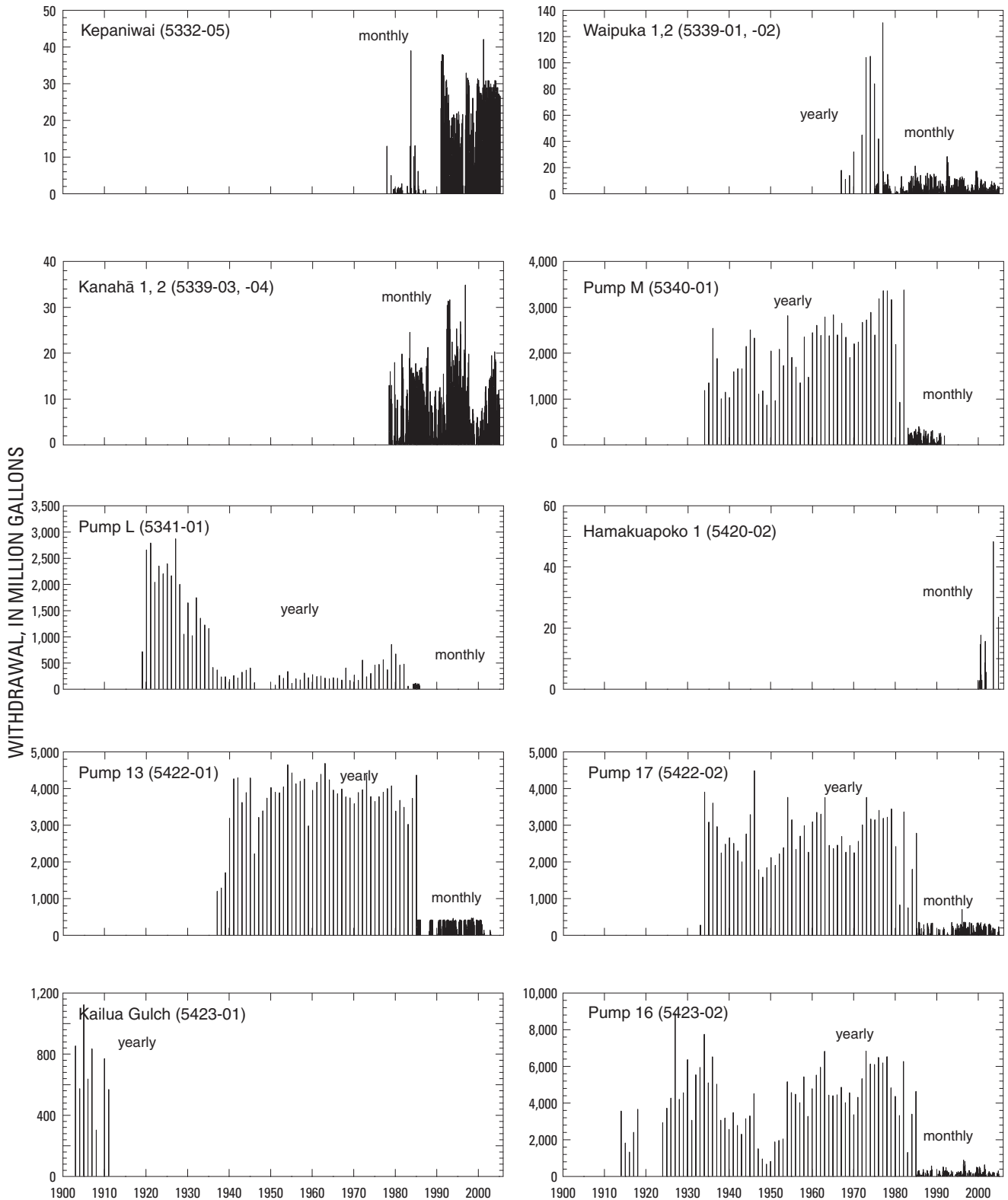


Figure B1.—Continued.

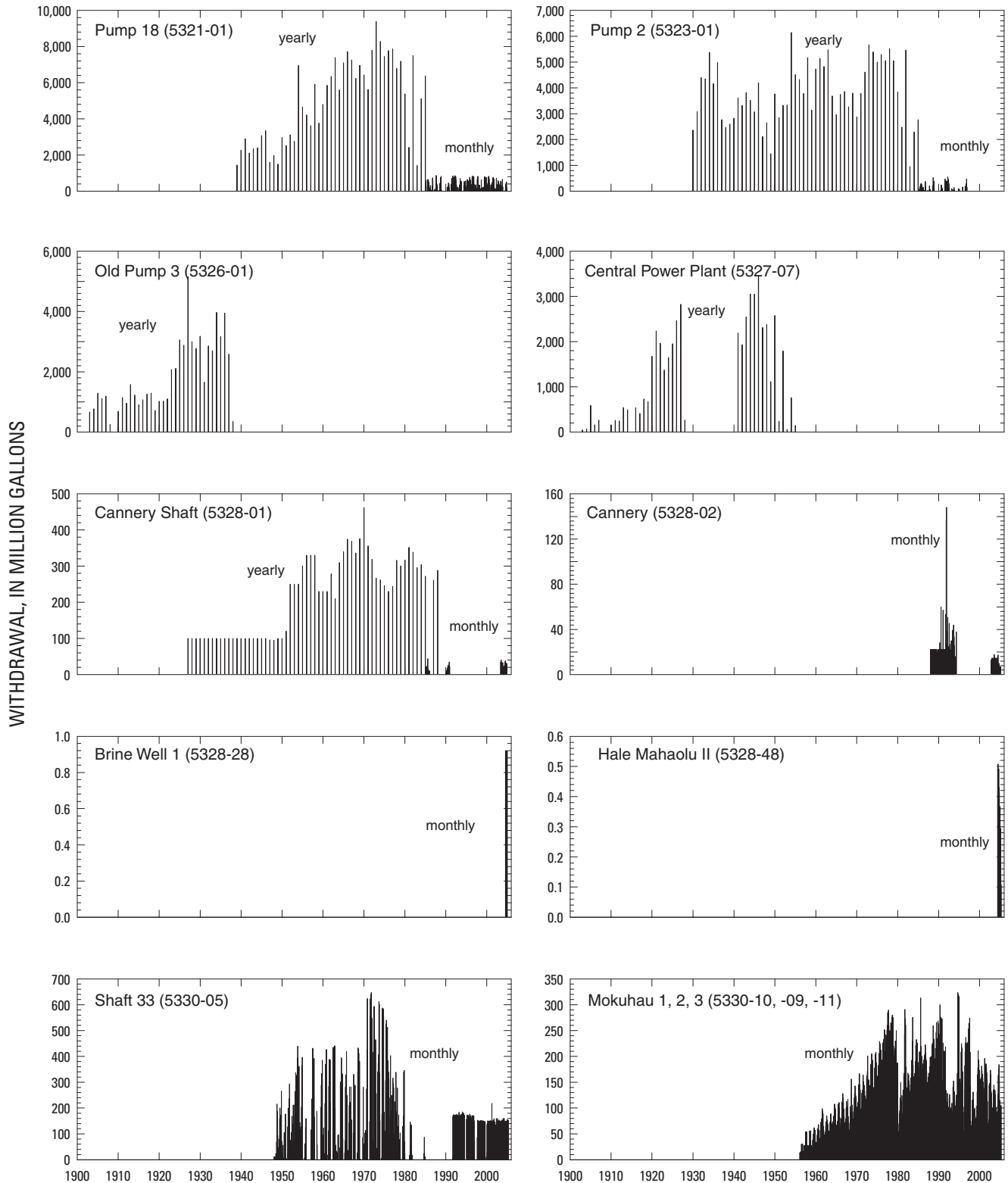


Figure B1.—Continued.

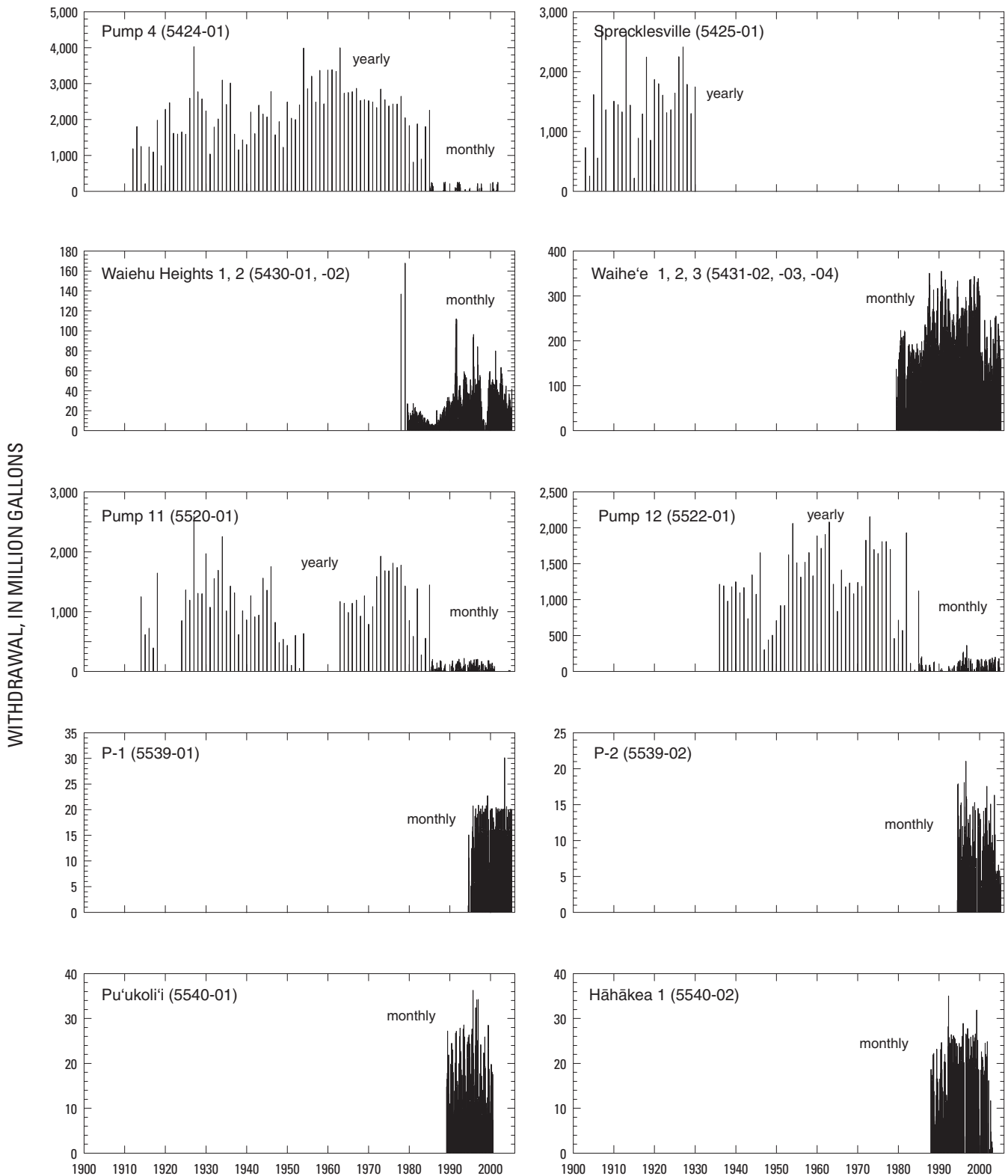


Figure B1.—Continued.

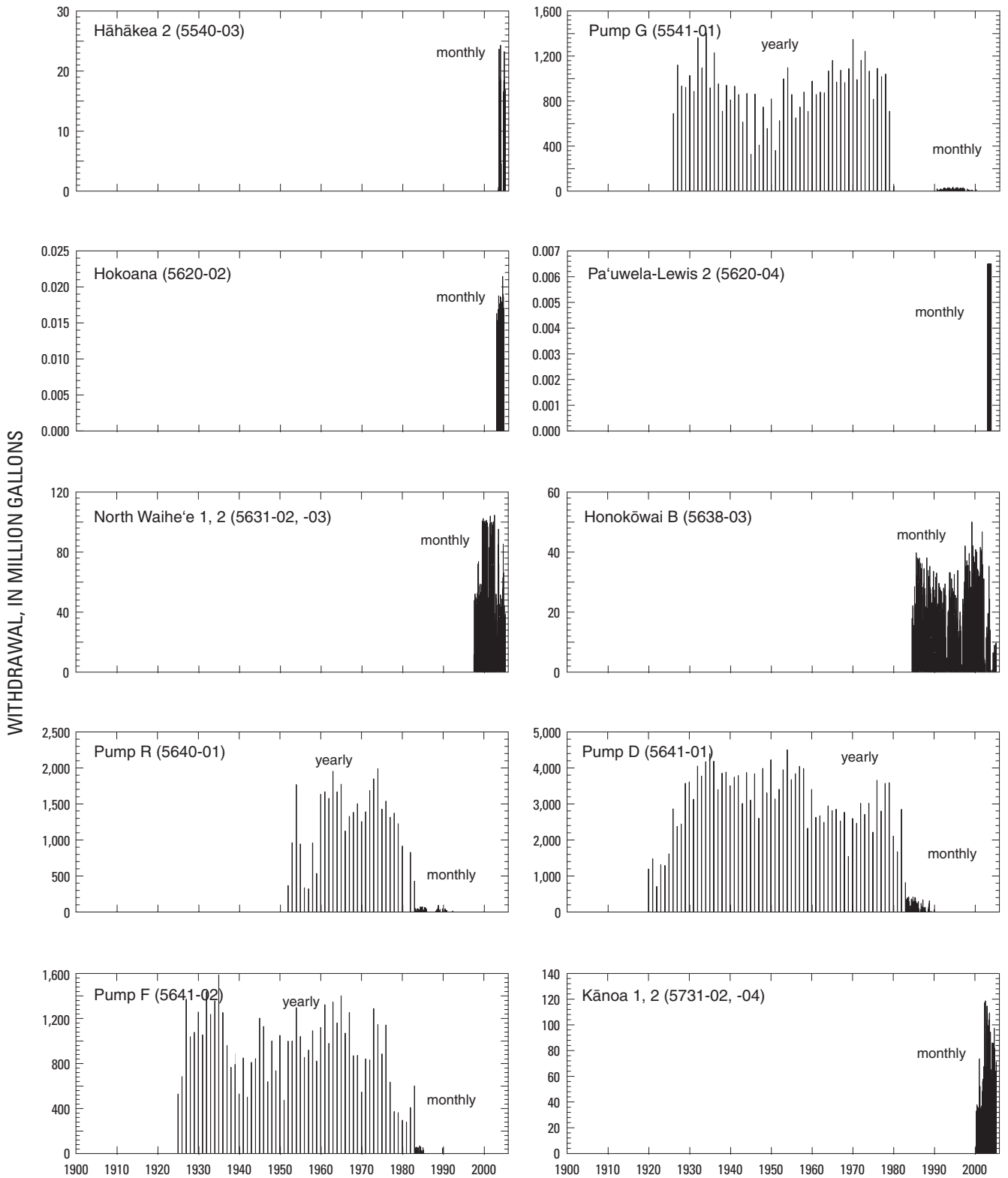


Figure B1.—Continued.

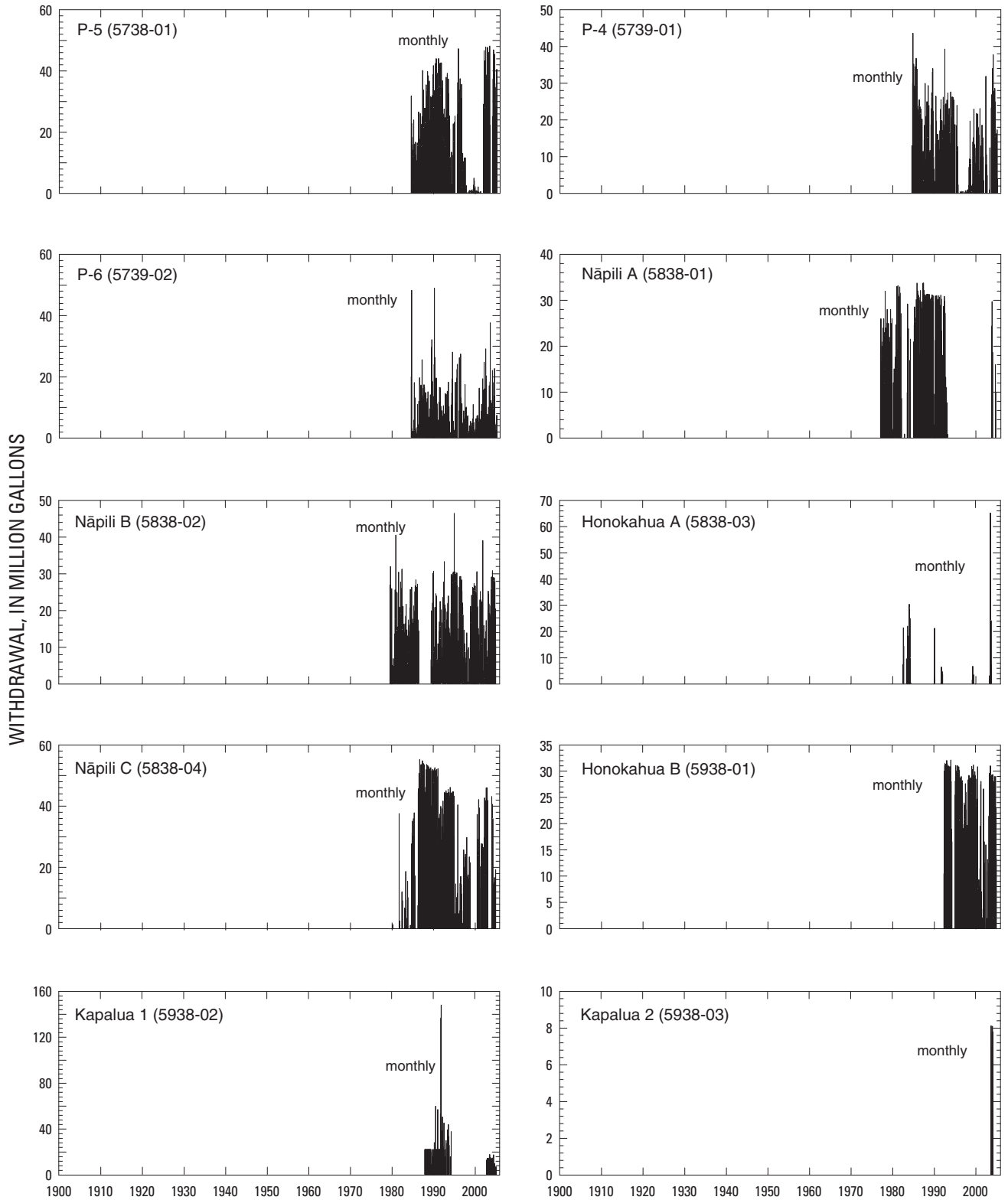


Figure B1.—Continued.

Appendix C. Properties of pumped wells in the central and west Maui study area, Hawai‘i.

Table C1. Properties of pumped wells in the central and west Maui study area, Hawai‘i.

Well no.	Well name	Year drilled	Altitude of top of open interval (feet relative to sea level)	Altitude of bottom of open interval (feet relative to sea level)
3826-01	Seibu 2	1978	6	-22
3826-02	Seibu 3	1978	7	-23
3826-03	Seibu 4	1978	7	-23
3926-02	Seibu 1	1977	9	-22
3926-03	Wailea 8	1976	-1	-29
3926-04	Seibu 5	1984	11	-19
3926-05	Seibu 6	1984	6	-24
3926-06	Seibu 8	1988	11	-19
3926-08	Seibu 10	1988	0	-24
3926-09	Seibu 11	1988	10	-20
3926-11	Mākena Surf	2002	-4	-14
4026-04	Wailea 4	1972	0	-31
4026-05	Wailea 6	1975	8	-31
4026-06	Wailea 7	1975	5	-20
4126-02	Wailea 2	1969	3	-17
4126-03	Wailea 3	1969	0	-21
4226-12	Wailea 5	1972	0	-23
4226-13	Wailea 9	1989	0	-20
4226-14	Wailea 10	1990	6	-14
4226-16	Maui Kama‘ole	2001	4	-26
4426-03	Kihei Maui R&T	1990	-3	-33
4427-03	Medo	1948	0	-14
4727-01	Pump 1 (shaft)	1900	0	-39
4822-01	Kula Meadows	2000	-6	-60
4825-01	Pump 3 (shaft)	1900	0	-47
4835-01	Pump P (shaft)	1934	0	-64
4837-01	Pump O (shaft)	1905	0	-40
4928-02	Pu‘unēnē (shaft)	1942	0	-3
4937-01	Pump N (shaft)	1933	0	-10
5021-01	Pukalani Golf Course	1972	-12	-52
5128-02	Pump 7 (shaft)	1926	0	-42
5129-01	Reynolds 1	1959	-32	-107
5131-01	Waikapū Tank	1999	-1	-101
5138-01	Launiupoko 1	1979	1	-44
5140-01	Puamana 1	1987	-3	-31

Table C1. Properties of pumped wells in the central and west Maui study area, Hawai'i.—Continued

Well no.	Well name	Year drilled	Altitude of top of open interval (feet relative to sea level)	Altitude of bottom of open interval (feet relative to sea level)
5140-02	Puamana 2	1987	-12	-45
5224-02	Pump 9 (shaft)	1938	0	-5
5226-01	Pump 5 (shaft)	1899	0	-45
5226-02	Pump 6 (shaft)	1934	0	-4
5227-04	Pump 8 (shaft)	1939	0	-4
5227-05	Pump 19 (shaft)	1952	0	-5
5228-17	Luana II-1	1986	-6	-38
5228-18	Luana III-2	1986	-5	-50
5228-20	'Elima Irrigation	1997	3	-49
5229-02	Maui Lani 1	1980	-12	-52
5229-03	Maui Lani 2	1980	-5	-25
5230-01	Ka Hale A Ke Ola	1997	-21	-51
5230-03	'Īao Tank			
5240-01	Pump C (shaft)	1897	0	-51
5240-03	Pump B (shaft)	1897	0	-20
5320-01	Hamakuapoko 2	1993	0	-32
5321-01	Pump 18 (shaft)	1938	0	-6
5323-01	Pump 2 (shaft)	1929	0	-42
5326-01	Old Pump 3 (shaft)	1898	0	-40
5327-07	Central Power Plant (shaft)	1894	0	-40
5328-01	Cannery Shaft (shaft)	1926	0	-4
5328-02	Cannery	not available	-120	-280
5328-28	Brine Well 1	1958	-278	-300
5328-48	Hale Mahaolu II	1979	9	-36
5328-51	'Akahi	1969	0	0
5330-05	Shaft 33 (shaft)	1946	30	-280
5330-09	Mokuhau 2	1953	-58	-247
5330-10	Mokuhau 1	1953	-69	-247
5330-11	Mokuhau 3	1967	not available	-251
5339-01	Waipuka 1	1962	4	-57
5339-03	Kanahā 1	1977	1	-52
5340-01	Pump M (shaft)	1933	0	-1
5341-01	Pump L (shaft)	1897	0	-34
5420-02	Hamakuapoko I	1992	0	-63
5422-01	Pump 13 (shaft)	1923	0	-4

Table C1. Properties of pumped wells in the central and west Maui study area, Hawai'i.—Continued

Well no.	Well name	Year drilled	Altitude of top of open interval (feet relative to sea level)	Altitude of bottom of open interval (feet relative to sea level)
5422-02	Pump 17 (shaft)	1932	0	-3
5423-01	Kailua Gulch (shaft)	1899	0	-5
5423-02	Pump 16 (shaft)	1899	0	-30
5424-01	Pump 4 (shaft)	1911	0	-35
5425-01	Sprecklesville (shaft)	1895	0	-50
5430-01	Waiehu Heights 1	1975	0	-338
5430-02	Waiehu Heights 2	1975	0	-206
5431-02	Waihe'e 1	1976	-1	-182
5431-03	Waihe'e 2	1976	-1	na
5431-04	Waihe'e 3	1981	-1	-156
5522-01	Pump 12 (shaft)	1933	0	-5
5539-01	P-1	1990	-1	-61
5539-02	P-2	1991	0	-63
5540-01	Pu'ukoli'i	1968	0	-28
5540-02	Hāhākea 1	1971	0	-20
5540-03	Hāhākea 2	1971	0	-20
5541-01	Pump G (shaft)	1923	0	-2
5620-02	Hokoana	1969	0	-6
5631-02	North Waihe'e 1	1981	-9	-106
5631-03	North Waihe'e 2	1981	-19	-106
5638-03	Honokōwai B	1976	10	-43
5640-01	Pump R (shaft)	1952	0	-14
5641-01	Pump D (shaft)	1897	0	-23
5641-02	Pump F (shaft)	1921	0	-20
5731-02	Kānoa 1	1999	3	-51
5731-03	Kūpa'a	1999	4	-49
5738-01	P-5	1982	4	-36
5739-01	P-4	1982	3	-54
5739-02	P-6	1982	1	-47
5838-01	Nāpili A	1971	0	-33
5838-02	Nāpili B	1972	1	-32
5838-03	Honokahua A	1978	0	-31
5838-04	Nāpili C	1979	-1	-21
5938-01	Honokahua B	1987	0	-20
5938-02	Kapalua 1	1989	13	-54
5938-03	Kapalua 2	1991	-2	-42

This page intentionally left blank

